COMPARISON OF DIFFERENT LOGGING TECHNIQUES FOR POROSITY DETERMINATION TO EVALUATE WATER SATURATION OF ZUBAIR RESERVOIR – EAST BAGHDAD FIELD

A THESIS

SUBMITTED TO THE COLLEGE OF ENGINEERING OF

THE UNIVERSITY OF BAGHDAD IN PARTIAL

FULFILLMENT OF THE REQUIREMENT FOR

THE DEGREE OF MASTER OF SCIENCE

IN PETROLEUM ENGINEERING

BY

SUDAD HAMEED HAMZA

(B.Sc.)

OCTOBER 1990

ABSTRACT

The purpose of this work is to evaluate the saturation profile of Zubair formation in East Baghdad Field, from log interpretation.

The relative accuracy of four methods of porosity evaluation, from three porosity logs (Neutron, Density and sonic logs), was tested against measured porosity from cores of eighty nine chosen intervals.

The accuracy of each method was evaluated statistically by calculating the correlation coefficient, standard deviation error, average percentage error and absolute average percentage error.

The crossplot technique (using triangle method) of Neutron and Density logs data was found to give the best statistical parameters, hence, it was used to calculate optimum porosity values.

It is concluded that the adoption of this method in porosity determination will result in more accurate water saturation determination particularly when using Archie's equation.

ACKNOWLEDGEMENTS

For his patience and encouragement, I am indebted to Dr. Riadh R. Al-Kattan who kindly supervised this work with valuable comments and advices.

For helpful technical advices and assistance, I am as ever indebted to Mr. Imad Jossif, head of logging section in reservoir and field development office and to my friend and colleague Adnan Sadic.

Also, I feel deeply appreciated to the head and members of the examining committee.

Special thanks to my brother Mr. M. Hameed and to Dr. Hayder M. Jaafer and my niece Meha for their constant readiness of being helpful.

Thanks to my colleagues Samira, Saad, Mohammed K., Mohammed E. and Medhat for their assistance in accomplishing this work.

Finally, my gratitude and thankfullness are devoted to my family for their patience and encouragement throughout the stages of this work.

NOMENCLATURE

Symbols:

a = Formation factor coefficient.

C_b = Compressibility of the rock frame, psi^{-1}.

C_f = Compressibility of the pore fluid, psi^{-1}.

C_{hc} = Compressibility of the hydrocarbon fluid, psi^{-1}.

C_P = Compressibility of the pore volume, psi^{-1}.

C_s = Compressibility of the grain material, psi^{-1}.

C_w = Compressibility of the water, psi^{-1}.

F = Formation factor.

G_b = Bulk sheer modulus.

m = Cementation factor.

n = Archie exponent (saturation exponent).

P = Shale fraction of the total formation volume.

R_{mf} = Mud-filtrate resistivity, Ω-m.

R_t = True formation resistivity, Ω-m.

R_w = Formation-water resistivity, Ω-m.

R_{wa} = Apparent formation-water resistivity, Ω-m.

R_{xo} = Flushed-zone resistivity, Ω-m.

S_w = Water saturation, fraction.

S_{xo} = Water saturation in the flushed zone, fraction.

V = Formation velocity, ft/sec.

V_{CL} = Clay volume, fraction.

V_f = Sonic velocity in the interstitial fluid, ft/sec.

V_{ma} = Sonic velocity in the rock matrix, ft/sec.

V_p = Compressional velocity, ft/sec.

V_{sh} = Shale volume, fraction.

α = Shale indicator, fraction.

Δt = Acoustic traveltime in formation, μsec/ft.

Δt_f = Acoustic traveltime in fluid, μsec/ft.

Δt_{ma} = Acoustic traveltime in rock matrix, μsec/ft.

σ = Poisson's ratio.

ϕ = Porosity, fraction.

$\bar{\phi}_{calc}$ = Average calculated porosity, fraction.

$\bar{\phi}_{meas}$ = Average measured porosity, fraction.

$\phi_{i\ calc}$ = Calculated porosity in well for ith layer, fraction.

$\phi_{i\ meas}$ = Measured porosity in well for ith layer, fraction.

ϕ_{sc} = Corrected porosity for shale content, fraction.

ϕ_D = Density-log apparent porosity, fraction.

ϕ_N = Neutron-log apparent porosity, fraction.

ϕ_{Nsh} = Neutron-log equivalent porosity of shale, fraction.

ϕ_m = Porosity derived from matrix method, fraction.

ϕ_F = Porosity derived from fluid method, fraction.

ϕ_A = Porosity derived from average method, fraction.

ρ_b = Bulk formation density, gm/cc.

ρ_f = Density of fluid, gm/cc.

ρ_{ma} = Density of rock matrix, gm/cc.

ρ_{sh} = Density of shale, gm/cc.

β = C_s/C_b.

Abbreviations:

AAP = Absolute Average Percentage Error.

APE = Average Percentage Error.

BHC = Borehole Compensated.

CF = Correlation Coefficient.

CNL = Compensated Neutron Log.

FDC = Formation Density Compensated.

GR = Gamma Ray.

CGR = Corrected Gamma Ray.

ILD = Induction Log Deep.

S_D = Standard Deviation Error.

LIST OF FIGURES

LIST OF TABLES

TABLE OF CONTENTS

CHAPTER ONE

INTRODUCTION

East Baghdad Field is one of the recently discovered Iraqi oil fields, having several pay Zones. Zubair formation is one of these zones at which we have executed this investigation.

Lithologically, Zubair formation is composed mainly of sandstone with some intervals of shaly sand and shale (particularly in the upper section).

The porosity of eighty nine intervals in the water bearing zone of six wells (EB-55, EB-56, EB-77, EB-79, EB-15, and EB-18) of this field was calculated by using the following available logs:-

1- Sonic log, BHC.

2- Density log, FDC.

3- Neutron log, CNL.

Neutron and Density logs are used either as single porosity indicator, using their basic equations, or in combinations, using a crossplot technique (triangle method). Hence, three porosity values are calculated from Neutron and Density logs for each interval.

On the other hand, the time-average equation was used to calculate porosity from the transit time of sound wave through the formation which was taken from sonic log. Therefore, Several comparisons can be made between porosity

values calculated from sonic log and that from other logs. The reference value in these comparisons is the core porosity. This porosity was measured in the laboratory by using saturation method with gas oil, at depths corresponding to same log intervals.

Log porosity should be corrected for shaliness. More than one method can be used for shale volume determination, some of these methods are:

1- Corrected Gamma Ray log, CGR.

2- ρ_b-ϕ_N crossplot using triangle method.

After the four porosity values have been calculated for each interval, we have used regression analysis (simple regression) and a statistical program to compare these values with those obtained from cores in order to get the correlation coefficient, average percentage error, absolute average percentage error and standard deviation error. Then we used the porosity values obtained from the triangle method to formulate a modified form of Archie equation to be used for water saturation determination.

The reason of using triangle method was that it shows a highest correlation coefficient and lowest percentage errors.

The modified Archie's equation is formulated by finding particular values for cementation factor (m) and the formation factor coefficient (a) for Zubair formation using Pikett method, in which, resistivity-porosity crossplots for the same intervals have been executed.

CHAPTER TWO

LITERATURE REVIEW

One of the main objectives in formation evaluation is the determination of water saturation (S_w). Importance of this objective comes from the essential part of saturation determination in reserve estimation.

Water saturation is defined as the fraction of pore space occupied by water. To determine 'S_w', many other petrophysical parameters should be known, either from well logging or from other sources, such as the porosity.

The most commonly used method for S_w determination is the Archie's equation[1]:-

$$S_w^n = \frac{FR_w}{R_t} \qquad \text{..... 2-1}$$

Where:

R_t = True formation resistivity, Ω-m,

F = Formation resistivity factor,

R_w = Formation-water resistivity, Ω-m, and

n = Saturation exponent.

This equation is directly applicable to the case of clean formation with homogeneous intergranular porosity, where it is found to give good results. It is also used for determination of 'S_w' in flushed zone, as follows,

$$S_{xo}^{n} = \frac{FR_{mf}}{R_{xo}} \qquad \text{..... 2-2}$$

Where:

S_{xo} = Water saturation in the flushed zone,

R_{xo} = Resistivity of flushed zone, Ω-m, and

R_{mf} = Mud-filtrate resistivity, Ω-m.

The formation resistivity factor (F) is defined by

$$F = \frac{a}{\phi^{m}} \qquad \text{..... 2-3}$$

Therefore Eq.(2-1) can be written as:-

$$S_{w}^{n} = \frac{a\ R_{w}}{\phi^{m}\ R_{t}} \qquad \text{..... 2-4}$$

Formation resistivity factor, as seen from Eq.(2-3) is a function of porosity, cementation factor (m) and formation factor coefficient (a). The cementation factor (m) was found to be a function of formation lithology, and to have essential effect on 'S_w' determination. It was also found that general values of m = n = 2 and a = 1 can be used to give reasonable results.

Determination of porosity is a vital step for the accurate determination of saturation, as can be seen from Archie's equation. The resistivity of formation water (R_w) can be obtained from direct laboratory measurement of formation water sample, or, alternatively, can be estimated

from well logs. Many methods were suggested for the determination of 'R_w'[2], which can serve as quick methods for Sw determination. Among these are

1- Pickett method

2- Hangle method

3- R_o/R_t, ratio method.

- Pickett Method[3]:- In this method, formation resistivity readings are to be cross-plotted against porosity on logarithmic co-ordinates. The lowermost points in this plot represent the water line (R_o line), and the intercept of this line with the Ø-axis (at Ø=100%) can be used to calculate 'R_w'.

  This method can be considered as a quick graphical solution for the determination of water saturation.

- Hingle Method[2]: In this method, across-plot is constructed of (log $1/\sqrt{R_t}$) against one porosity log reading. Formation density (ρ_b), sonic transit time (Δt), and formation factor can be used in this semi-logarithmic cross-plot. As in pickett method, line is drawn through the lowest resistivity points, that represent the water zone, and 'R_w' value can be calculated from the slop of this line. This plot can also be used for direct graphical determination of 'S_w'.

- Ratio Method[4]:- In this method, resistivity readings of two zones around the well bore are taken into consideration. The first zone is the invaded zone next to the well bore, which is affected by mud filtrate. The

second is the uninvaded zone, which corresponds to the original conditions in the formation.

The ratio of the flushed zone resistivity to the unflushed zone resistivity can be shown to have the following form, according to Archie's equation:-

$$R_{xo}/R_t = \frac{R_{mf}}{R_w} (S_w/S_{xo})^2 \quad \text{..... 2-5}$$

When the following empirical relationship is substituted:-

$$S_{xo} = S_w^{1/5} \quad \text{..... 2-6}$$

Solving the equation for 'S_w':

$$S_w = \left(\frac{R_{xo}/R_t}{R_{mf}/R_w}\right)^{5/5} \quad \text{..... 2-7}$$

When 'R_w' is known, water saturation can be determined directly from Eq.(2-7).

Another method that can be used for 'R_w' and 'S_w' determination, is the apparent water resistivity method[5]. This method employs the determination of minimum 'R_{wa}' by using the following equation (in assuming that $S_w=1$)

$$R_{wa} = \frac{R_t}{F} \quad \text{..... 2-8}$$

When several intervals of water bearing zone have the same values of $(R_{wa})_{min}$, there is a fair amount of certainty

that this value corresponds to 'R_w'. Therefore, when 'R_w' is known from this method, 'S_w' can be calculated by substituting Eq.(2-7) in Eq.(2-1)

$$S_w = \sqrt{\frac{R_w}{R_{wa}}} \qquad \text{..... 2-9}$$

All the above mentioned methods are based on Archie's equation, and are mostly valid for clean formation.

Determination of porosity from logs has been discussed by neumerous numbers of articles. In this section, an attempt will be made to summarise some of the essential articles dealing with sonic and radioactive logs as porosity indicators.

2-1 Sonic log:

The principle of sonic logging tool is based on the propagation of elastic vibrations in the formation. Sonic logging is a recording of the transit time of sound wave as it travels through one foot in the formation, i.e. is a measure of sonic velocity in the formation.

Since the mid-1950's, the sonic log has become one of the most commonly used methods for porosity determination in oil and gas reservoirs[6].

Although the sonic log can be run in both compacted and uncompacted formations, its record in the later case needs to be corrected. The correction procedure was suggested by Tixier et al[7].

They also found that the sonic reading should be corrected for shaliness and fluid content.

Besides porosity determination, sonic logs can be used for fracture location, geological correlation, and with neutron and/or density logs, for identification of lithology. Similar to most other logging measurements, the sonic log reading is not a direct porosity value, but rather the time required by the sound wave to travel between two points through the formation, i.e., sonic velocity in the formation. These measured (Δt's) or velocities must then be transformed into porosity. The transformation procedure is affected by many factors, among which are[8]:-

- Degree of shaliness.
- Effective stress.
- Type and pressure of pore fluid.
- Matrix materials.
- Degree and nature of cementation.
- Temperature.

The transformation of sonic reading into porosity had been discussed by many authors, as follows:-

Wyllie et al. (1956, 1958)[9,10] have developed an average velocity equation as a conclusion of substantial Laboratory work to describe velocities measured on a pile of lucite-aluminum discs. This equation was used to calculate the porosity of fluid filled pores:-

$$\frac{1}{V} = \frac{\phi}{V_L} + \frac{1-\phi}{V_{ma}} \quad \text{..... 2-10}$$

Where:

V = Formation velocity, ft/sec,

ϕ = Fractional porosity,

V_L = Sonic velocity in the interstitial fluid, ft/sec, and

V_{ma} = Sonic velocity in the material constituting the matrix of the rock, ft/sec.

In terms of transit time (Δt), and for porosity determination, the time average equation can be written as:-

$$\phi = \frac{\Delta t - \Delta t_{ma}}{\Delta t_f - \Delta t_{ma}} \quad \text{..... 2-11}$$

Where Δt, Δt_{ma} and Δt_f are the respective transit times of the sound energy expressed in μsec/ft.

Wyllie et al.[9] compared the velocities from equation with actual velocities obtained from cores measurements at atmospheric pressure. They repeated the comparison in 1958 under different pressures to simulate in situ conditions[10].

They reported that "whereas all the experimental data show a considerable degree of dependence of velocity upon porosity, there is also a considerable scatter of data which must represent the influence of other factors such as the matrix material, grain size, distribution and shape of

cementation, type of liquid in pores, pressure and temperature".

It can be noticed that the time average equation is the simplest model, and the mostly used equation in determination of formation porosity since it was developed by wyllie et al. (1956). This is because of its simplicity and intuitively reasonable appearance as compared with other theoretical equations.

Millican[11] (1960) has developed a method of log interpretation in the Delaware sand, in which the effects of shale content can be recognized and used for correction of porosity calculation.

He stated that "the shale content may be considered as an additive to the sand matrix, and as such may be included as part of the matrix in any proposed relation between sonic velocity and porosity".

Therefore, he added the shale as a second matrix material to Wyllie equation:

$$\frac{1}{V} = \frac{\phi}{V_L} + \frac{P}{V_{sh}} + \frac{1-P-\phi}{V_{ma}} \qquad \text{..... 2-12}$$

Where, P is the shale fraction of the total volume. In terms of Δt's and for porosity calculation, the equation may be formed as:

$$\phi = \frac{\Delta t - \Delta t_{ma}}{\Delta t_f - \Delta t_{ma}} - P \frac{\Delta t_{sh} - \Delta t_{ma}}{\Delta t_f - \Delta t_{ma}} \qquad \text{..... 2-13}$$

It seems obvious that the second term of Eq.(2-13) is a correction term for the presence of shale within the sand, i.e., it represents a porosity reduction term.

With presence of Sonic and Gamma Ray logs, he presented Eq.(2-12) on a graphical chart to determine the porosity for both clean and shaly sand, as shown in Fig.(2-1).

Geertsma[12] (1961) showed that the effect of porosity on formation velocity can be accounted for, through the compressibilities:-

$$V_p^2 = \left[\frac{\beta}{Cs} + \frac{4}{3} Gb + \frac{(1-\beta)^2}{(1-\phi-\beta)\, Cs + \phi\, Cf} \right] \frac{1}{\rho_b} \qquad \ldots 2\text{-}14$$

Where, V_p is the compressional velocity (ft/sec), ρ_b is the bulk density (gm/cc), C_s and C_f the compressibilities (psi^{-1}) of the matrix grain material and the pore fluid, respectively.

The bulk shear modulus (Gb) is defined as:

$$Gb = \frac{3(1-2\sigma)}{2\, C_b\, (1+\sigma)} \qquad \ldots 2\text{-}15$$

Poisson's ratio of the empty rock frame is 'σ' and β is C_s/C_b, where 'C_b' is the compressibility of the rock frame, which is defined as:

$$C_b = \phi\, C_p + C_s \qquad \ldots 2\text{-}16$$

where, 'C_p' is the compressibility of the pore volume. The pore fluid compressibility is defined as:

$$C_f = S_w C_w + (1-S_w) C_{hc} \quad \ldots\ldots\ldots\ldots\ldots\ldots \quad 2\text{-}17$$

where, C_{hc} is the compressibility of the hydrocarbon fluid and C_w is the compressibility of the water.

Use of Eq.(2-14) to predict porosity is obviously far less attractive than empirical correlations due to the number of parameters and the involved calculations.

Kokesh et al.[13] (1965) have suggested a completely new logging system, which is the borehole compensated sonic system, in which the errors caused by irregular borehole diameter have been overcome.

Meese[14] (1974) have used a statistical approach to derive relationships between transit time (Δt) and porosity for reservoir rock which has either linear or logarithmic statistical properties.

He stated that "If the rock properties are distributed (statistically) in a linear fashion, the well-known time-average equation is derived":-

$$\Delta t = \Delta t_f . \phi + \Delta t_{ma} (1-\phi) \quad \ldots\ldots\ldots\ldots\ldots\ldots \quad 2\text{-}18$$

And if the properties (particularly transit times) are distributed statistically in a logarithmic fashion, an analogous logarithmic-time-average equation is derived:-

$$\Delta t = (\Delta t_{ma})^{1-\phi} . (\Delta t_f)^{\phi} \quad \ldots\ldots\ldots\ldots\ldots\ldots \quad 2\text{-}19$$

He compared the logarithmic time average equation and the usual (linear) time average equation with laboratory data for certain carbonates, as shown in Fig.(2-2). He concluded that, there is a very good agreement between the logarithmic equation and laboratory data.

Problems rising when using the time average equation, particularly when it fails to predict the porosities in high formation porosity ranges (over 25%), have urged Raymer et al.[15] (1980) to propose a new empirical model to transform the transit times to porosities over the entire theoretical porosity range, from 0.0 to 100%, as shown in Fig.(2-3). This figure shows a comparison between their proposed transform and time average equation for V_{ma} = 1800 ft/sec and V_{ma} = 19,500 ft/sec.

One drawback of their suggested transform is that they could not find a single algorithm or equation for translating the transit times to porosities over the entire porosity ranges (0-100%). For that reason, they divided the entire range into segments, as follows:-

a- For the range of porosity from 0% to 37%, they proposed the following equation:-

$$V_1 = \sqrt{\frac{\rho_{ma}}{\rho}}\,(1-\phi)^{1.9}\,V_{ma} \qquad \text{..... 2-20}$$

where, ρ is the bulk density of the mixture and ρ_{ma} is the matrix density. This equation was suggested to be used in porosity determination for zones saturated with water.

However, if the zones are saturated with other fluid, the following equation was proposed:-

$$V_1 = (1-\phi)^2 V_{ma} + \phi V_f \quad \ldots\ldots\ldots\ldots\ldots\ldots\ldots \quad 2\text{-}21$$

where, $\Delta t_1 = 10^6 / V_1$

b- For the range of porosity from 47% to 100%, the proposed equation is:-

$$\Delta t_2 = \sqrt{\frac{\rho \phi \Delta t_f^2}{\rho_f} + \frac{\rho(1-\phi) \Delta t_{ma}^2}{\rho_{ma}}} \quad \ldots\ldots\ldots\ldots \quad 2\text{-}22$$

c- For 37% to 47% porosity range, the proposed equation is:-

$$\Delta t = \frac{0.47 - \phi}{0.1} \Delta t_1 + \frac{\phi - 0.37}{0.1} \Delta t_2 \quad \ldots\ldots\ldots \quad 2\text{-}23$$

or

$$\Delta t = \frac{0.47 - \phi}{0.1} \Delta t_1 + \frac{\phi - 0.37}{0.1} \Delta t_f \quad \ldots\ldots\ldots \quad 2\text{-}24$$

2-2 Radioactive logs

Neutron, Density and Gamma Rays logs are the most widely used radioactive logs in the field of formation evaluation, particularly for porosity and shale volume determination. The first logging operation using radiation of nuclear origin was performed in the begining of 1940's to

record the natural gamma radiation emitted by the formation crossed by bore holes[2]. The gamma radiation has been widely used in well logging because of its high penetration power to investigate through the formation and the casing.

Other purposes of radioactive logs in addition to porosity and clay volume determination are the lithology determination, gas bearing zones detection, formation density, ... etc.

Neutron logging device emits neutrons that responds to the hydrogen content in the formation, which includes hydrogen of liquid present in pore space, matrix and in clay lattice (if the formation contains clay).

Density logging device measures the bulk density (matrix and fluid densities) by emitting Gamma Ray into the formation. The Gamma Ray logging device measures the natural radioactivity of the formation.

Since the most of radioactive minerals exist in shales and clays, the Gamma Ray log considered to be the most widely used log as a shale or clay indicator.

2-2-1 Evaluation of porosity

The neutron and density logs have been in use for many years as porosity indicators. They can be used as single indicators, combined to each other in crossplot techniques, or combined to other logs (such as sonic), for better evaluation of porosity.

The Density log measures the bulk formation density, therefore, porosity derived from this log will represent the total formation porosity[16].

Neutron log responds to the hydrogen content of the formation. Hydrogen ions exist mainly in the pore filling fluids, but they can be also found in the matrix and in clays (in the cases of shaly formation). When this is the case, the neutron porosity needs to be corrected for hydrogen content of matrix and shale.

The effective porosity can be estimated by crossplot technique of density-neutron data, and it was noticed that calculated effective porosity by this technique provides the most meaningful measurement of in-situ porosity[17].. Various methods have been proposed by many authors that deal with these two radioactive logs as porosity indicating devices.

An approach of porosity determination for thin beds from Neutron logs has been proposed by Edwards and Simpson[18] (1955). Actually they developed an equation to correct the deflections of Neutron logs in thin beds. They also introduced the scintillometer into the field of radioactivity logging to make it possible to determine bed thickness accurately.

Wahl et al.[19] (1964) proposed a new density logging tool in which the effects of the mud cake and hole irregularities could be overcome. This tool was called the compensated formation density tool, FDC.

They concluded that the tool gives good measurements for more accurate densities without needing mud cake and borehole irregularities corrections, hence, more accurate porosities will be obtained by applying the following equation:-

$$\rho_b = \rho_{ma}\ (1-\phi) + \rho_f(\phi) \qquad \text{..... 2-25}$$

Where:

ρ_b = Formation bulk density, gm/cc,

ρ_f = Fluid density, gm/cc, and

ρ_{ma} = Matrix density, gm/cc.

Neutron-Density crossplot has been proposed by Schlumberger company[20] (1968) for better porosity evaluation. The method was called 'The Duel Mineral Method'. It accounts for the presence of more than one mineral in the formation matrix. Both 'ϕ_N' and 'ρ_b' are plotted on a specially designed chart, see Fig.(2-4). Each line represents one mineral. The points so cross-plotted on the chart can be used for direct porosity and lithology determination.

Poupon et al.[21] (1971) proposed a new method (complex lithology method), which is more general than the Duel Mineral Method because it takes into account the effects of the shaliness and hydrocarbon on the porosity and lithology determination. The method was used in a computer program called CORIBAND, which facilitates the numerous

amount of cross-plotting and other correction techniques that required specially when dealing with complex lithology.

A comparison has been made between the compensated Neutron log, CNL, (which overcomes the mud cake and bore hole irregularities effects) and the epithermal Neutron tools by Truman et al.[22] (1972). They concluded that the determined shale content and porosity by the CNL-density crossplot are more accurate than those determined by previous Neutron (such as SNP)-Density crossplot by computations.

A program for hand-held calculators have been developed by Ching and Krug[23] (1978) for crossplot analysis in which the FDC-CNL-GR and deep investigation resistivity logs can be used. This program can be considered as a quick method to determine effective porosity, shale content and water saturation.

Ching and Krudwing[24] (1980) have modified the proposed quick method of density-Neutron crossplot analysis (using hand-held calculators) by WU and Krug[23] (1978), by means of using polar coordinates that made the program more compact, efficient and more quicker in determination of shale content, porosity and water saturation.

Swulius[25] (1986) suggested a new technique to transform Neutron log deflections into accurate Neutron porosity log. In that method, he used computers to analyze and rescale the Neutron log deflections to a more accurate porosity log. Then an equation was derived in which the

corresponding porosities to the neutron log deflections can be obtained.

2-2-2 Evaluation of clay volume

Many logs can be used as shale or clay indicators, the most common are SP, Neutron, Density and Gamma Ray logs.

The clay volume can be calculated by single log or by a combination of two or more logs. The following is a review of the most interesting researches dealing with radioactive logs as a shale or clay indicators:-

Poupon and Gaymard[26] (1970) discussed the evaluation of clay logs as clay indicators. They stated that "each clay indicator is calibrated in such a way that it gives either a good approximation of the volume of clay when the conditions are favorable for that particular indicator, or an upper limit of the clay volume".

They used, in addition to the resistivity, SP and sonic logs, the radioactivity logs as clay indicators that include Gamma Ray log as a single clay indicator and Neutron log as either a single clay indicator or combined clay indicator with Density log.

It has been reported that when there is more than one lithology within the formations (such as limestone and sand stone), the use of one (VCL = 0 line) in cross-plotting of neutron-density data is not favorable. However, it's preferable to divide the formation into intervals, taking

the lithology into account, and to define for each interval the appropriate VCL = 0 line.

Heslop[27] (1974) proposed a new method to calculate the clay volume using Gamma Ray log. His method included a new technique to estimate the shale and sand lines by using Gamma Ray-Density crossplot and Neutron-Density crossplot. He had also calculated the clay volume by using the X-Ray diffraction for 357 feet of examined samples. He found that there was a linear relationship between the determined clay volumes by x-ray diffraction and those determined by Gamma Ray response for the same interval. Therefore, Heslop stated that "the Gamma-ray response to clay content of elastic rocks is linear".

A new logging tool has been suggested by Serra et al.[28] in 1980's (Natural Gamma ray spectroscopy, NGS), whose reading can be analysed to determine the nature and qualities of the radioactive materials, and considered to be an improved shale indicator. This tool has responded to the existence of thorium, uranium and potassium within the formation, and by applying the following equations, the percentage volumes of these radioactive minerals within shale can be found:-

$$(V_{sh})_{Th} = \frac{Th - Th_{min}}{Th_{sh} - Th_{min}} \quad \ldots\ldots\ldots\ldots\ldots\ldots \quad 2\text{-}26$$

$$(V_{sh})_U = \frac{U - U_{min}}{U_{sh} - U_{min}} \quad \ldots\ldots\ldots\ldots\ldots\ldots \quad 2\text{-}27$$

$$(V_{sh})_K = \frac{K - K_{min}}{K_{sh} - K_{min}} \quad \ldots\ldots\ldots\ldots\ldots\ldots \quad 2\text{-}28$$

Upon the determination of U, Th, and K by application of the weighted least squares solution, the total gamma ray response can then be found by linear combination:-

$$GR = ATh + BU + CK \quad \ldots\ldots\ldots\ldots\ldots\ldots\ldots \quad 2\text{-}29$$

Where A,B,C are coefficients obtained from a special test procedure of the log tool.
and this shale indicator defined as follows:-

$$(V_{sh})_{GR} = \frac{GR - GR_{min}}{GR_{sh} - GR_{max}} \quad \ldots\ldots\ldots\ldots\ldots\ldots \quad 2\text{-}30$$

They stated that "the uranium is associated with radioactive minerals other than those found in shale, so it is generally not a reliable shale indicator".

Because of that, they have eliminated the uranium contribution from the total gamma ray response:-

$$GR_s = ATh + CK \quad \ldots\ldots\ldots\ldots\ldots\ldots\ldots\ldots \quad 2\text{-}31$$

Where GR_s is the uranium free gamma ray response, and this shale indicator is defined as follows:-

$$(V_{sh})_{GR_s} = \frac{GR_s - GR_{smin}}{GR_{ssh} - GR_{smax}} \quad \text{..... 2-33}$$

Thus, they concluded that GR_s log is a better shale indicator than GR log.

Quirein, et al.[29] (1981) suggested a new approach in which the clay volumes and associated clay bound water volumes from log data can be determined. The regression techniques for log data and core data used in this approach to provide first-order estimates of how each logging tool responds to expected clay or minerals types.

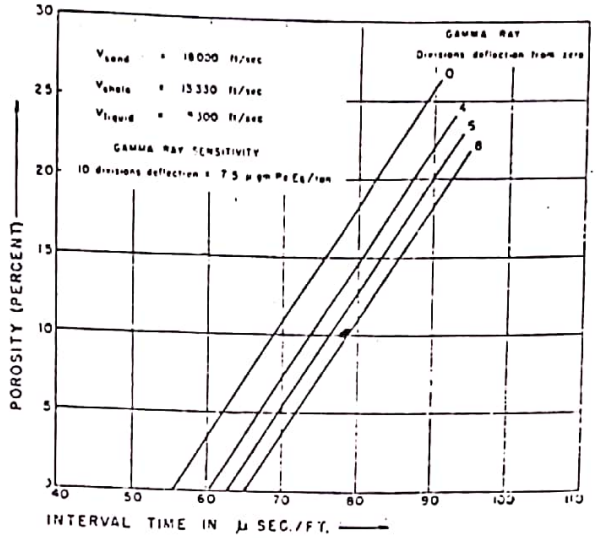

Fig.(2-1) Theoretical plot of porosity vs transit time with increasing shale as indicated by Gamma Ray deflection

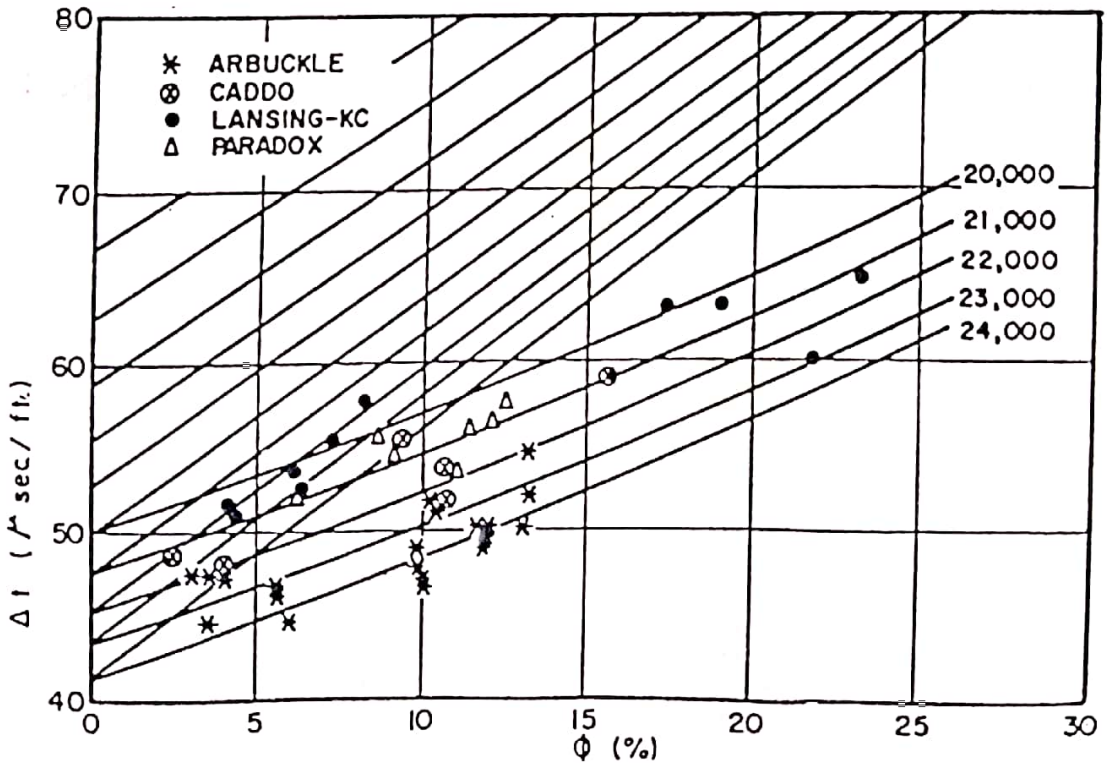

FIGURE(2-2) POROSITY VS TRAVEL TIME
(P_{axt} = 2000 psi , P_f = 0 , BRINE SATURATED)

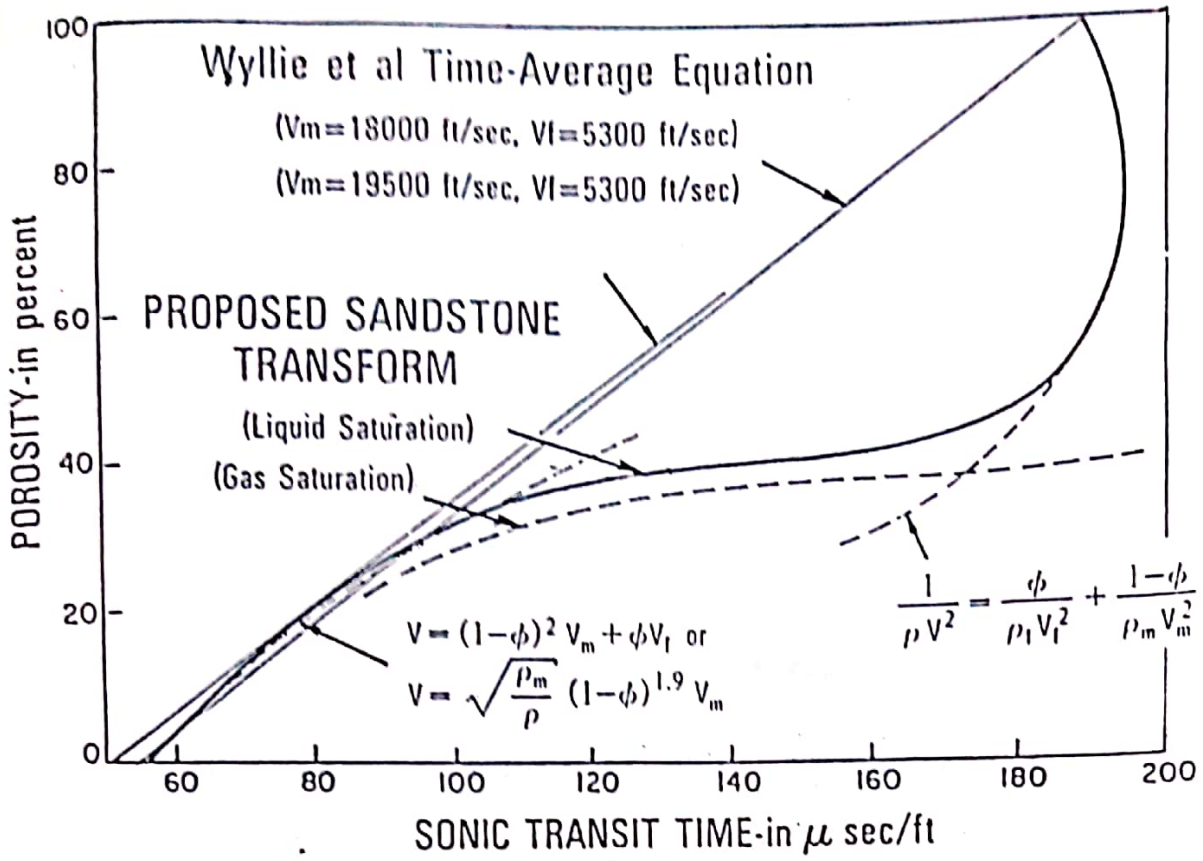

Fig.(2-3) The proposed sonic transit time-to porosity transform, showing comparison to Wyllie time-average equation (1956) and to suggested algorithms by Rayner et al. (1980).

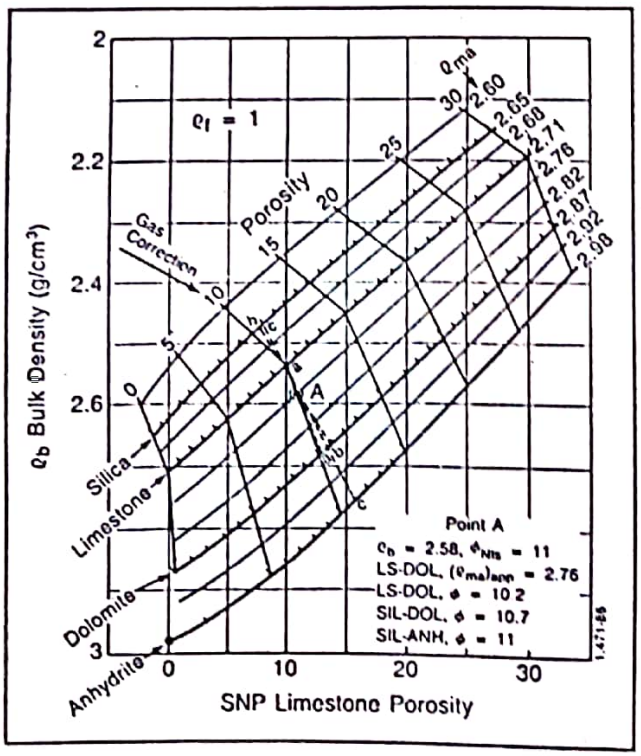

Fig. 2-4—Neutron-density crossplot scaled with interpolated ρ_{ma} lines.

CHAPTER THREE

DETERMINATION OF POROSITY BY LABORATORY MEASUREMENTS AND SONIC LOG

3-1 Laboratory measurements:-

In order to have accurate correlation between the core analysis and the well logs interpretation, all porosity values that can be measured from the cores and enable us to compare it with the well logs were measured. This part includes the description of the apparatus used and the experimental procedure. Calibrations for each apparatus, if needed, were done before beginning of the runs.

3-1-1 Preparing and cleaning the core samples:-

Eighty Nine plugs were cut from the cored section of 6 wells of the Zubair formation-East Baghdad oil field. The cutting were both in vertical and horizontal directions, using one diameter of core drill (1 inch) and water as a coolant.

The core samples that were used for porosity by mercury injection measurements, were cleaned in soxhlet extractor, (see Fig.3-1) by refluxing them with a mixture of equal volume of pure benzene (C_6H_6), toluene (C_7H_8) and methanol (CH_3OH), until no change in the colour of the

mixture occures. After the samples had been dried in the oven, they were ready for testing.

3-1-2 Measurement of porosity:-

The porosity values, as shown in Table (A-1), of the six wells had been measured by using core samples of 1 inch diameter and (1-1.5) inch long by saturation method using gas oil with density=0.82 gm/cc as a saturation liquid. Figure 3-2 shows the schematic diagram of saturation apparatus.

3-2 Statistical Analysis

A correction factor of a value of 0.95 is used as an average correction for the whole porosity values that measured experimentally in order to use these values as reference in evaluating the porosity values that calculated from logs.

We have used statistical analysis between the two variables, the measured porosity from core and the calculated porosity from sonic log, in which the following correlation parameters are calculated:-

1- Average percentage error, APE.

2- Absolute average percentage error, AAPE.

3- Standard deviation error, SD.

The average percentage error was the most investigating used parameter in comparing the performance of various correlation combination, APE, defined as:-

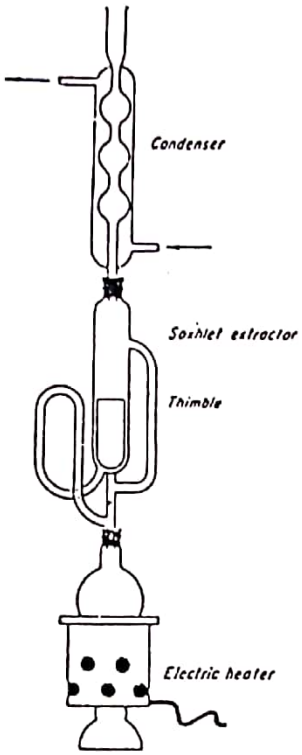

Fig.(3-1) Soxhlet extractor

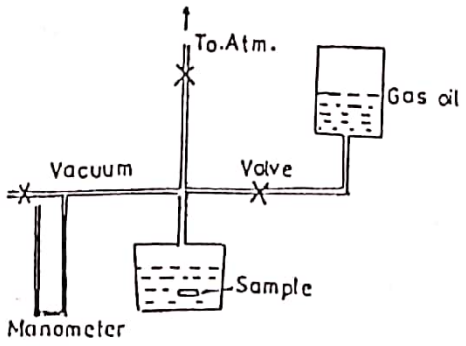

Fig.(3-2) Saturation apparatus

$$(APE)_i = \frac{\phi_{i\ calc} - \phi_{i\ meas}}{\phi_{i\ meas}} * 100 \quad \ldots\ldots\ldots\ldots 3\text{-}1$$

Where

ϕ_{icalc} = calculated porosity in well for ith sandstone layer,

ϕ_{imeas} = measured porosity in well for ith sandstone layer.

The definition of each of these parameters is as follows:-

$$APE = \sum_{i=1}^{n} \frac{(APE)_i}{n} \quad \ldots\ldots\ldots\ldots 3\text{-}2$$

$$AAPE = \sum_{i=1}^{n} \frac{|(APE)_i|}{n} \quad \ldots\ldots\ldots\ldots 3\text{-}3$$

$$SD = \sum_{i=1}^{n} [(APE)_i - APE]^2 / (n-1) \quad \ldots\ldots\ldots\ldots 3\text{-}4$$

(Where n is the number of data points). These parameters are represented graphically in Fig.(3-3).

It should be noted that the magnitude of the average percentage error, APE, will be apparently small when negative errors cancel positive errors. The absolute average percentage errors overcome this cancelling effect by transforming all negative errors to equal magnitude positive errors. Therefore, this parameter is always greater than

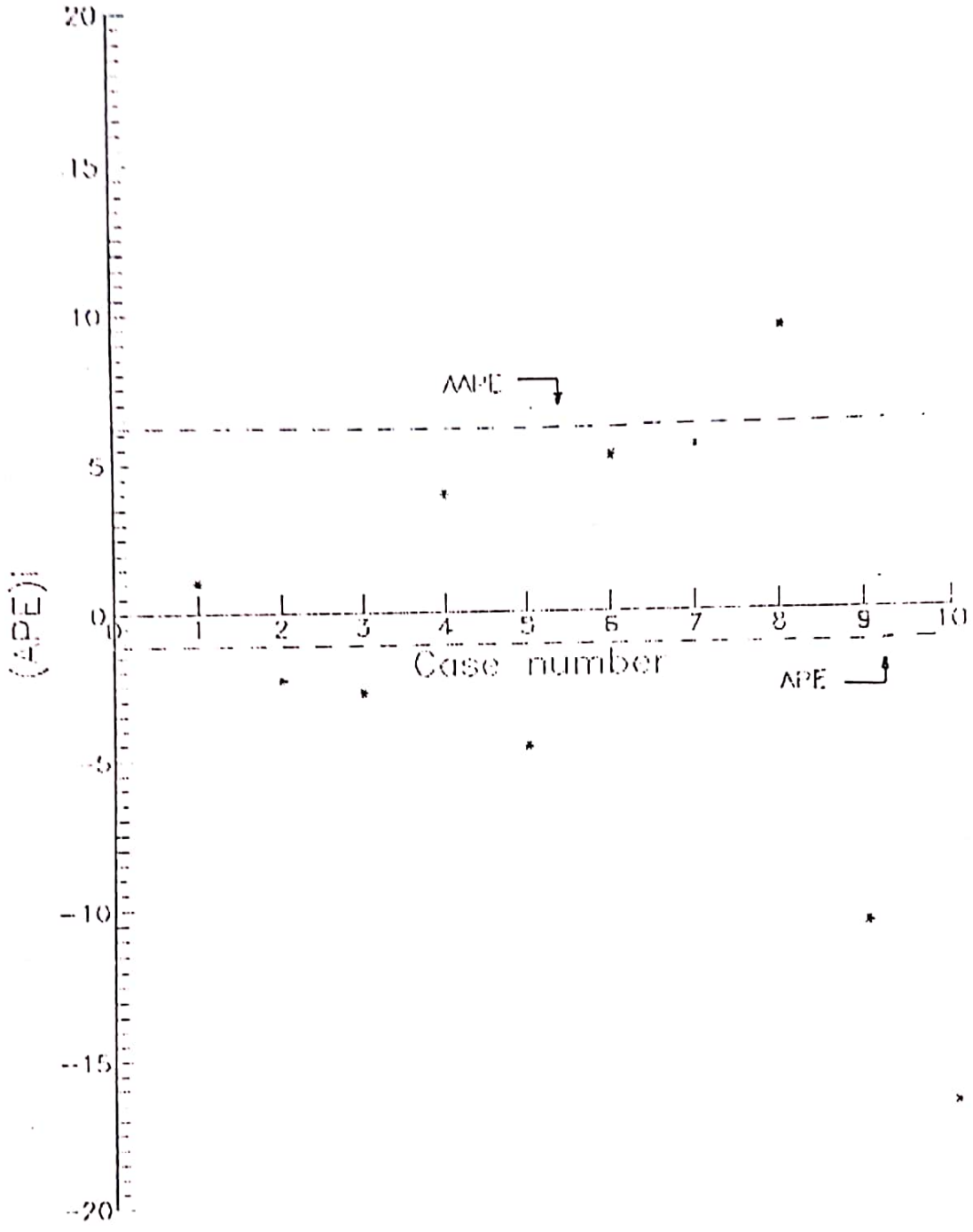

Fig.(3.3) Graphical Representation of statistical parameters.

zero, and it equals zero if -and only if- the error for all cases in the sample is zero(30).

The standard deviation is a measure of the scattering of errors about the average percentage error.

For completeness, regression analysis (simple linear regression) of calculated porosity from cores was performed in order to calculate their correlation coefficient.

The correlation coefficient is defined as:-

$$CF = \frac{\sum_{i=1}^{n} (\phi_{i,calc} - \bar{\phi}_{calc})(\phi_{i,meas} - \bar{\phi}_{meas})}{\sqrt{\sum_{i=1}^{n} (\phi_{i,calc} - \bar{\phi}_{calc})^2 \sum_{i=1}^{n} (\phi_{i,meas} - \bar{\phi}_{meas})^2}} \quad \ldots 3\text{-}5$$

Where:

$\bar{\phi}_{calc}$ = average calculated porosity

$$= \sum_{i=1}^{n} \phi_{i,calc}/n \quad \ldots 3\text{-}6$$

$\bar{\phi}_{meas}$ = average measured porosity

$$= \sum_{i=1}^{n} \phi_{i,meas}/n \quad \ldots 3\text{-}7$$

The correlation coefficient measures the accuracy of the linear relationship between the calculated and measured porosity data. In a linear regression, line of a correlation coefficient of (+1.0) indicates that all data points lie

exactly on the line; conversely a correlation coefficient of (0.0) indicates that no linear relationship exists between the regressed variables[30]. The computer program used in these calculations is given in appendix 'A'.

3-3 Determination of porosity by sonic log

The basic model was used for porosity calculation from sonic log is the time average equation, which is the classical method. This model is discussed below.

3-3-1 Time average equation

The first transformation of the measured sonic transit time into quantitative evaluation of porosity was developed by Wyllie et al.[9] (1956). Since then, this equation was adopted to transform acoustic velocity or transit time to porosity particularly for compact clean sandstone formations[6].

Equation (2-10) is the time average equation defined in terms of velocities.

This equation could be also defined in terms of transit times,

$$\Delta t = \phi \, \Delta t_f + (1-\phi) \, \Delta t_{ma} \qquad \ldots\ldots\ldots\ldots\ldots\ldots\ldots\ldots \quad 3\text{-}8$$

Where Δt, Δt_{ma} and Δt_f are the respective transit times of the sound energy expressed in μsec/ft.

The use of equation (3-8) requires knowledge of matrix and fluid transit times.

In the case of the water bearing zone of Zubair Sand, Δt_{ma}=51.3 μsec/ft (compacted sandstone) and Δt_f=189 μsec/ft (water filled pores) were used (see Table 3-1)[34,7]. These values were adopted considering clean sandstone in the intervals selected. This equation is derived to describe the transit time of sound wave through the matrix and pore fluids. Hence, in the existence of any shale within the rock, the derived porosity from the equation must be corrected for the shale content by using the following empirical equation developed by Texier et al.[7] (1959), which was widely accepted in sonic log interpretation:-

$$\phi_{sc} = \phi_s * \frac{1}{2-\alpha} \qquad \text{..... 3-9}$$

Where:

ϕ_{sc} = Corrected porosity for shale content,

ϕ_s = Derived porosity from Wyllie equation, and

α = Shale indicator (α = 1-V_{sh}).

This correction was applied on all log intervals selected, after the porosity values of those intervals have been calculated using the time average equation. A graphical representation of these values versus those derived from cores at corresponding depths is shown in Fig.(3-4), in which the following correlation parameters (using the statistical and regression program) were calculated.

SD	AAPE	APE	CF
12.511	11.576	-11.555	0.922

It is obvious from these high percentages errors, that time average equation gives unsatisfactory results when it is used for porosity determination of Zubair formation-East Baghdad oil field.

Comparison plots have been also prepared in Figs. (4-26c) through (4-31c), in which, the calculated porosity values using Wyllie equation and those measured from cores are plotted versus depths.

It is indicated, through these figures, that an obvious distinction between the porosity values measured from core samples and those calculated from sonic log (using time average equation) is occured.

Table (3-1)

Values of sonic velocity and transit time for common rock matrix, materials and casing.

Medium	V_{ma} (ft/sec)	Δt_{ma} (μsec/ft)
Sandstone	18000-19500	55.5-51.3
Limestone	21000-23000	47.6-43.5
Dolomite	23000	43.5
Anhydrite	20000	50.0
Salt	15000	66.7
Casing (iron)	17500	57.0
Air (atm. pressure)	1100	909
Water	5300	189
Oil	4200	238

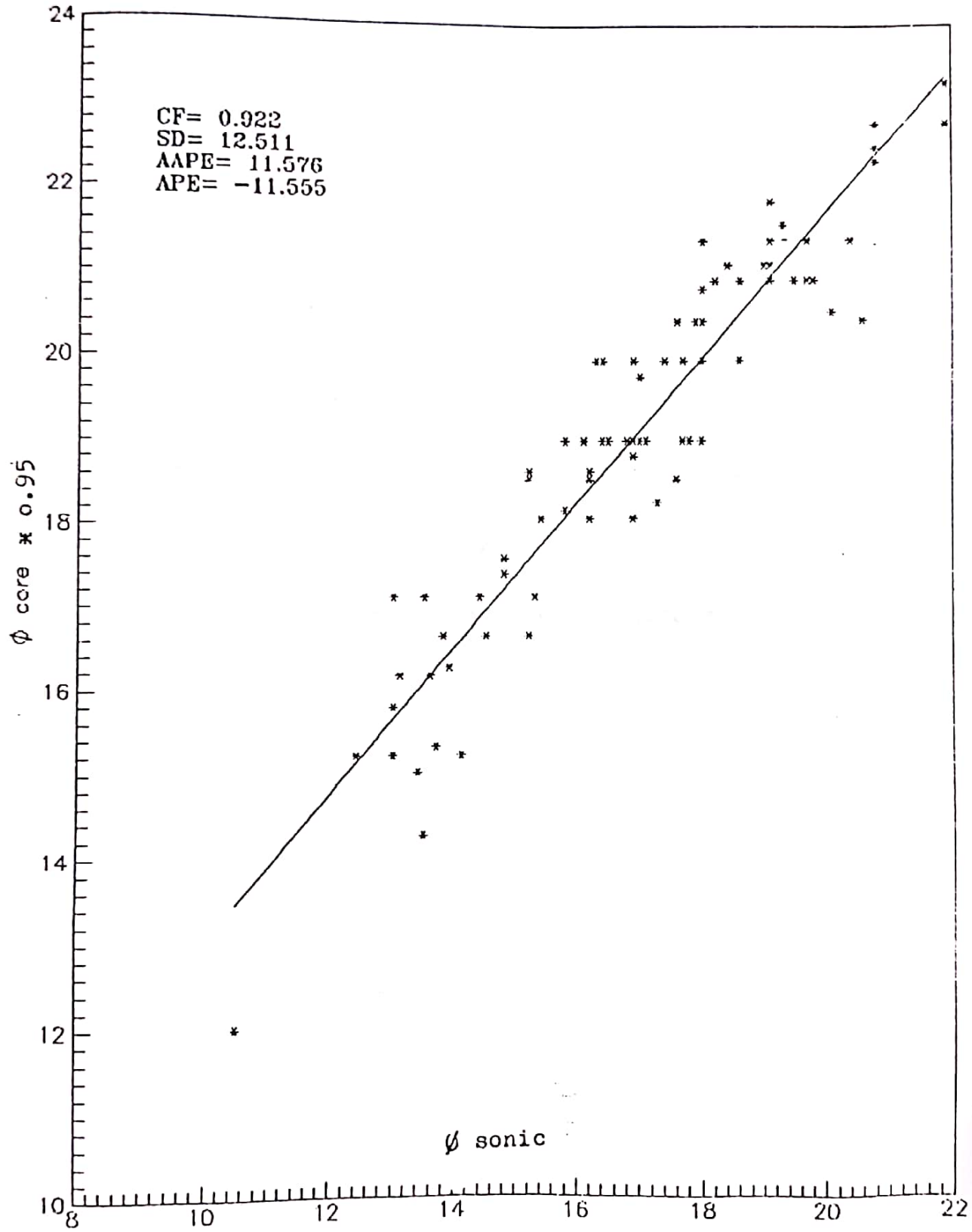

Fig.(3-4) Plot of Øcore vs. Øsonic (using Wyllie equation) for the Wells of Zubair formation-East Baghdad field.

CHAPTER FOUR

DETERMINATION OF POROSITY

BY

RADIOACTIVE LOGS

In this chapter, the available radioactivity logs (Neutron, Density & Gamma Ray) will be used for calculating porosity. Since shale affects every logging measurements, porosity values calculated from these logs need to be corrected for shaliness.

Radioactive logs will be used, in addition to porosity determination in a given interval, as shale indicators for that interval, as described below.

4-1 Determination of shale volume

The shale volume (V_{sh}) for each chosen interval was determined by using Gamma Ray, Neutron and Density logs.

Gamma Ray log was used as a single shale indicator, by the following basic relationship:-

$$V_{sh} = \frac{GR - GR_{min}}{GR_{max} - GR_{min}} \qquad \ldots\ldots\ldots\ldots\ldots\ldots\ldots\ldots 4\text{-}1$$

Where:

GR_{min} = Radioactivity reading in clean formations,

GR_{max} = Radioactivity reading in shale formations, and

GR = Radioactivity reading from log.

Neutron and Density logs were used in combinations through crossplot techniques.

In fact, two types of Gamma Ray curves are available, the first is the standard (total) Gamma Ray curve (SGR), in which the reading represents a linear combination of Potassium, Thorium and Uranium amounts, as defined by the following equation[28]:-

$$SGR = ATh + BU + CK \quad \ldots\ldots\ldots\ldots\ldots\ldots\ldots\ldots \quad 4\text{-}2$$

Where A,B,C are coefficients obtained from a special test procedure of the log tool.

The second type is the corrected Gamma Ray curve, CGR, in which, a Uranium free measurement is recorded. It is simply a linear combination of Gamma Rays from thorium and potassium only, as defined by the following equation:-

$$CGR = ATh + CK \quad \ldots\ldots\ldots\ldots\ldots\ldots\ldots\ldots \quad 4\text{-}3$$

Because of the existence of Uranium in association with radioactive minerals other than those found in shale, such as organic materials, the corrected Gamma Ray log is believed to be a better shale indicator, and was used for determining shale volume for each interval by using Eq.(4-1), however, the 'CGR' log was not available in all the wells investigated, therefore, the data of 'SGR' log taken for sand bodies in wells where 'CGR' log is recorded (EB-55, EB-56, EB-77, EB-79), at depths of those missing 'CGR' log in Wells (EB-18, EB-15) are used in the regression

program to give a linear relationships that can be used to determine CGR values from SGR log data, as shown in Figs. (4-1) through (4-8), in which, a straight line equation and correlation coefficient for each sand body of missing 'CGR' log wells are determined.

'CGR' and 'SGR' logs data are replotted together, as shown in Fig.(4-9) to give a single general equation of its representative line, which can be applied to each interval of Zubair formation.

As it was mentioned earlier, the Neutron and Density logs are used in combinations through the technique of cross plot to determine shale volume. In this technique the triangle method[31] was used.

The use of more than one shale indicator is recommended, as the calculated shale volume from any one method can often be overestimated[26]. Therefore, the lowest calculated value of the three methods was used in the correction of porosity derived from logs.

4-2 Determination of porosity

Neutron and density logs were used as single indicators and in combinations to determine porosity value for each chosen interval, as described below:-

4-2-1 Single porosity indicator

Through the recorded densities, the density log was used as a single porosity indicator to determine the

porosity for intervals with no shale content using the following basic equation[32]:-

$$\phi_D = \frac{\rho_{ma} - \rho_b}{\rho_{ma} - \rho_f} \quad \ldots\ldots\ldots\ldots\ldots\ldots\ldots\ldots \quad 4\text{-}4$$

Where:

ρ_b = Formation bulk density, gm/cc,

ρ_{ma}= Matrix density, gm/cc, and

ρ_f = Fluid density, gm/cc.

For intervals containing shale, the following equation was used[33]:-

$$\rho_b = \phi_D \rho_f + (V_{sh}) \rho_{sh} + (1-\phi_D-V_{sh}) \rho_{ma} \quad \ldots\ldots\ldots \quad 4\text{-}5$$

Where,

ρ_{sh} is density reading in shale section, gm/cc.

In the use of the previous equation, we have to select matrix and fluid densities. According to our case (water saturated sand stone intervals), 2.65 gm/cc can be adopted as matrix density and 1.0 gm/cc as pore-filling fluid density, as shown in Table (4-1), in which, densities from density log and actual densities of most common materials encountered in formations are tabulated[34].

Table (4-1)

Actual density and 'FDC' derived porosity for different materials commonly encountered in boreholes.

	Formula	Actual density	FDC density
Quartz	SiO_2	2.654	2.648
Calcite	$CaCO_3$	2.710	2.710
Dolomite	$CaCO_3MgCO_3$	2.870	2.876
Anhydrite	$CaSO_4$	2.960	2.977
Sylvite	KCl	1.984	1.863
Halite	NaCl	2.165	2.032
Gypsum	$CaSO_4 2H_2O$	2.300	2.351
Fresh water	H_2O	1.000	1.000
Salt water	200,000 ppm	1.146	1.135
Oil	n (CH_2)	0.850	0.85
Gas	$C_{1.1}H_{4.2}$	ρ_g	$1.325\rho_g - 0.188$

Neutron log was also used as a single shale indicator for porosity determination.

The porosity value of each chosen interval was calculated from neutron log by directly reading its response. To use this value of porosity for comparison with that calculated from other logs, it should be corrected for shale content by using the following basic equation:-

$$\phi_{sc} = \phi_N + \phi_{Nsh} \cdot V_{sh} \quad \ldots\ldots\ldots\ldots\ldots\ldots\ldots \quad 4\text{-}6$$

Where:

$\emptyset_{Nsh}$ = Measured porosity from Neutron log in the shale section, and

Vsh = Shale volume, %.

4-2-2 Two-curves porosity indicator

Through this phase of work, neutron and density data were used to determine porosity employing the crossplot technique.

In this technique the triangle method was used, in which, the derived porosity values ($\emptyset_N$) from neutron log were plotted versus the derived density values at the same depths, for each well, as shown in Figs.(4-10) through (4-15).

According to the two manners of using the Neutron and Density logs in porosity determination, there will be three porosity values obtained for each chosen interval.

These three values were plotted versus the corresponding core porosity as shown in Figs.(4-16) through (4-18), in which, correlation coefficient, standard deviation error, average percentage error and absolute average percentage error for each of them were calculated, as shown in Table (4-2).

The calculated results of log porosities obtained by the three approaches are compared with the corresponding core porosity as shown in Figs.(4-19) through (4-24), for the six wells:

- Figures 26a to 31a for porosity values derived from Neutron log.
- Figures 26b to 31b for porosity value determined by (ϕ_N-ρ_b) crossplot (using triangle method)
- Figures 26d to 31d for porosity values derived from density log.

Table (4-2)

Correlation parameters for Neutron and Density logs as single indicators and in combinations

Method	APE	AAPE	SD	CF
Neutron log	1.699	4.870	6.853	0.906
Density log	1.262	5.048	7.4931	0.883
ϕ_N-ρ_b crossplot (using triangle method)	2.276	4.591	6.244	0.923
ϕ_N-ρ_b crossplot (using published chart)	13.096	13.096	14.739	0.884

Through its lowest percentage errors and highest correlation coefficient, as seen from Table (4-2), the ϕ_N-ρ_b crossplot (using triangle method) is the best method that can be used for more accurate determination of porosity than other methods for Zubair formation-East Baghdad oil field.

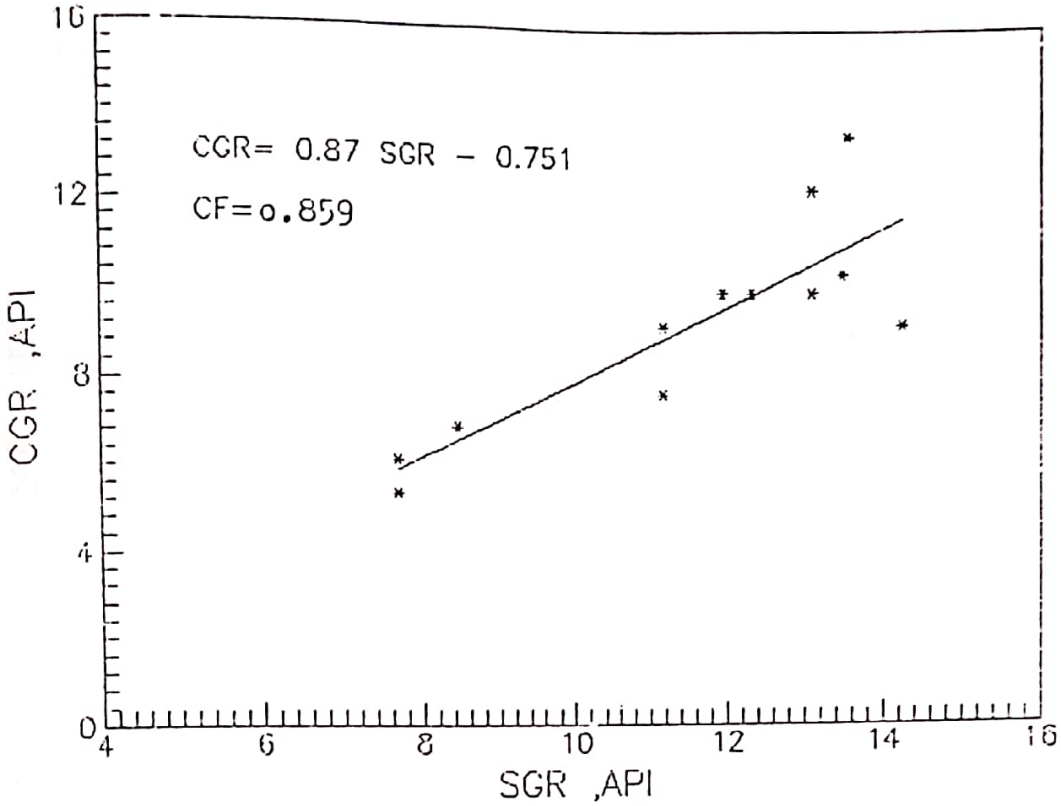

Fig.(4 - 1) Corrected gamma ray-Standard gamma ray relationship for sand body No. 1 .

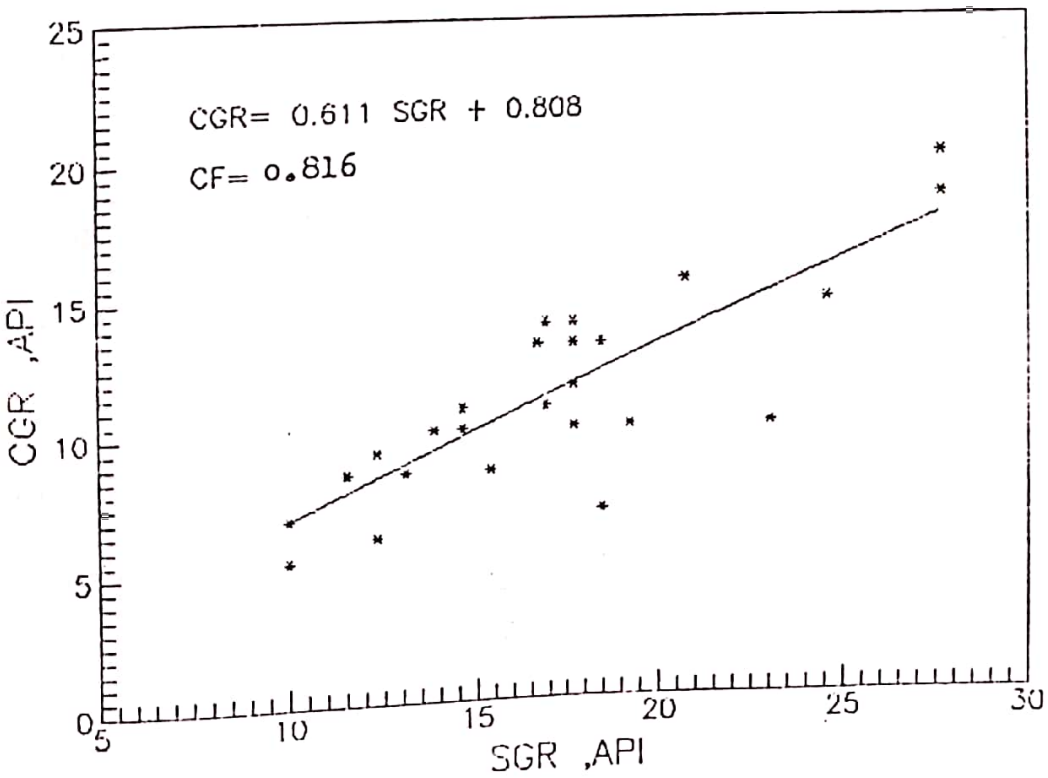

Fig.(4 - 2) Corrected gamma ray-Standard gamma ray relationship for sand body No. 2 .

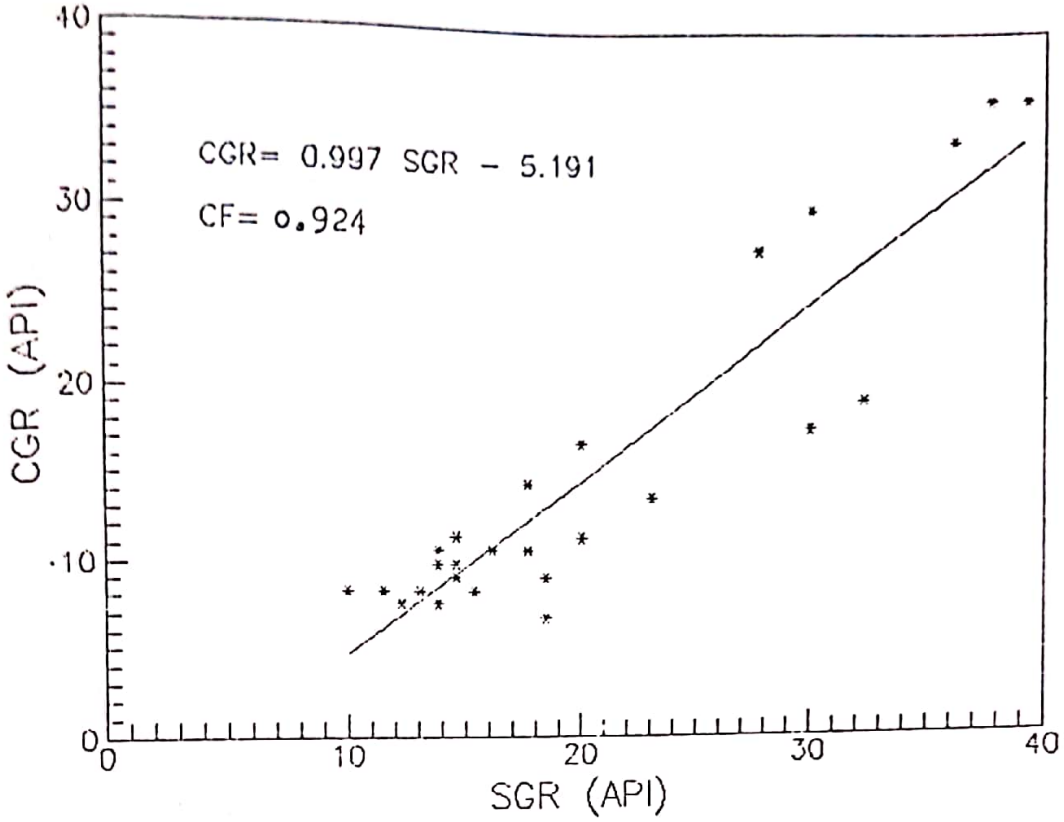

Fig.(4 - 3) Corrected gamma ray-Standard gamma ray relationship for sand body No. 3 .

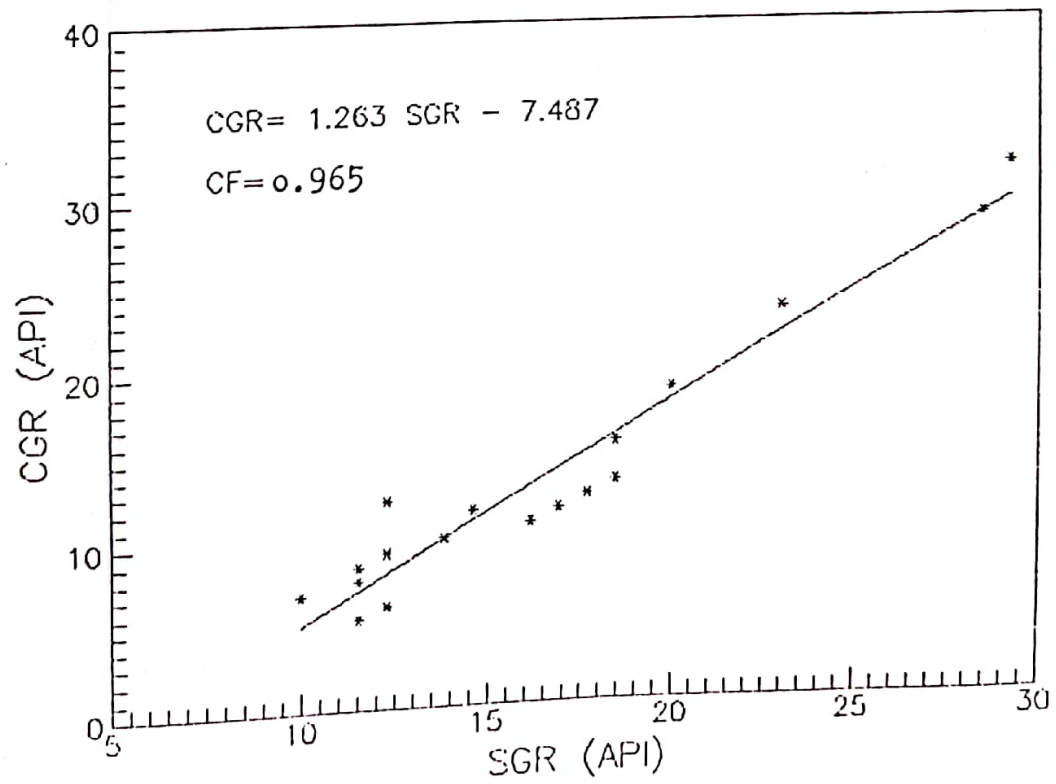

Fig.(4 - 4) Corrected gamma ray-Standard gamma ray relationship for sand body No. 4 .

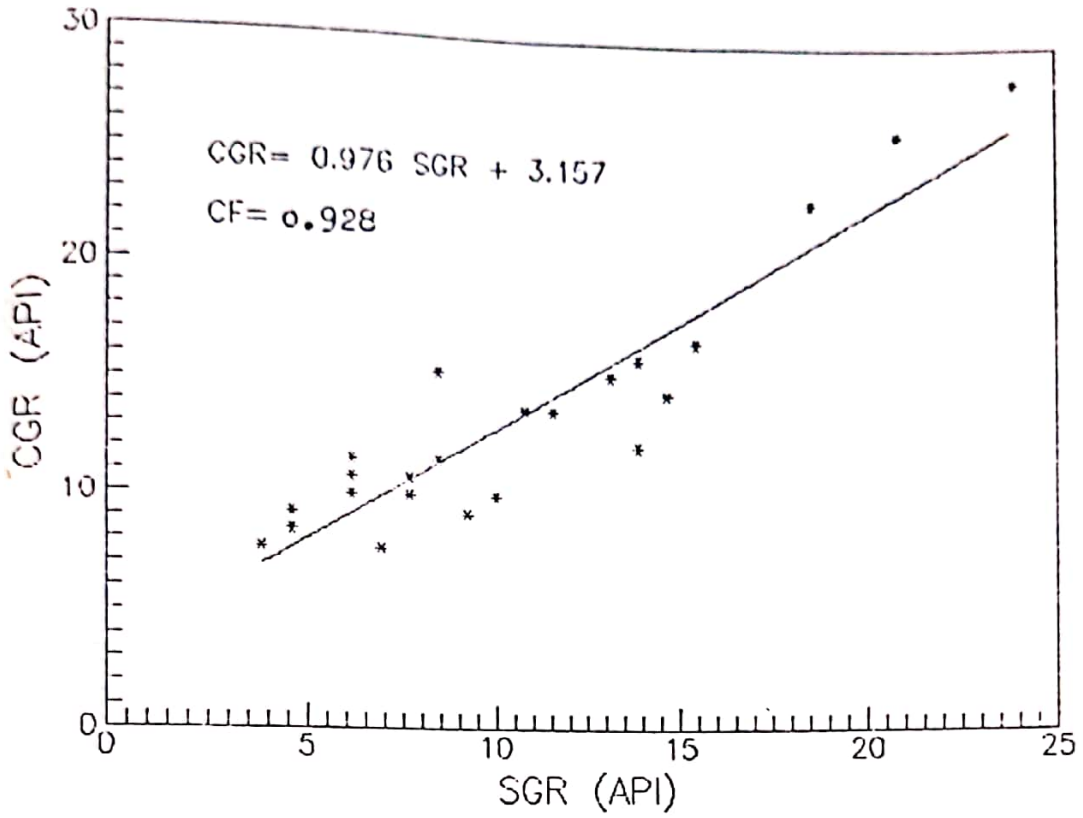

Fig.(4 -5) Corrected gamma ray-Standard gamma ray relationship for sand body No. 5 .

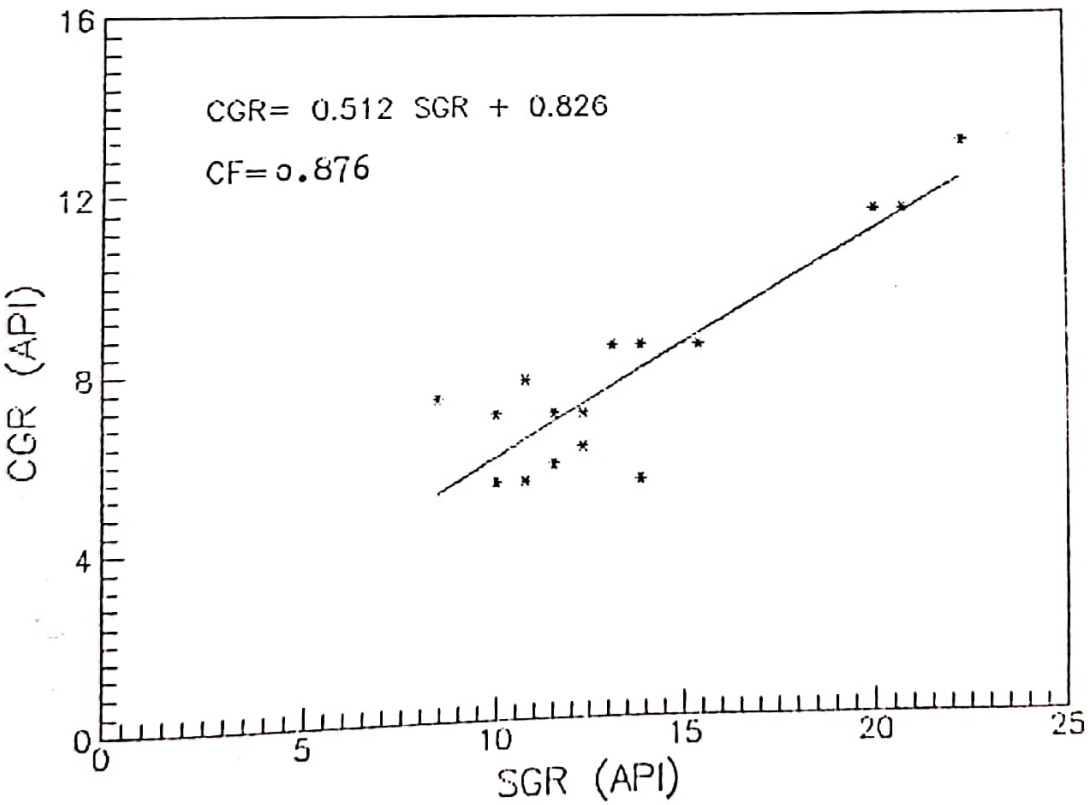

Fig.(4 - 6) Corrected gamma ray-Standard gamma ray relationship for sand body No. 6 .

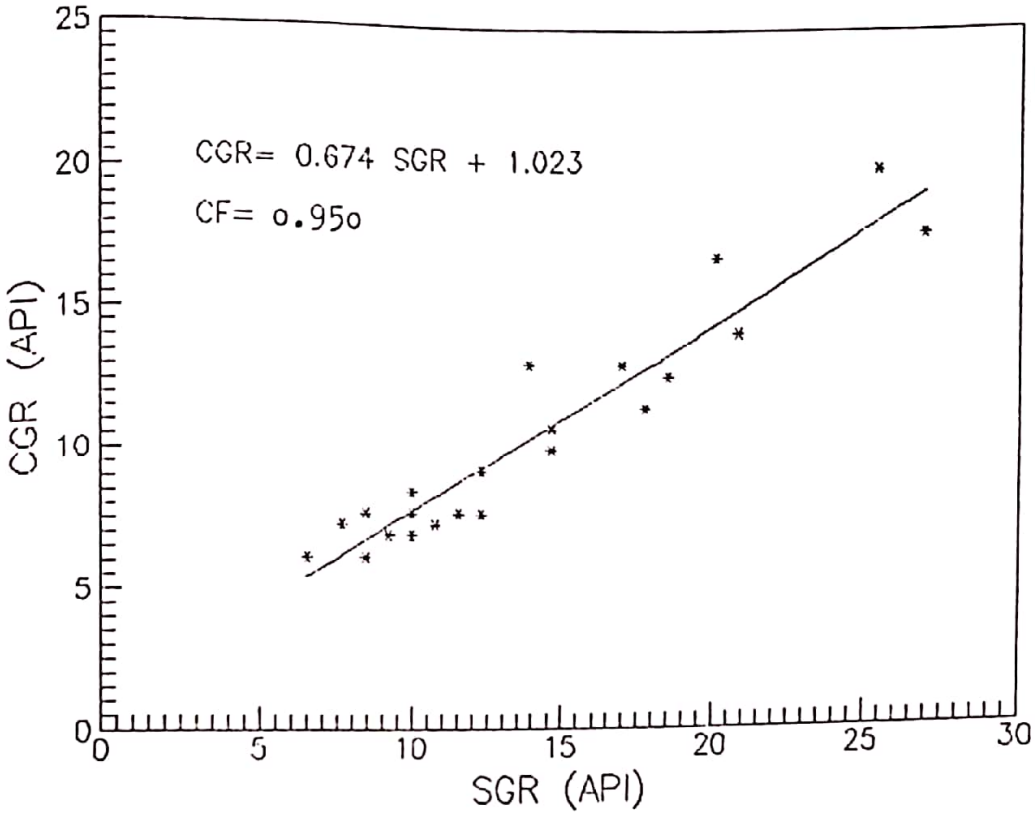

Fig.(4 - 7) Corrected gamma ray–Standard gamma ray relationship for sand body No. 7 .

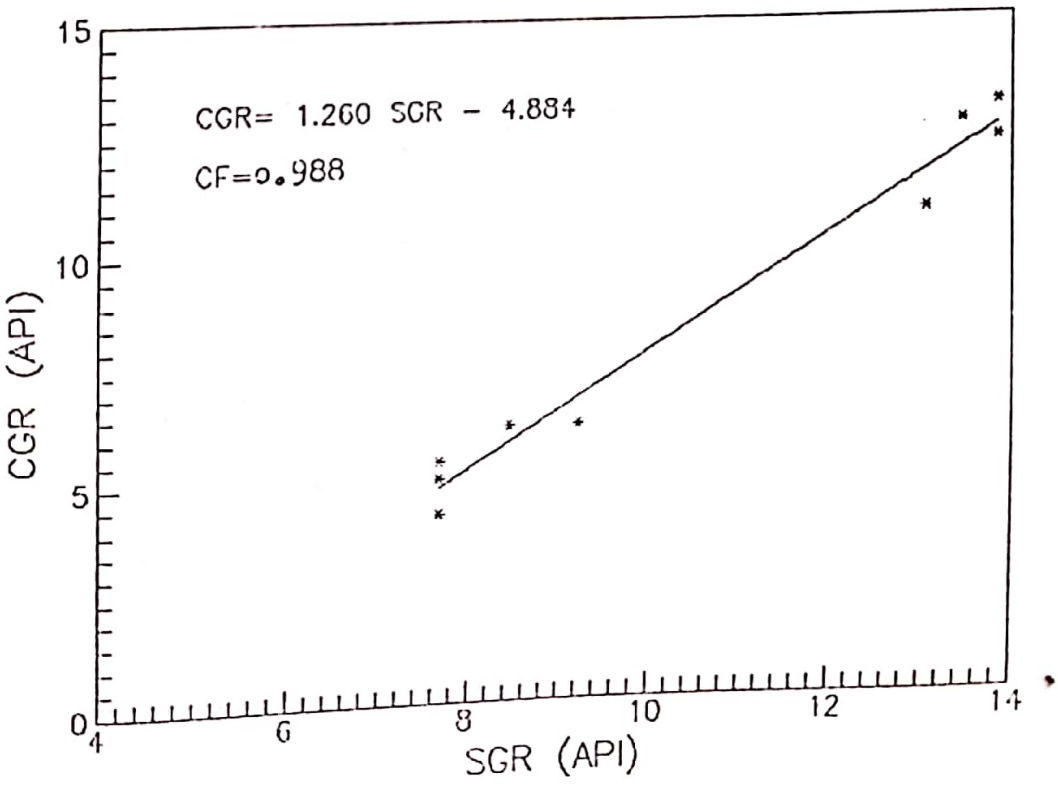

Fig.(4 - 8) Corrected gamma ray–Standard gamma ray relationship for sand body No. 8 .

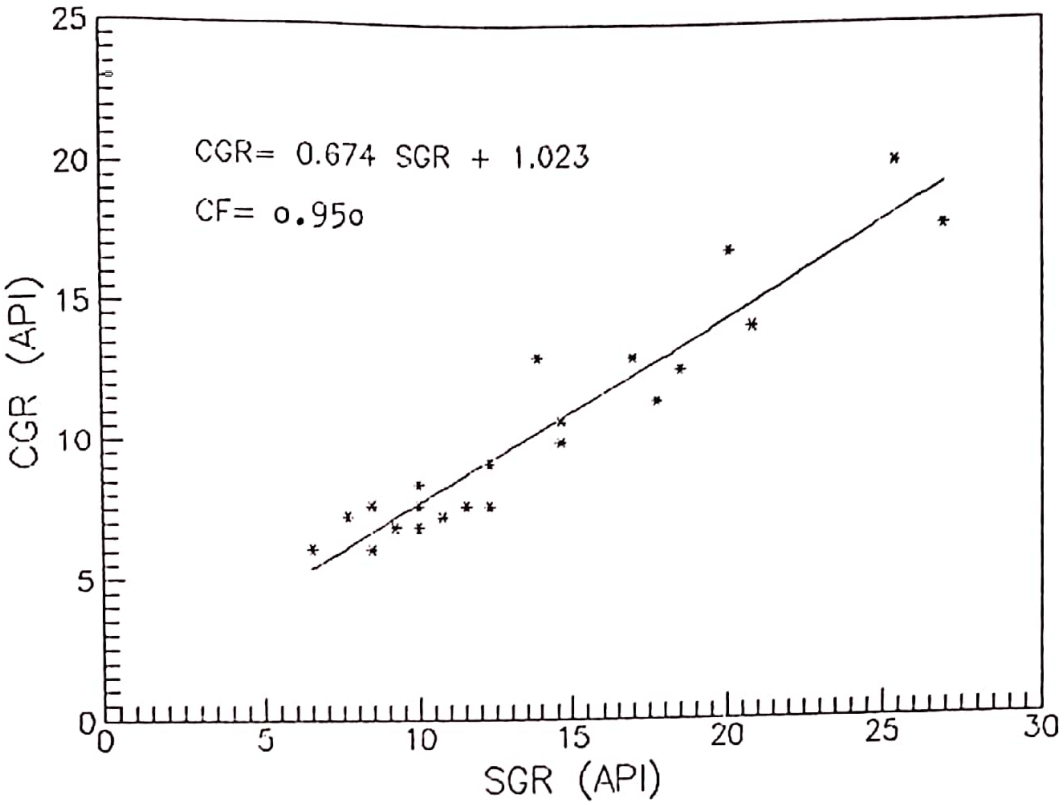

Fig.(4 - 7) Corrected gamma ray–Standard gamma ray relationship for sand body No. 7 .

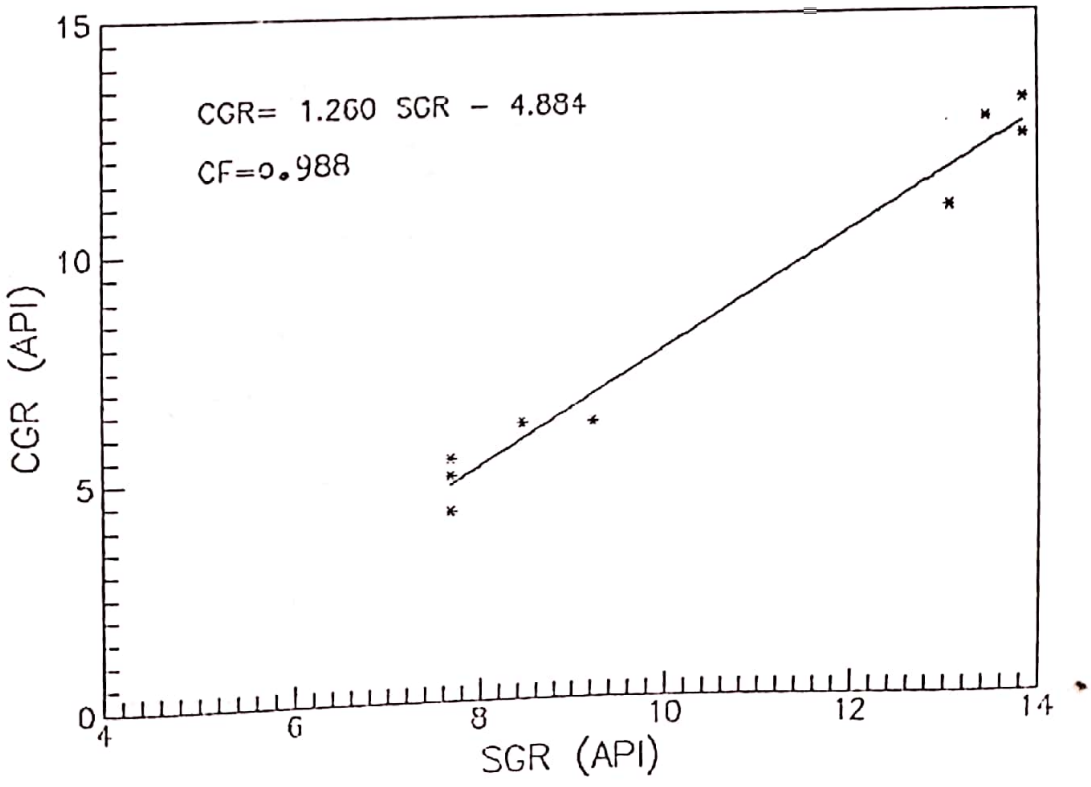

Fig.(4 - 8) Corrected gamma ray–Standard gamma ray relationship for sand body No. 8 .

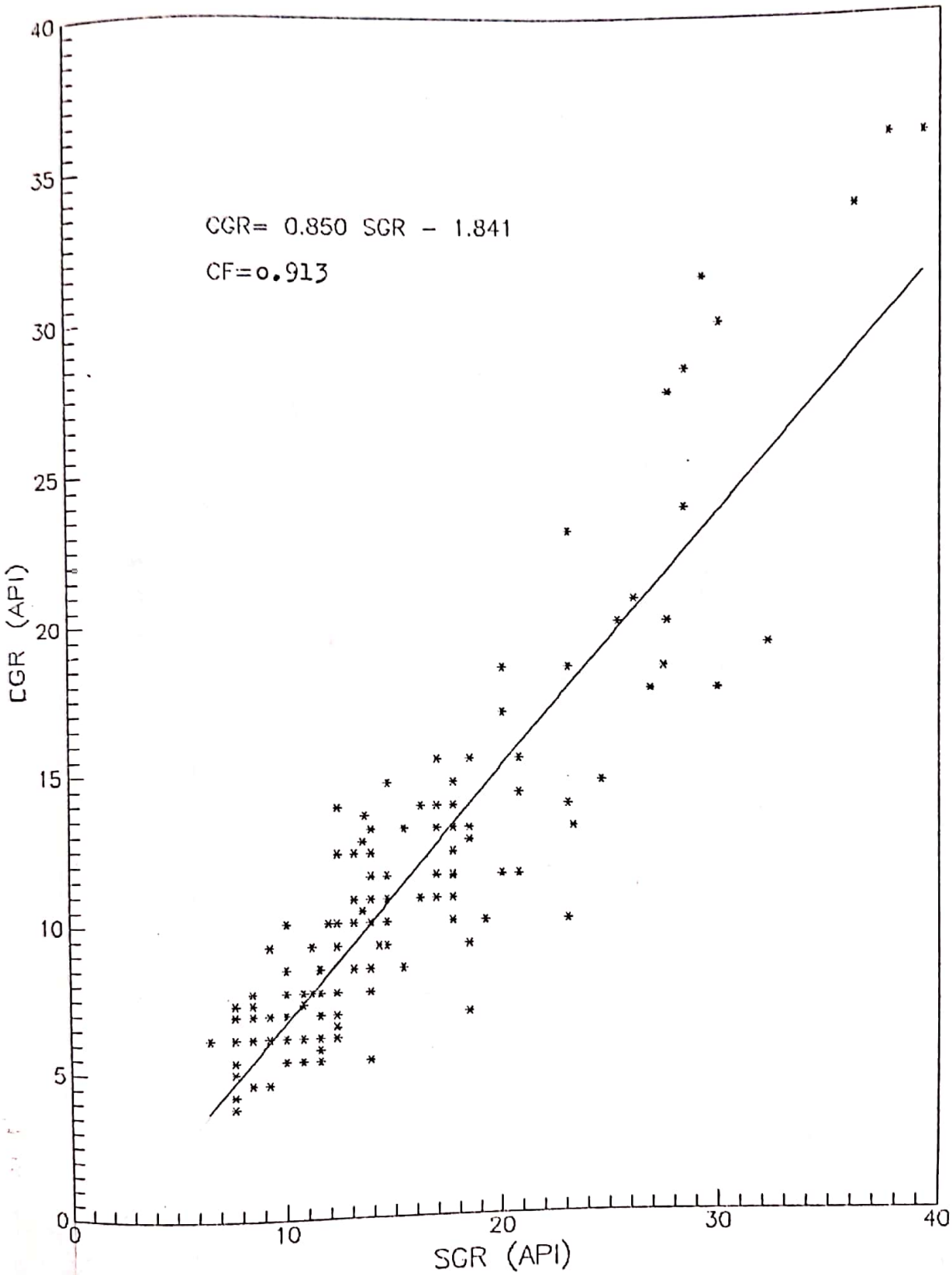

Fig.(4- 9) Corrected gamma ray–Standard gamma ray relationship for the sand bodies of Zubair Formation.

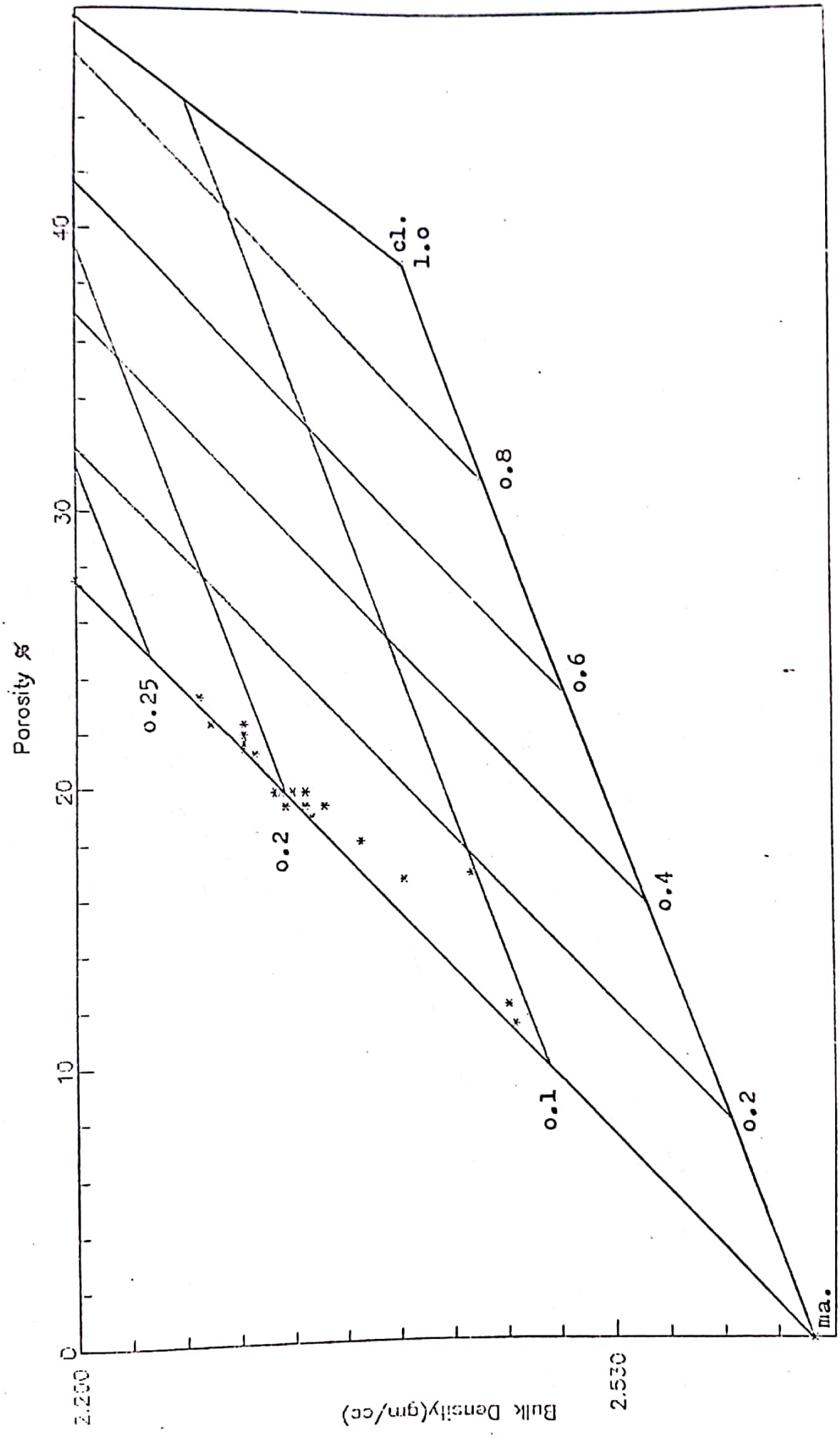

Fig.(4-1a) Bulk density-Øneutron cross plot of Well No.(FB-55).

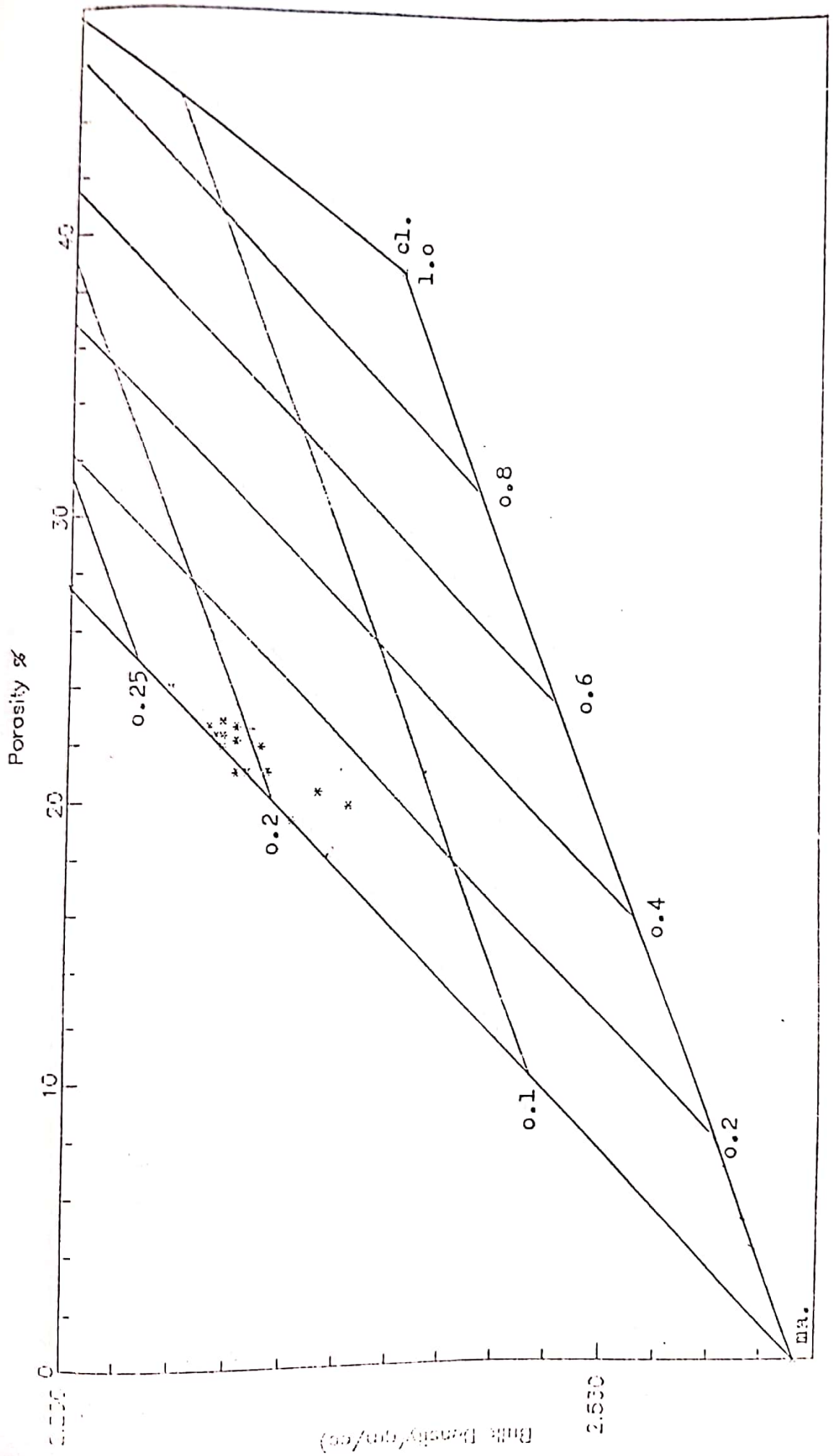

Fig.(4-11) Bulk density-Sheutron cross plot of Well No.(IE 50).

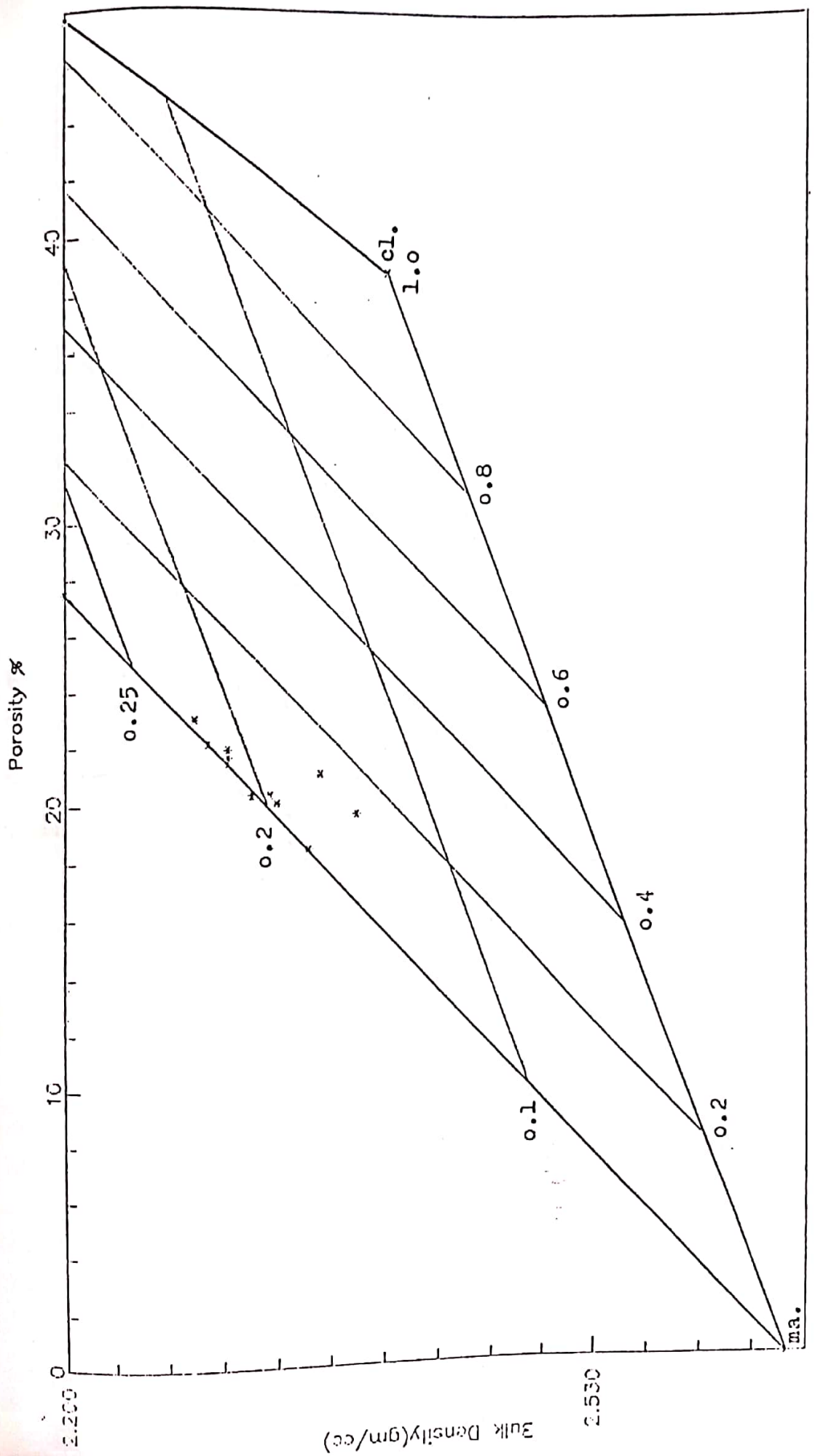

Fig.(4-12) Bulk density–ϕneutron cross plot of Well No.(EB-79).

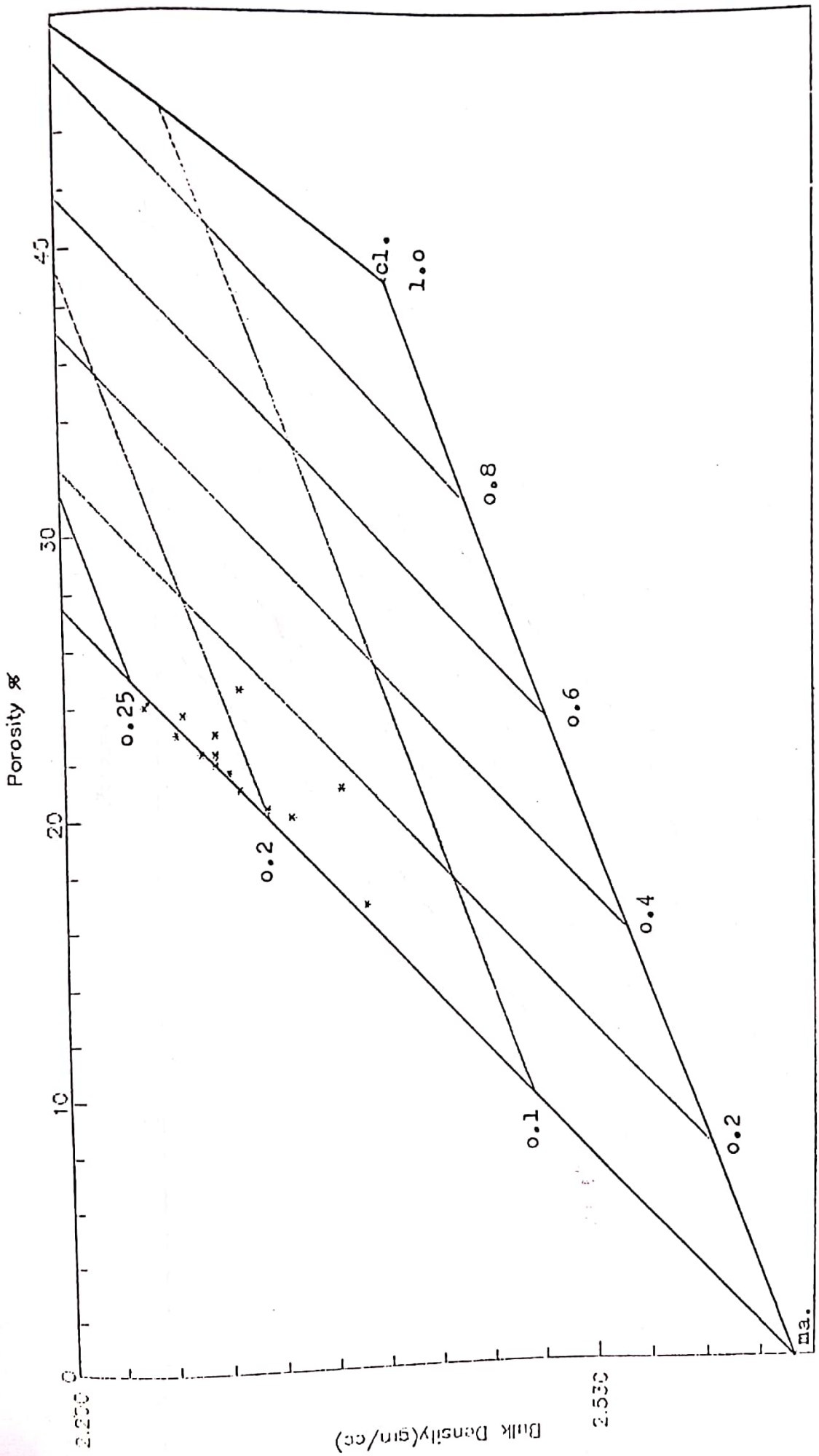

Fig.(4-13) Bulk density-Øneutron cross plot of Well No.(EB-77).

Fig.(4-1.4) Bulk density-Øneutron cross plot of Well No.(EB-15).

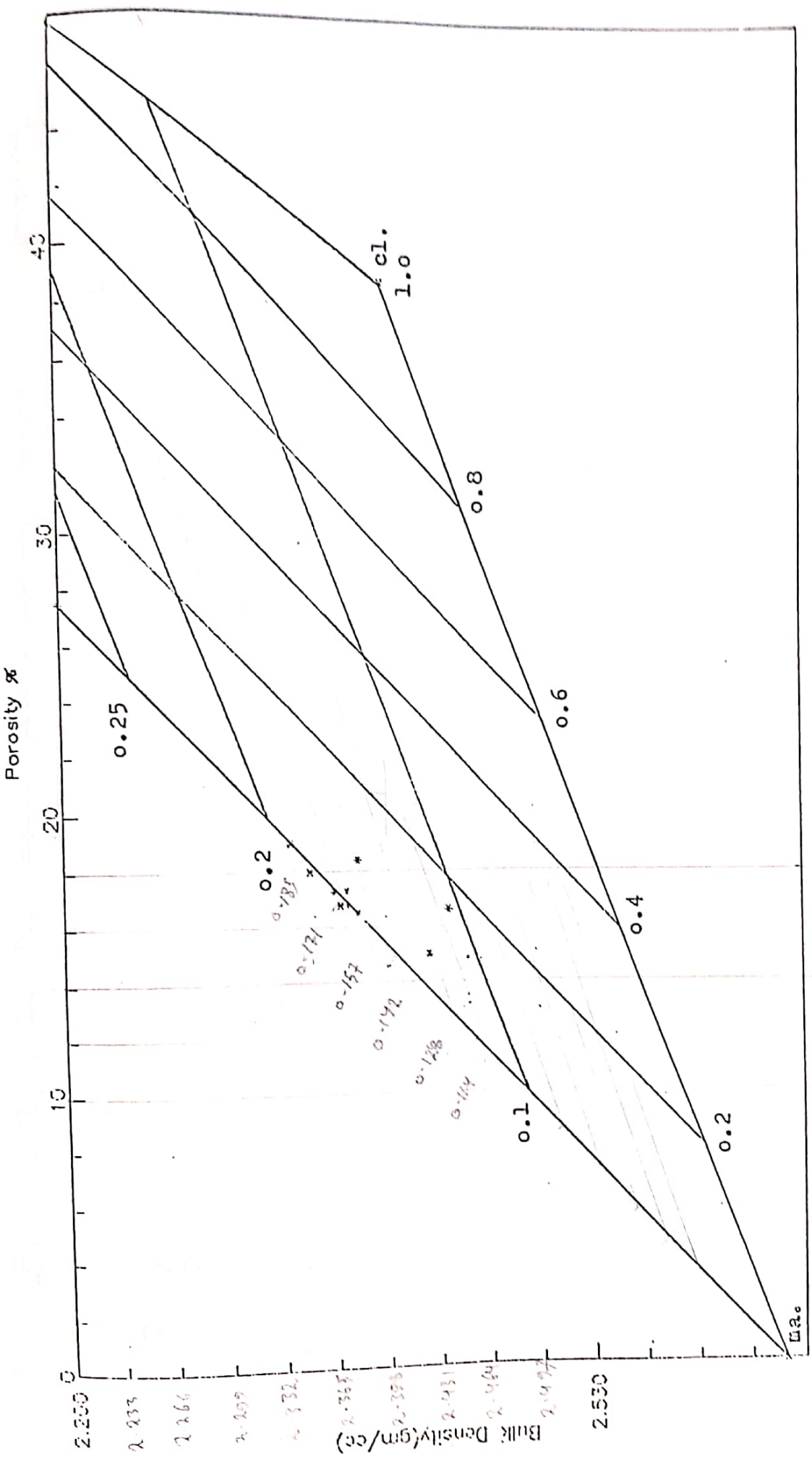

Fig.(4 – 15) Bulk density–Øneutron cross plot of Well No.(EB–18).

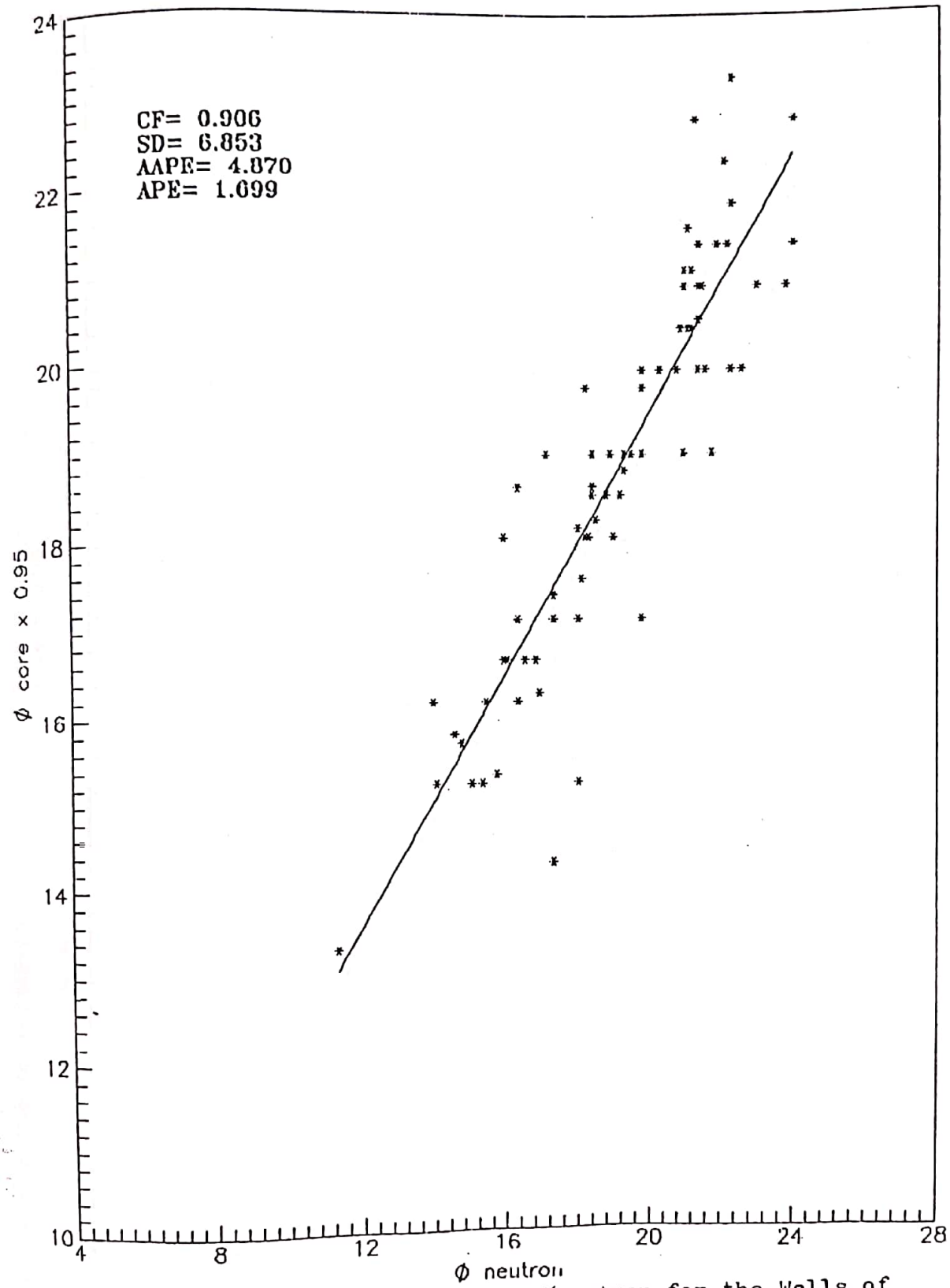

Fig.(4-I6) Plot of ϕcore vs. ϕneutron for the Wells of Zubair formation-East Baghdad field.

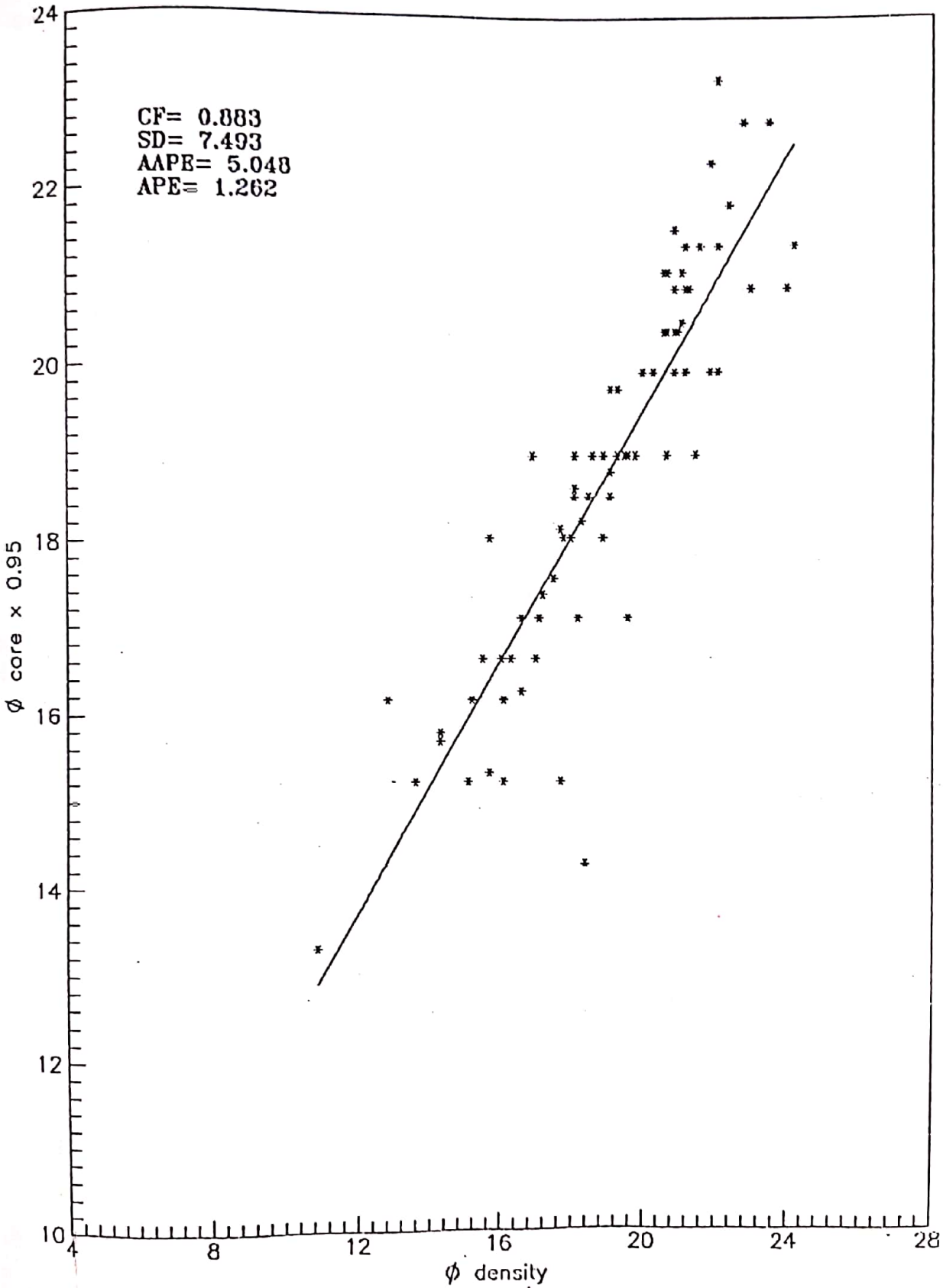

Fig.(4-17) Plot of Øcore vs. Ødensity for the Wells of Zubair formation-East Baghdad field.

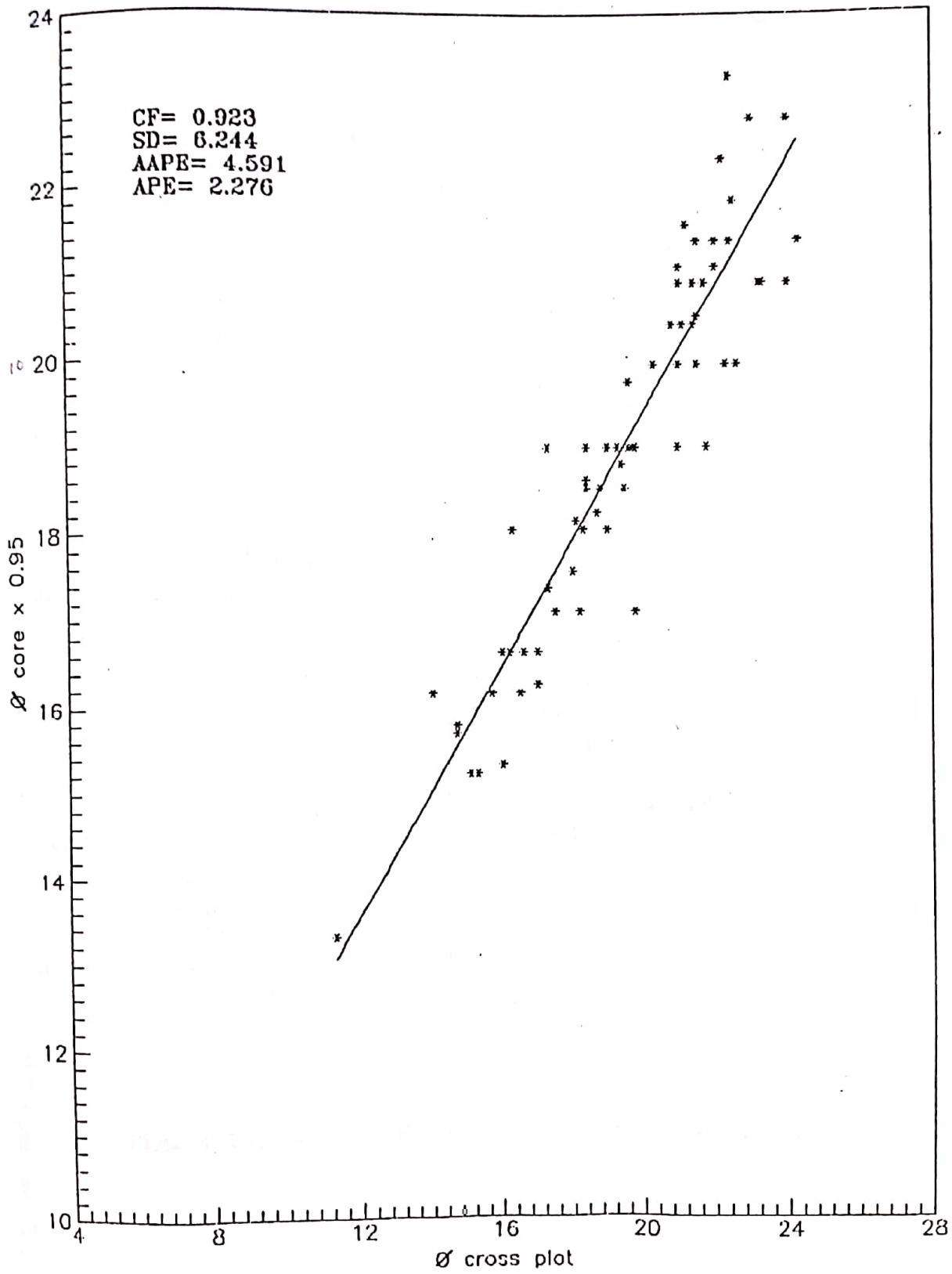

Fig.(4-I8) Plot of Øcore vs. Øcrossplot for the Wells of Zubair formation-East Baghdad field.

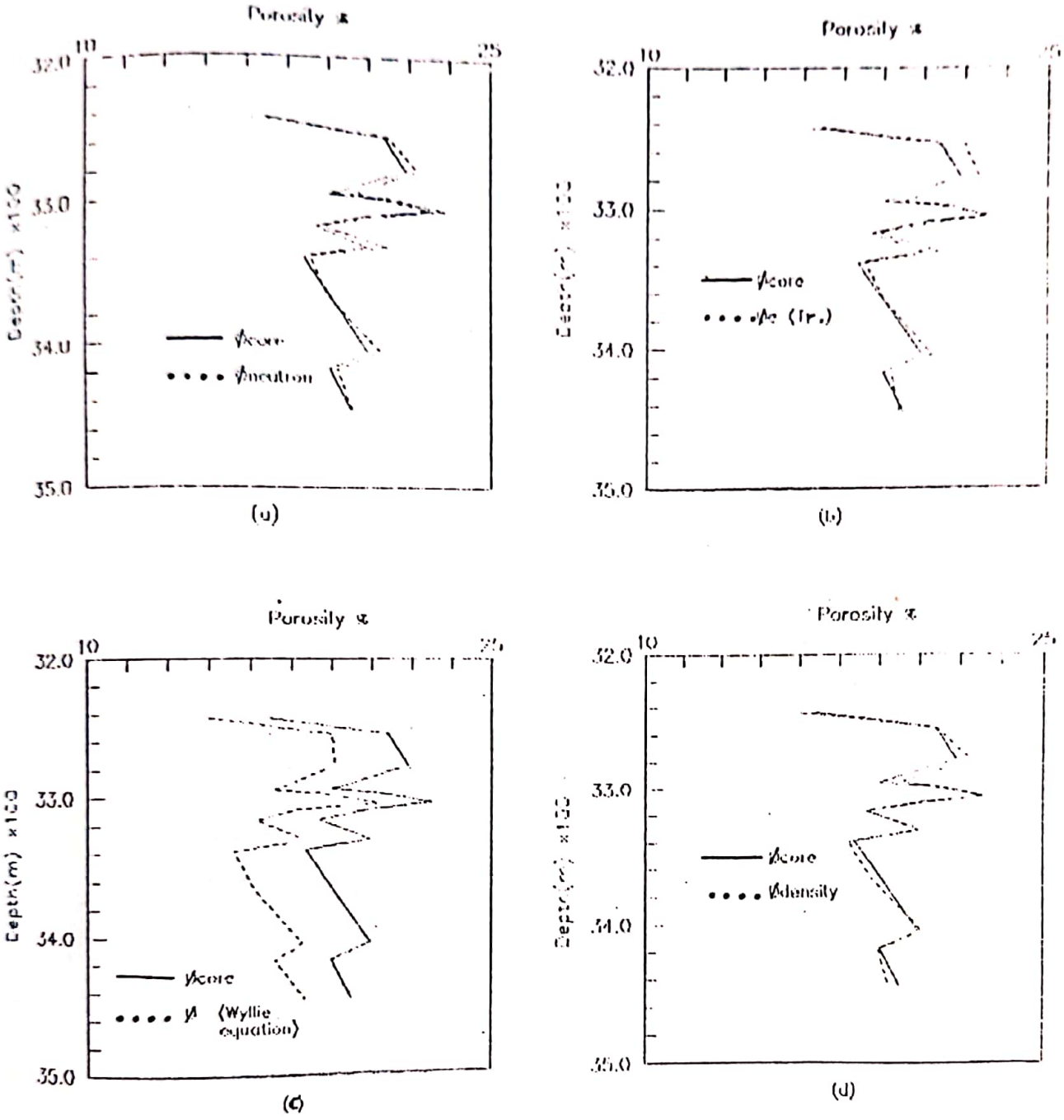

Fig.(4-I9) Øcore - Ølog comparisons for Well No.(EB-55).

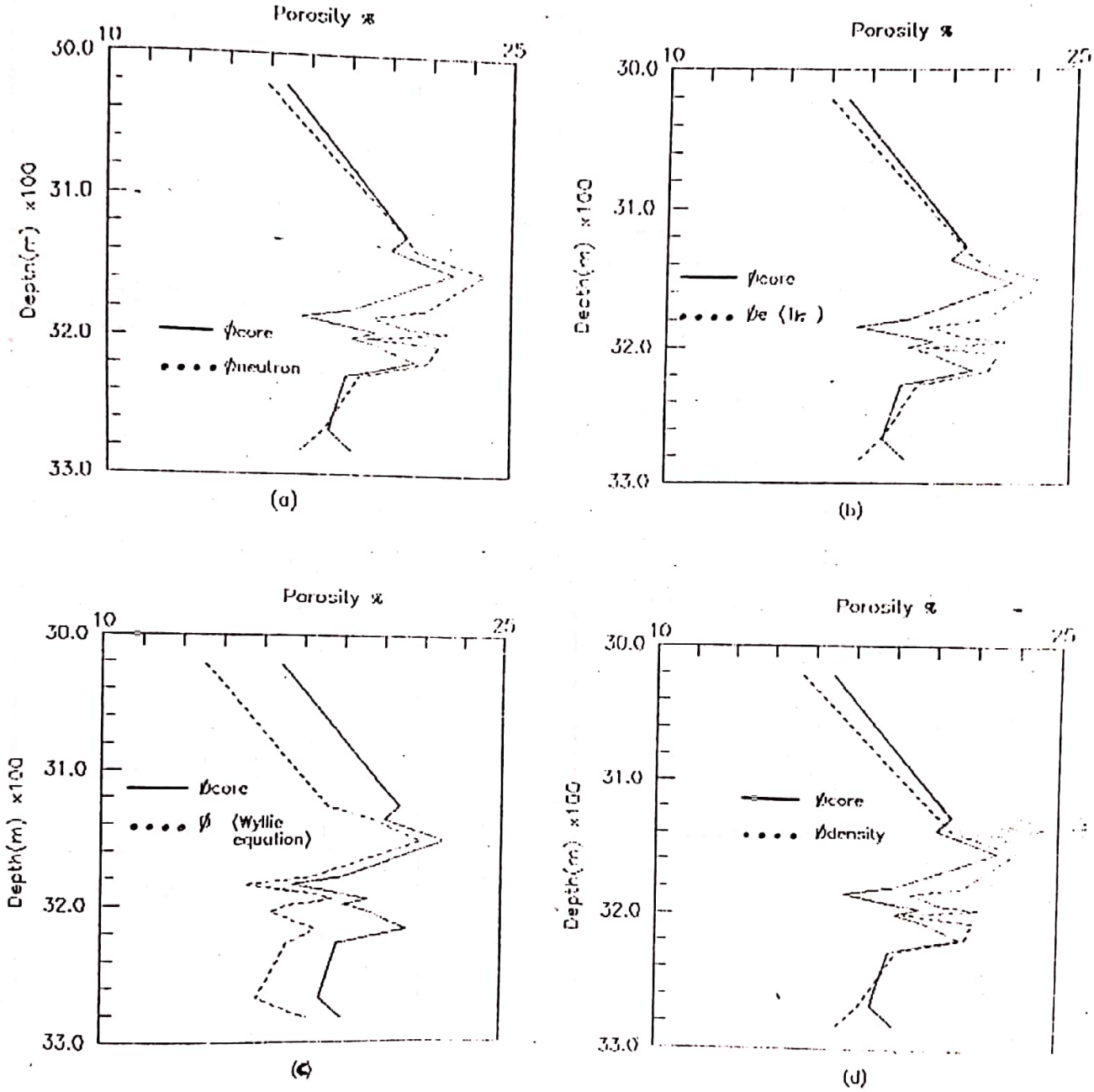

Fig.(4-2o) Øcore - Ølog comparisons for Well No.(EB-56).

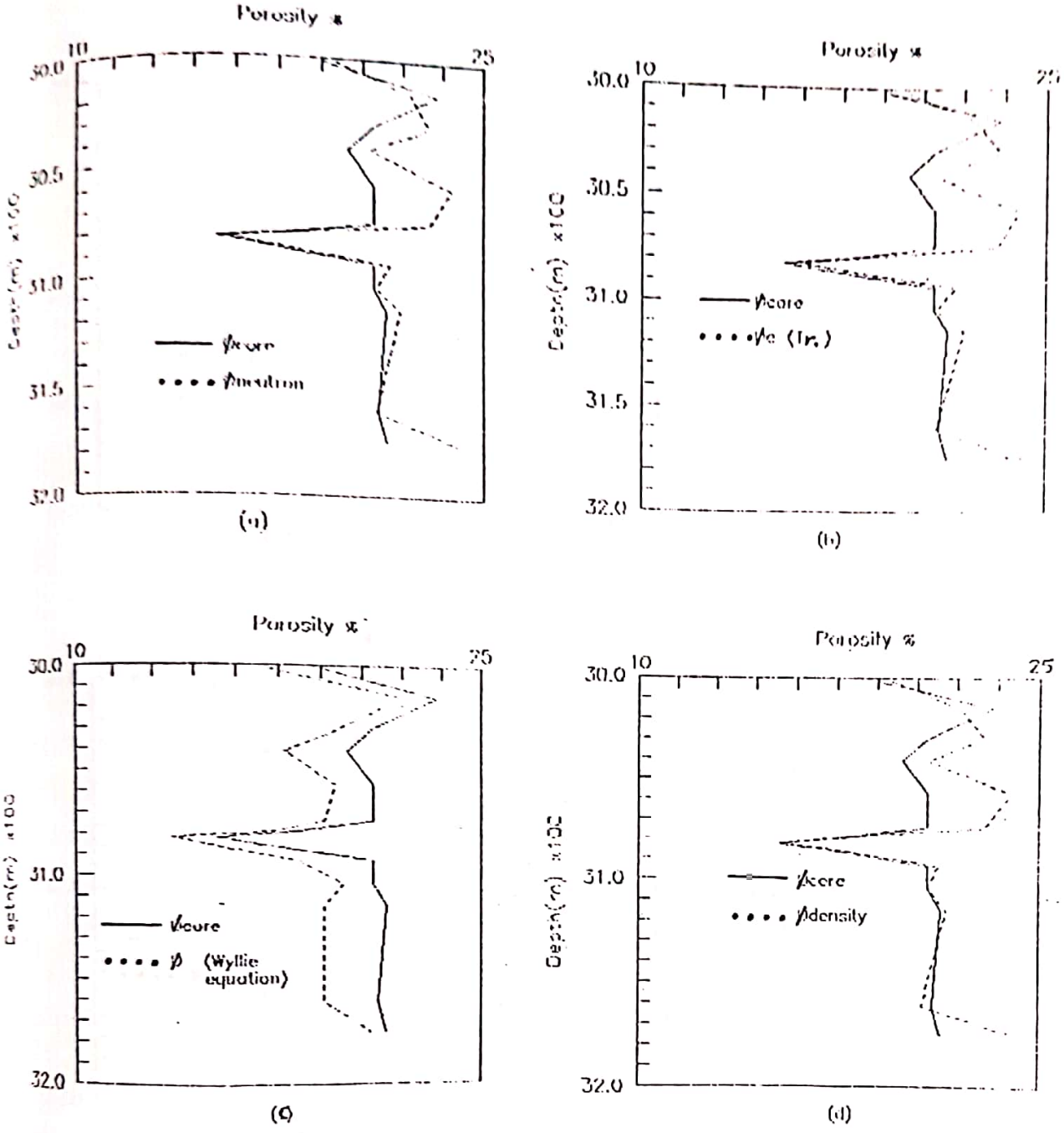

Fig.(4-2I) Øcore - Ølog comparisons for Well No.(EB-77).

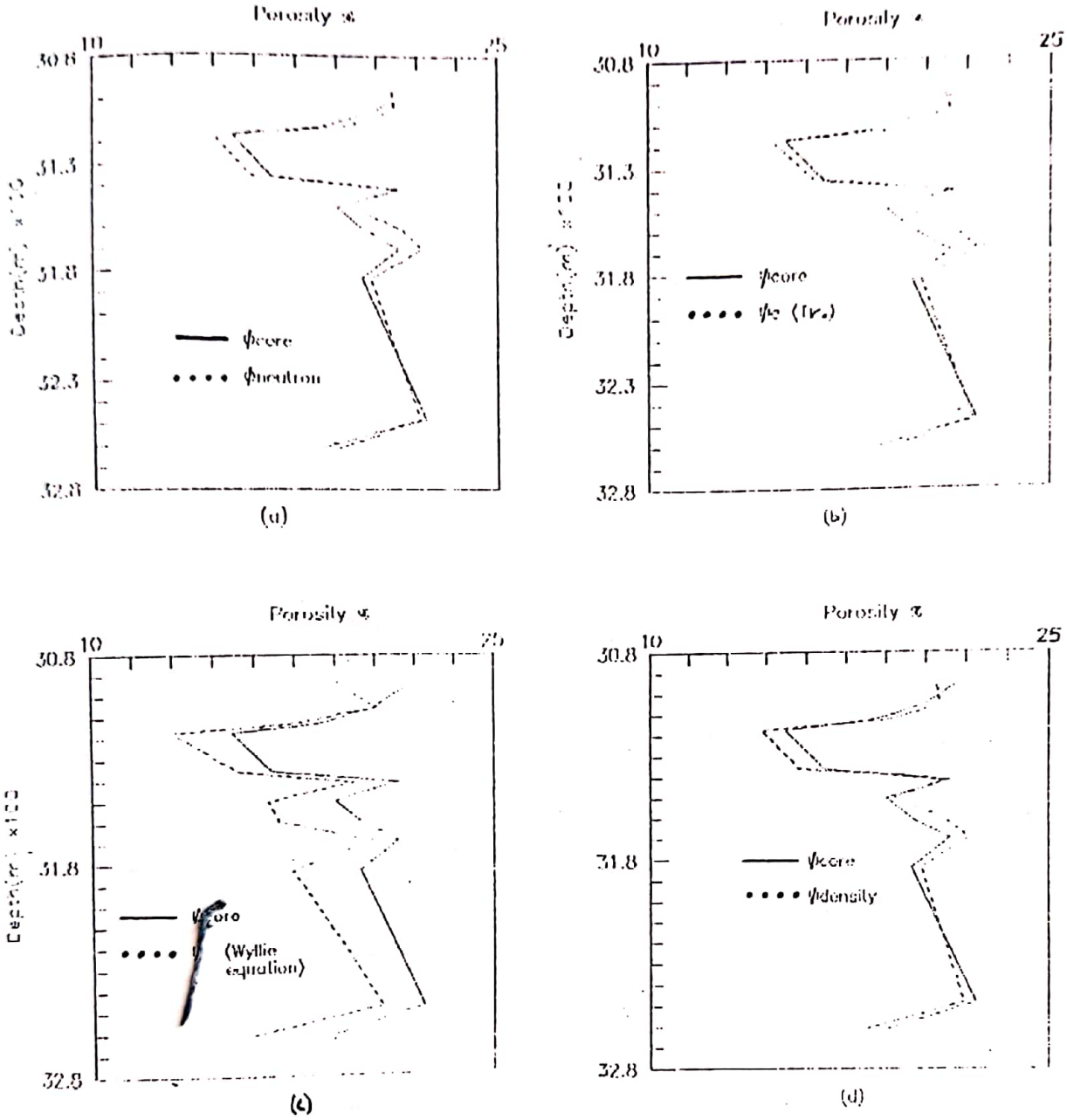

Fig.(4-22) Øcore - Ølog comparisons for Well No.(EB-79).

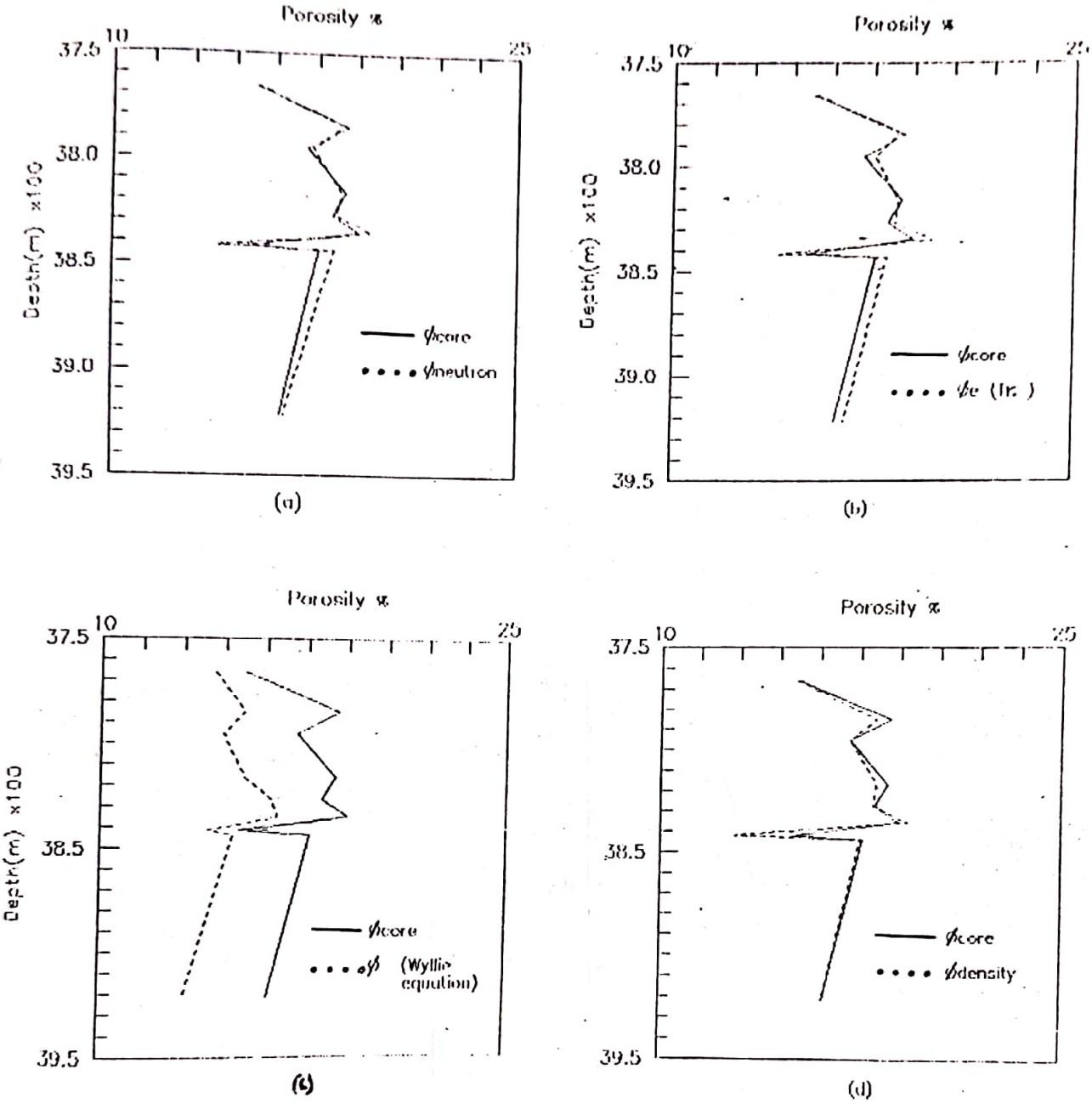

Fig.(4-23) Øcore - Ølog comparisons for Well No.(EB-I5).

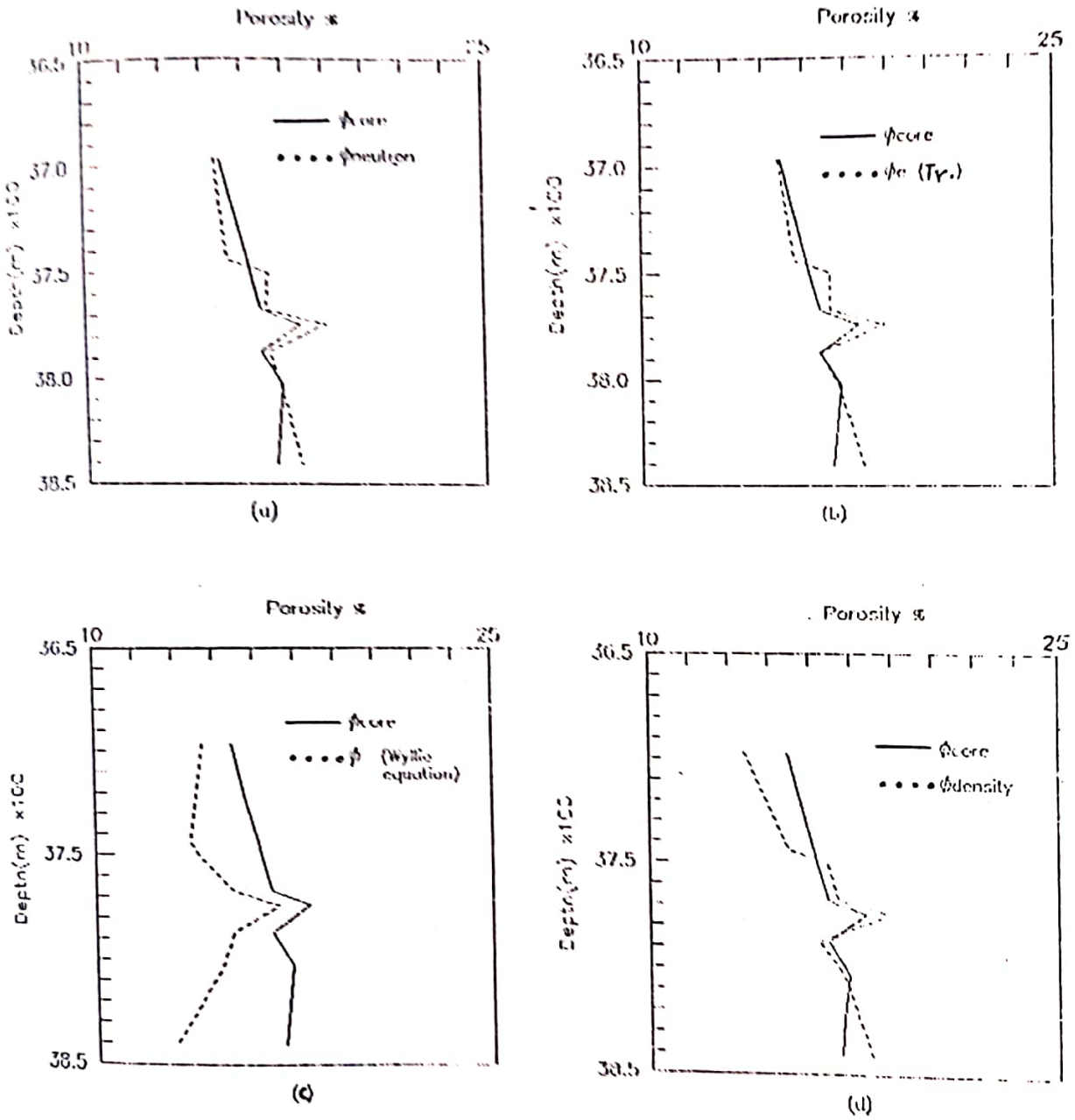

Fig.(4-24) Øcore - Ølog comparisons for Well No.(EB-I8).

CHAPTER FIVE

DETERMINATION OF WATER SATURATION

In the previous chapters, porosity was calculated by several methods, so as to select the best porosity value, to be used for saturation determination, due to its significant effect on 'Sw' calculation. The methods discussed are:-

1- Neutron log as a single porosity indicator,

2- Density log as a single porosity indicator,

3- Neutron-Density crossplot, using triangle method,

4- Sonic log, using the time average equation.

Core porosities were also measured, and used as reference values.

We have noticed through the comparisons made between the porosities derived from those methods and core porosities, Neutron log and the crossplot technique (using triangle method) yield favorable correlation parameters, when compared with other used methods.

Through the application of the triangle method in porosity calculation, it was found to give the highest correlation coefficient and lowest percentage errors. Therefore, triangle method was adopted to obtain porosity to be used in determination of water saturation by Archie's equation.

These calculated porosity values were also used in a crossplot technique (Pickett Method)[3], where they are plotted versus calculated resistivity values at the same depths in order to get specific values of the cementation factor (m) and the formation coefficient factor (a) of the Zubair formation, as explained below.

5-1 Determination of m and a

The generally accepted values of cementation factor (m) and formation coefficient factor (a) are 2.0 and 1.0, respectively.

These values were used extensively in references as typical values of these parameters. However, it was found by many authors that the values of those parameters may vary between formations, that will gave appreciable effect on the saturation determination from log analysis, by such methods as Archie's:-

$$S_w^n = \frac{a\, R_w}{\phi^m\, R_t} \qquad \text{..... 5-1}$$

It was also found that 'm' has more effect on saturation calculation than that of 'a', as shown in Fig. (5-1)[35]. Hence, 'm' is considered as being the most interested parameter to be calculated through the use of Pickett method.

The theoretical basis of Pikett method can be easily derived from the logarithmic expansion of Archie's equation,

relying on the classical value of n = 2 , as follows,

$$\log R_t = -m\log\phi + \log aR_w - 2\log S_w \quad \ldots\ldots\ldots\ldots 5\text{-}2$$

The method mentioned above suggests to solve graphically the values of water resistivity (R_w) and water saturation (S_w). The graphical determination of saturation will not be considered here.

For 'R_w' determination, it can be noticed from the above equation that when S_w= 100% (in the water bearing Zone), a linear relationship exists between resistivity and porosity:

$$\log R_t = -m\log\phi + \log aR_w \quad \ldots\ldots\ldots\ldots\ldots\ldots 5\text{-}3$$

The line represented by this equation should pass through the lowest resistivity points of the plot of log R_t versus logϕ.

In our application, as only water bearing Zones were selected for porosity determination, this line represents the best fit line through all the points.

The slope of this line is numerically equal to 'm', as seen from the above equation. The intercept of the line at ϕ= 100%, is related to 'R_w' and 'a' by

$$\log(\text{intercept}) = \log(aR_w) \quad \ldots\ldots\ldots\ldots\ldots\ldots 5\text{-}4$$

Therefore, in our case, Pickett method was used to determine specific values of 'm' and 'a' for Zubair

formation, knowing that the value of 'R_w' is 0.018 Ω-m, as calculated from the available 'R_{wa}' log and laboratory measurements.

The method was used to determine 'm' and 'a' values of each individual well, as shown in Figs.(5-2) through (5-7), in which, 'm' represents the slope of best fitting line (R_o line) and 'a' is calculated from its intercept at $\emptyset$ = 100% using Eq.(5-4).

To calculate a more accurate water saturation for any interval of Zubair formation and for finding a modified and particular form of Archie's equation for this formation, Pickett method was applied for the whole data from all wells, as shown in Fig.(5-8), in which, the value of m= 1.917 and a= 0.583 was calculated. By substituting these values in Eq.(5-2), the following form of Archie's equation was obtained:-

$$S_w = \sqrt{\frac{0.010}{\emptyset_{Tr}^{1.917}\ R_t}} \qquad \text{..... 5-5}$$

Where,

$\emptyset_{Tr}$ is the calculated porosity using the triangle method.

5-2 Practical application of the Modified Archie's equation

We have used Eq.(5-5) to calculate the water saturation of some of clean sand stone intervals selected from the Zubair formation, as shown in Table (5-1).

Table (5-1)

Sw data obtained from Modified Archie's equation

for some selected intervals of

Rubair formation

Well No.	Depth (m)	Rt	ϕ_e%	Sw%
EB-55	3400	20	13	16.1
	3457	20	16.3	13.0
EB-79	3030	30	6	27.7
	3070	17	10.5	21.5
EB-77	3135	30	5.5	30.1
EB-55	3007	5.5	16.3	24.8
	3150	6.0	15	25.7
EB-15	3553	4.0	10.5	44.4
	3720	80	7.3	13.9
EB-18	3505	18	5.3	40.3
	3855	1.7	14.1	51.2

Where, formation resistivity values (R_t's) has been taken from induction log (ILD).

To check the validity of the calculated water saturation by this modified and particular form of Archie's equation, it was checked against flow test results in corresponding intervals of the same wells.

This qualitative check indicates that saturation values obtained by our modified equation are in good agreement with well test results.

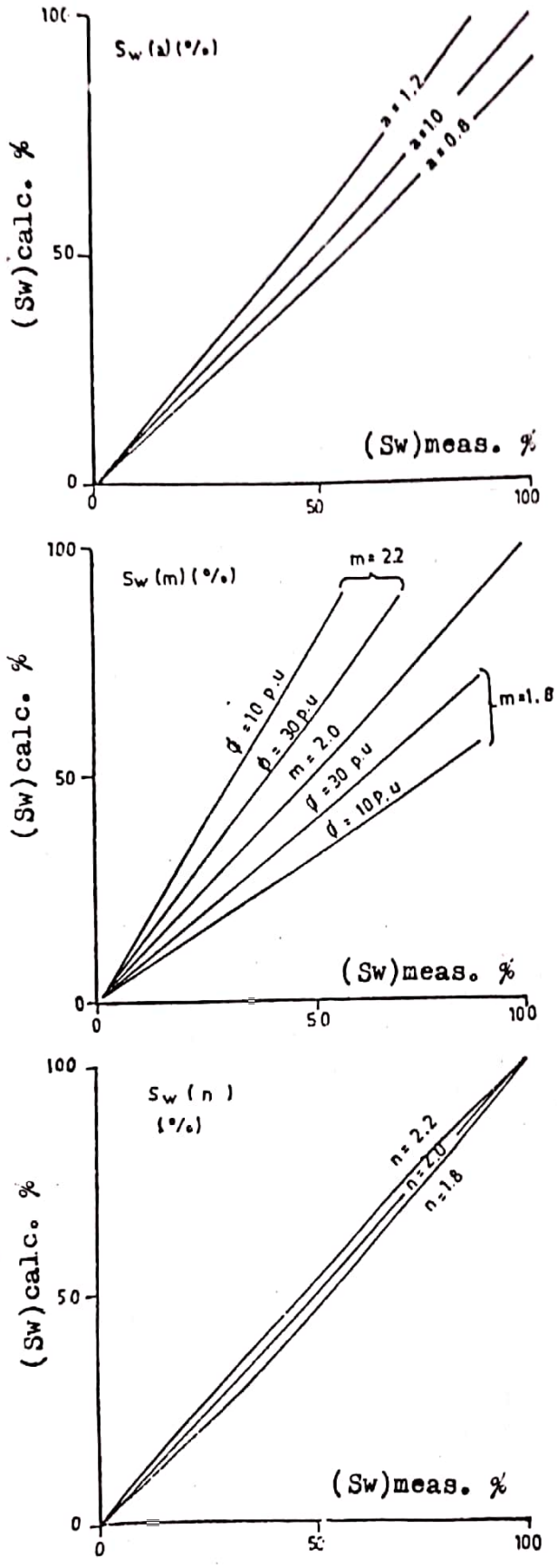

Fig.(5-I) The effect of m, a and n on the clculated value of 'Sw'.

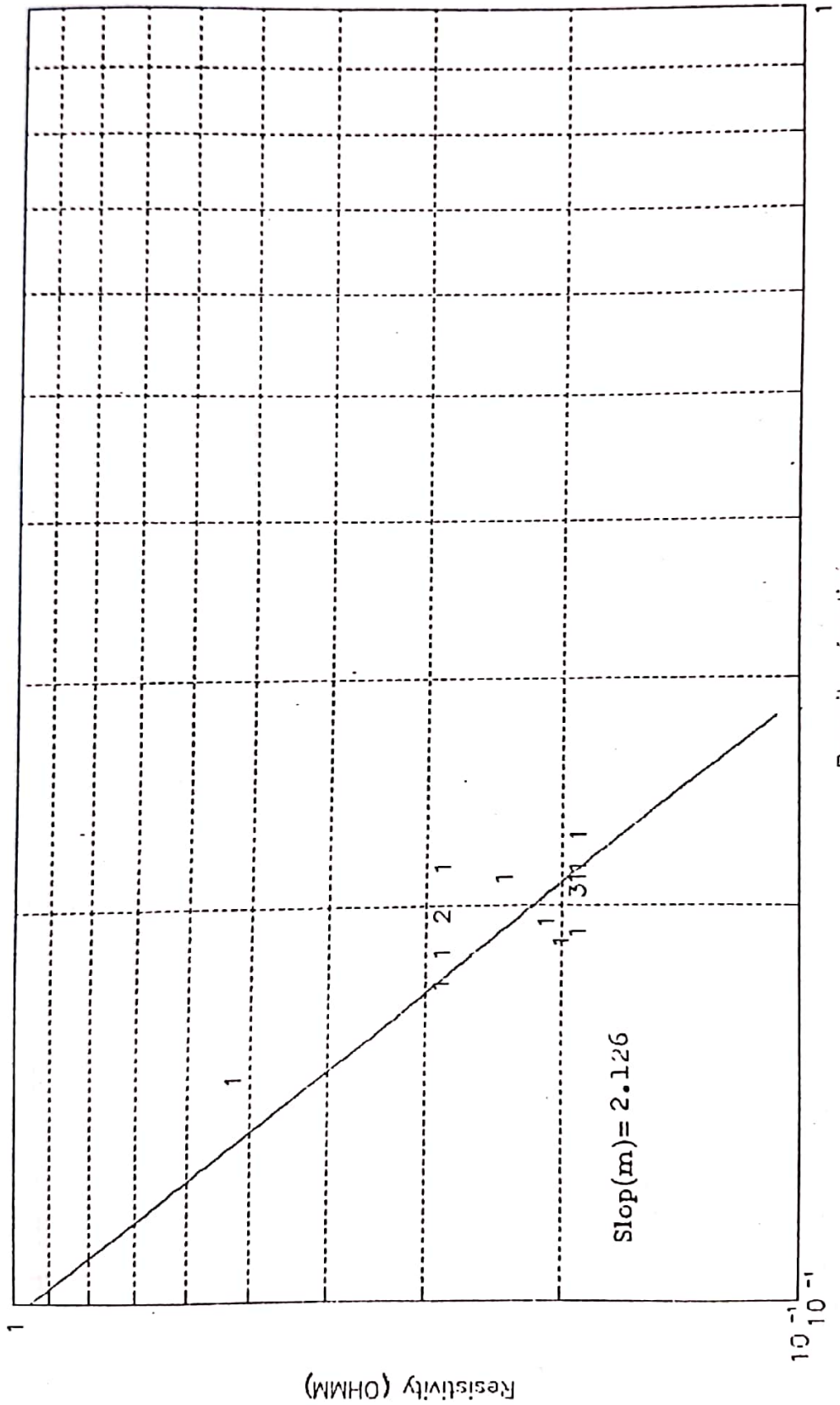

Fig.(5 - 2) Resistivity – Porosity cross plot for Well No.(EB–55) .

Fig.(5 - 3) Resistivity – Porosity cross plot for Well No.(EB–56) .

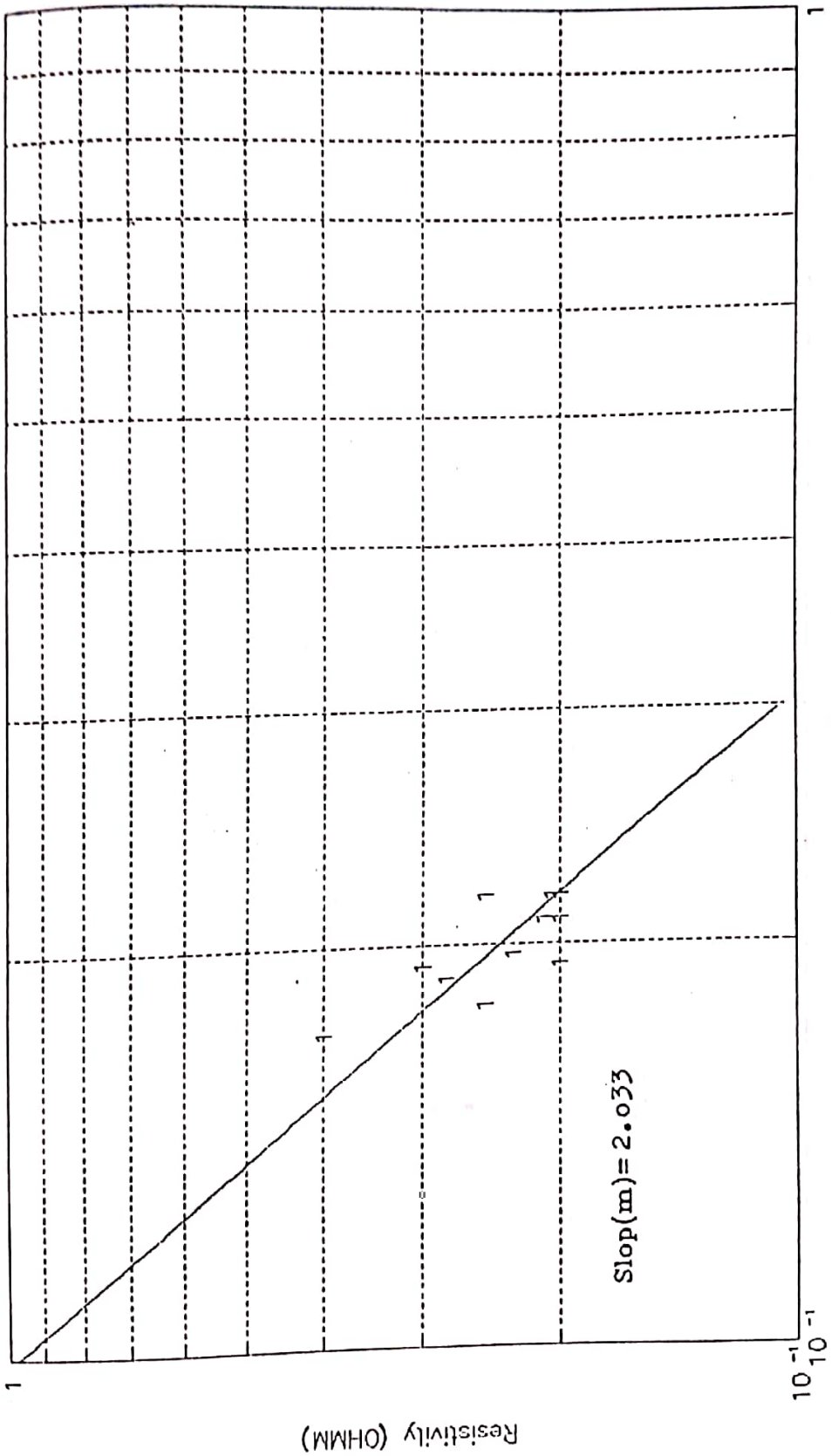

Fig.(5 - 4) Resistivity – Porosity cross plot for Well No.(EB–79) .

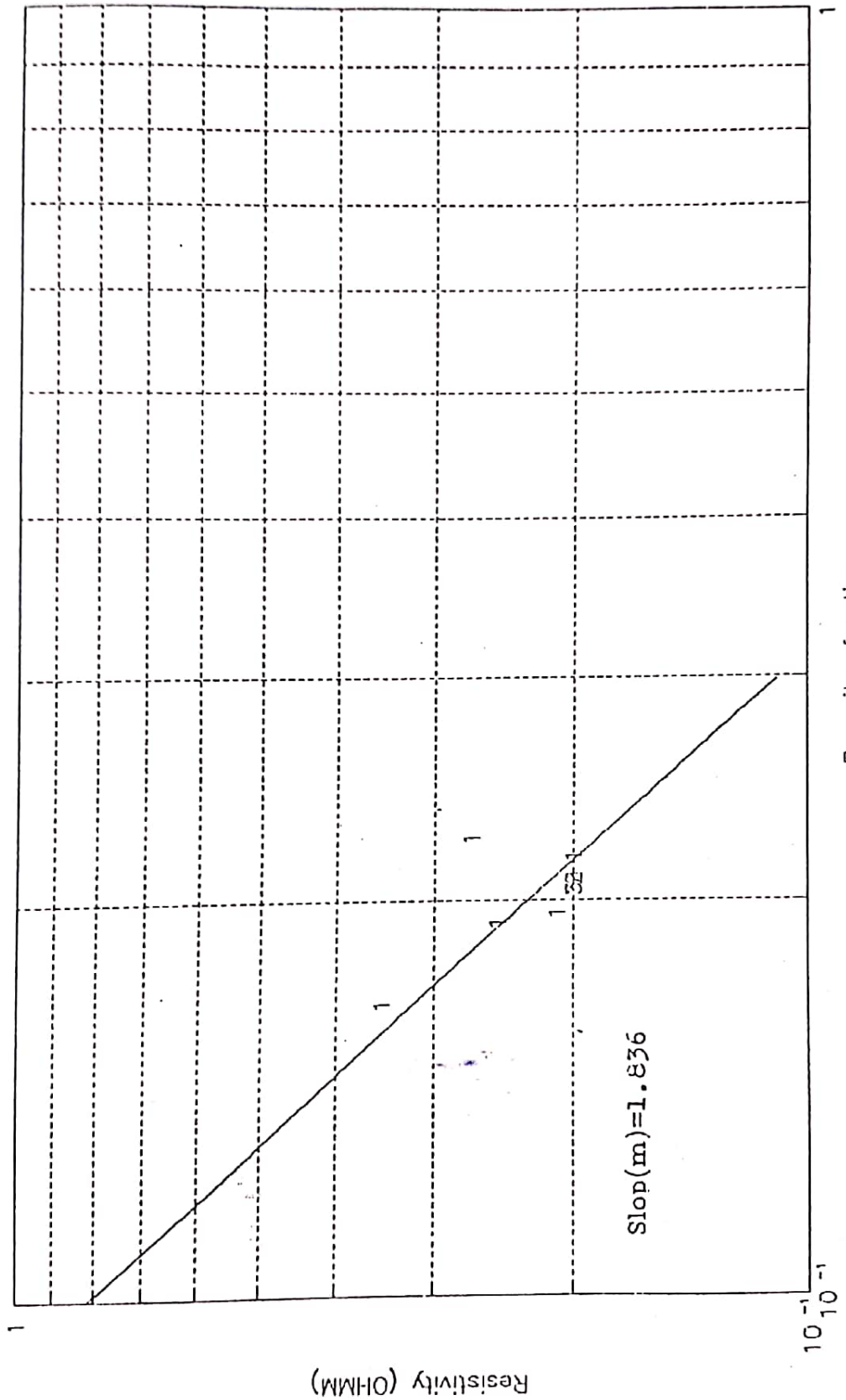

Fig.(5 - 5) Resistivity - Porosity cross plot for Well No.(EB-77) .

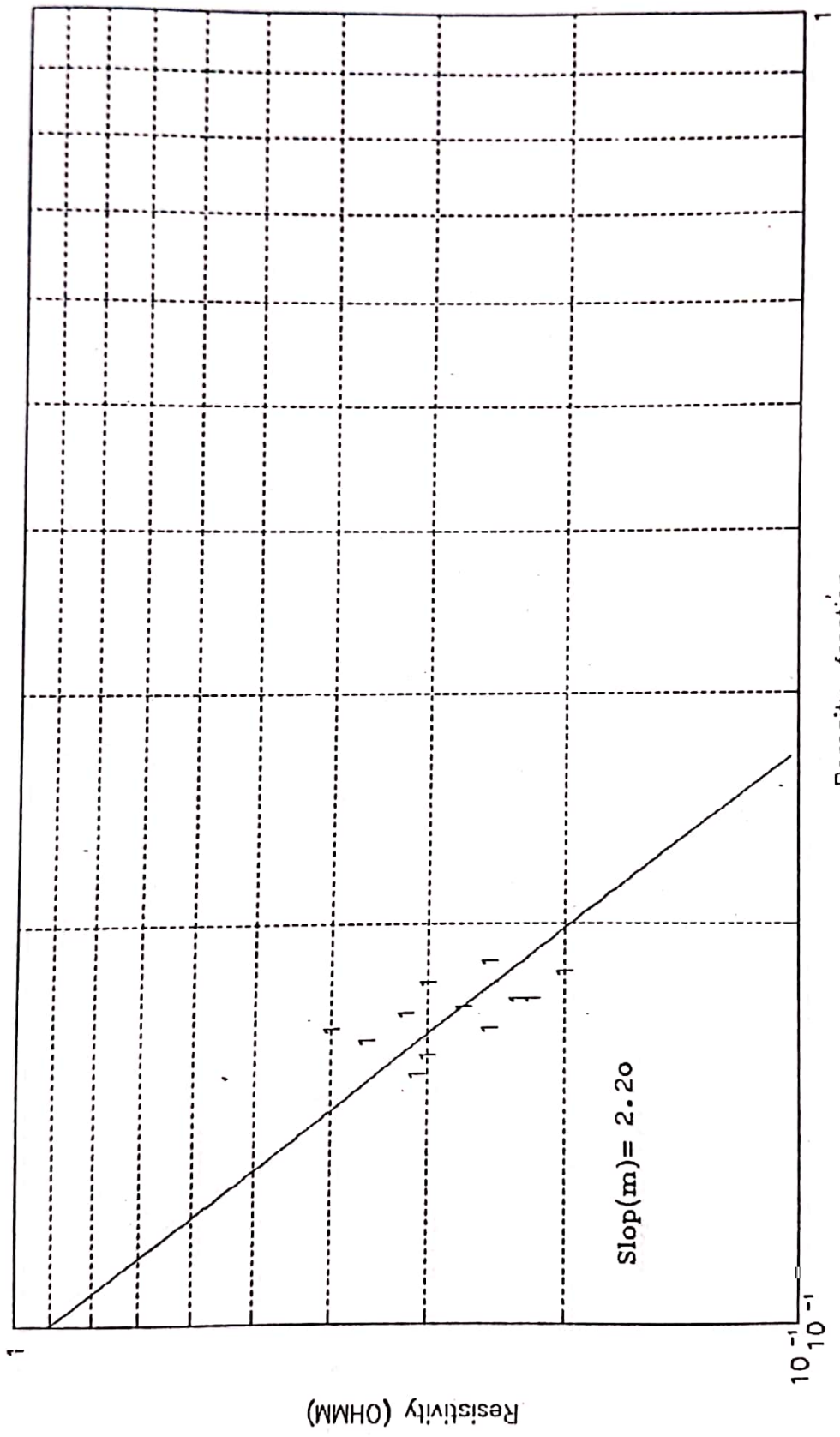

Fig.(5 - 6) Resistivity – Porosity cross plot for Well No.(EB–15) .

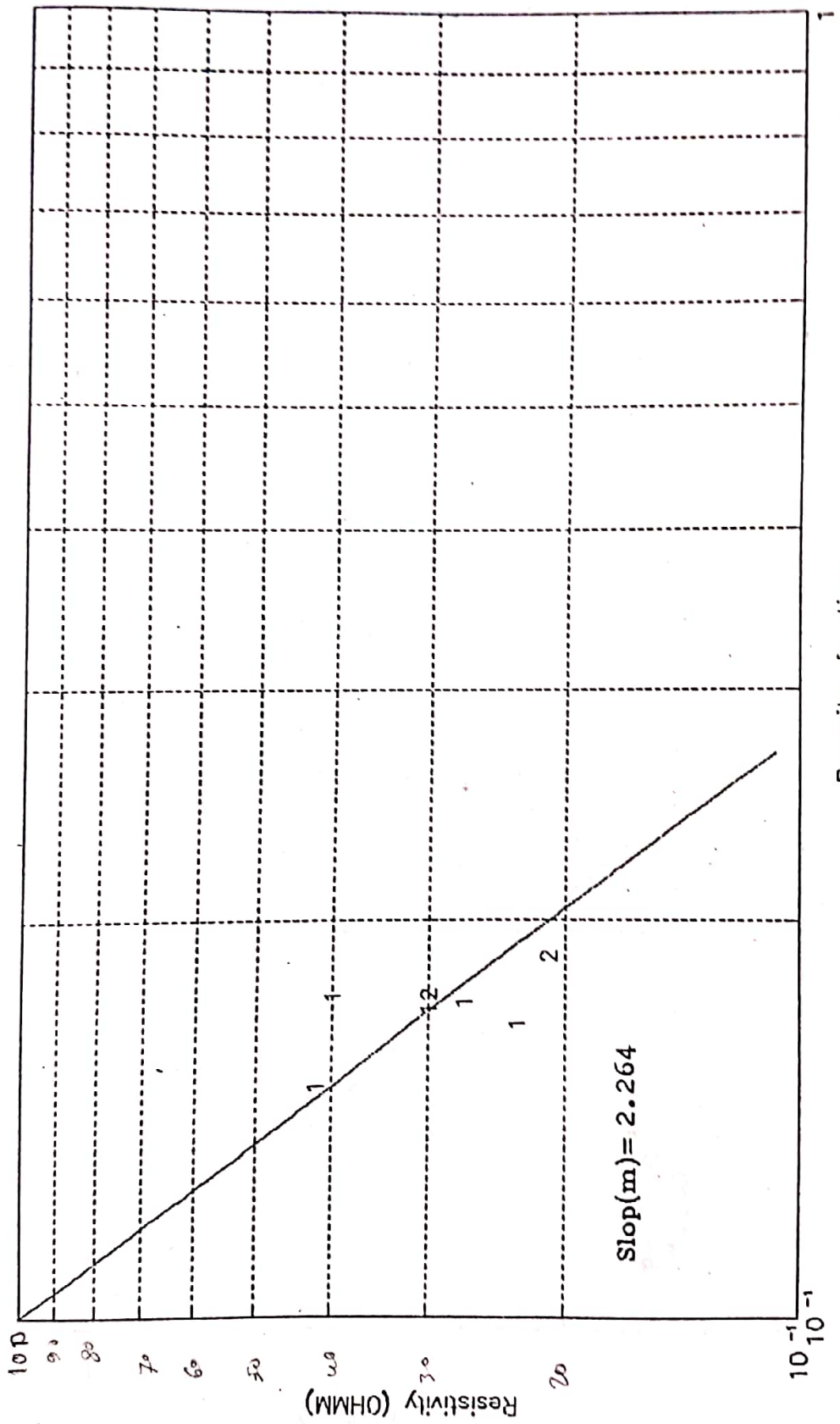

Fig.(5 - 7) Resistivity – Porosity cross plot for Well No.(EB–18) .

Fig.(5 - 8) Resistivity – Porosity cross plot for the Wells .

CHAPTER SIX

CONCLUSIONS & RECOMMENDATIONS

6-1 Conclusions:-

Relying on log interpretation and statistical analysis, some significant observation have been made. Although some of these observations are new conclusions, others merely represent the qualitative substantiation of general knowledge.

The results of this study indicate that:-

1- The statistical programme used to compare porosity values derived from logs and core porosity is found to give good correlation parameters.

2- Through its high percentage errors, obtained from statistical programme, the time average equation used in porosity determination of Zubair formation gives unsatisfactory results when compared with results obtained from other methods.

3- Through the statistical programme, it is found that effective porosity (ϕ_e) obtained by ρ_b-ϕ_N crossplot (using triangle method) gives the best correlation parameters when compared with core porosity.

4- Because 'CGR' log is unavailable in all the tested wells; a new technique for shale volume determination from 'SGR' log is used. Good values of 'V_{sh}' are obtained by using the derived equations from this technique.

5- A modified and particular from of Archie equation for Zubair formation is developed to be used with good confidence, when comparing its results with flow tests, for saturation determination in the clean sections of this formation.

6-2 Recommendations

For further investigations, the following pertinent recommendations are proposed:

1- Although, the run of Neutron and Density logs costs $8.35 per foot while the run of Sonic log costs $1.96 per foot[36], the use of ϕ_N-ρ_b crossplot technique (using triangle method) for porosity determination of Zubair formation is recommended.

2- A similar study can be performed by using other regression techniques to obtain better correlation parameters.

3- To extend the work, it is recommended to use other models for determination of water saturation (S_w), such as Volan, Coriband ... etc.

REFERENCES

1. Archie, G.E., "The Electrical Resistivity Log as an Aid in Determining Some reservoir Characteristics", J. Pet. Tech., 1942.
2. Robert, "Encyclopedia of Well Logging", 1984.
3. Pickett, G.R., "A Review of Current Techniques for Determination of Water Saturation from Logs", J. Pet. Tech., Nov. 1966.
4. Dumanoir et al., "R_{xo}/R_t Methods for Wellsite Interpretation", SPWLA, May 7-10, 1972.
5. Hilchie, D.W., "Applied Openahole Log Interpretation", 1978.
6. Hartley, "Factors Affecting Sandstone Acoustic Compressional Velocities and an Examination of Empirical Correlation Between Velocities and Porosities", SPWLA, June 23-26, 1981.
7. Tixier et al., "Sonic Logging", AIME, Vol.216, 1959.
8. Han et al., "Velocity Measurement and Empirical Modeling in Sandstones", SPWLA, June 9-13, 1986.
9. Wyllie et al., "Elastic Wave Velocities in Heterogeneous and Porous Media", Geophysics, Vol.21, PP.21-70, 1956.
10. Wyllie et al., "An Experimental Investigation of Factors Affecting Elastic Wave Velocities in Porous Media", Geophysics, Vol.23, PP.459-493, 1958.
11. Marcus, "The Sonic Log and the Delaware Sand", J. Pet. Tech., Jan. 71-75, 1960.

12. Geertsma, Velocity Log Interpretation, "The Effect of Rock Bulk Compressibility", SPEJ, Dec., 1961.

13. Kokesh et al., "A New Approach to Sonic Logging and Other Acoustic Measurements", J. Pet. Tech., March, 1965.

14. Meese,. "Statistical Methods Derive Equation for Calculating Porosity from Sonic Travel-Time Data", SPWLA, June 2-5, 1974.

15. Raymer et al., "An Improved Sonic Transit Time-To-Porosity Transform", SPWLA, July 8-11, 1980.

16. Patchett and Coalson, "The Determination of Porosity in Sandstone and Shaly Sandstone. Part Two, Effects of Complex Mineralogy and Hydrocarbons", SPWLA, July 6-9, 1982.

17. Heslop, "Porosity in Shaly-Sands", SPWLA, June 4-7, 1974.

18. Edwards and Simpson, "A method for Neutron Derived Porosity Determination for Thin Beds", AIME, Vol.204, 1955.

19. Wahl et al., "The Dual Spacing Formation Density Log", J. Pet. Tech., December, 1964.

20. Schlumberger Log Interpretation Principles, Schlumberger Ltd., (1969).

21. Poupon et al., "Log Analysis in Formation With Complex Lithologies", J. Pet Tech., August, 1971.

22. Truman et al., "Progress Report on Interpretation of Dual-Spacing Neutron Log (CNL) in The U.S.", SPWLA, May 7-10, 1972.

23. Ching and Krug, "Density-Neutron Crossplot Analysis For Shaly Gas Sands Using Hand-Carried Calculators", The Log Analyst, July-August, 1978.

24. Ching and Krudwig, "Density-Neutron Crossplot Analysis Using Polar Coordinates", The log analyst, July-August, 1980.

25. Swulius, T.M., "Porosity Calibration of Neutron Deflection Logs", SACROC Unit, J. Pet. Tech., April, 1986.

26. Poupon and Gaymard, "The Evaluation of Clay Content From Logs", SPWLA, May 3-6, 1970.

27. Heslop, "Gamma-Ray Log Response of Shaly Sandstones", The log analyst, September-October, 1974.

28. Serra et al., "Theory, Interpretation and Practical Application of Natural Gamma Ray Spectroscopy", SPWLA, July 8-11, 1980.

29. Quirein et al., "Estimation of Clay Types and Volumes From Well Log Data - An Extension of The Global" Method", SPWLA, June 23-26, 1981.

30. Leslie, "Determination of Optimum Combination of Pressure Loss and PVT Property Correlations for Predicting Pressure Gradients in Upward Two-Phase Flow, 1982.

31. Alger et al., "Formation Density Log Applications in Liquid - Filled Holes", J. Pet Tech., March, 1963.

32. Compbell and Wilson, "Density Logging in The Gulf Cost Area", J. Pet. Tech., July, 1958.

33. Schlumberger, "Log Interpretation". Vol. (I) Principles, 1972.

34. Schlumberger, "Log Interpretation, Principles and Applications", 1987.

35. Watfa, M., "Carbonate Interpretaions in The Middle East", Schlumberger MEA Internal Publication, 1982.

36. Schlumberger, L-11, 1982.

APPENDIX A

STATISTICAL PROGRAM

```
10 DIM PM(100),P1(100),P2(100),P3(100),P4(100),P5(100),P6(100),P7(100),P8(100)
20 AM=0:A1=0:A2=0:A3=0:A4=0:A5=0:A6=0:A7=0:A8=0
30 'LPRINT "NO.  CORE   WYLL.  MATR.  FLUID   AVER.  EFFE.  NEUT.  DENS.  CHART"
40 'LPRINT "=========================================================================="
50 FOR I=1 TO 82:READ PM(I),P1(I),P2(I),P3(I),P4(I),P5(I),P6(I),P7(I),P8(I)
60 AM=AM+PM(I):A1=A1+P1(I):A2=A2+P2(I):A3=A3+P3(I):A4=A4+P4(I)
70 A5=A5+P5(I):A6=A6+P6(I):A7=A7+P7(I):A8=A8+P8(I):'LPRINT I;
80 LPRINT USING "#####,##";PM(I);P1(I);P2(I);P3(I);P4(I);P5(I);P6(I);P7(I);P8(I)
90 NEXT I
100 LPRINT "ABSOLUTE AVERAGE PERCENT ERROR ANALYSIS OF METHODS"
110 LPRINT "=============================================="
120 T1=0:T2=0:T3=0:T4=0:T5=0:T6=0:T7=0:T8=0
130 C1=0:C2=0:C3=0:C4=0:C5=0:C6=0:C7=0:C8=0
140 S1=0:S2=0:S3=0:S4=0:S5=0:S6=0:S7=0:S8=0
150 A1=A1/82:A2=A2/82:A3=A3/82:A4=A4/82:A5=A5/82:A6=A6/82:A7=A7/82:A8=A8/82:
    AM=AM/82
160 R1=0:R2=0:R3=0:R4=0:R5=0:R6=0:R7=0:R8=0
170 O1=0:O2=0:O3=0:O4=0:O5=0:O6=0:O7=0:O8=0
180 B1=0:B2=0:B3=0:B4=0:B5=0:B6=0:B7=0:B8=0
190 PRINT "NO.  WYLL.   MATR.   FLUID   AVER.   EFFE.   NEUT.   DENS.  CHART"
200 FOR I=1 TO 82
210 E1=100*)P1(I)-PM(I))/PM(I):T1=T1+E1:S1=S1+E1^2:C1=C1+(P1(I)-A1)*(PM(I)-AM)
    :R1=R1+(P1(I)-A1)^2:O1=O1+(PM(I)-AM)^2:B1=B1+ABS(E1):EE1=ABS(E1)
220 E2=100*(P2(I)-PM(I))/PM(I):T2=T2+E2:S2=S2+E2^2:C2=C2+(P2(I)-A2)*(PM(I)-AM)
    :R2=R2+(P2(I)-A2)^2:O2=O2+(PM(I)-AM)^2:B2=B2+ABS(E2):EE2=ABS(E2)
230 E2=100*(P3(I)-PM(I))/PM(I):T3=T3+E3:S3=S3+E3^2:C3=C3+(P3(I)-A3)*(PM(I)-AM)
    :R3=R3+(P3(I)-A3)^2:O3=O3+(PM(I)-AM)^2:B3=B3+ABS(E3):EE3=ABS(E3)
240 E4=100*(P4(I)-PM(I))/PM(I):T4=T4+E4:S4=S4+E4^2:C4=C4+(P4(I)-A4)*(PM(I)-AM)
    :R4=R4+(P4(I)-A4)^2:O4=O4+(PM(I)-AM)^2:B4=B4+ABS(E4):EE4=ABS(E4)
250 E5=100*(P5(I)-PM(I))/PM(I):T5=T5+E5:S5=S5+E5^2:C5=C5+(P5(I)-A5)*(PM(I)-AM)
    :R5=R5+(P5(I)-A5)^2:O5=O5+(PM(I)-AM)^2:B5=B5+ABS(E5):EE5=ABS(E5)
260 E6=100*(P6(I)-PM(I))/PM(I):T6=T6+E6:S6=S6+E6^2:C6=C6+(P6(I)-A6)*(PM(I)-AM)
    :R6=R6+(P6(I)-A6)^2:O6=O6+(PM(I)-AM)^2:B6=B6+ABS(E6):EE6=ABS(E6)
270 E7=100*(P7(I)-PM(I))/PM(I):T7=T7+E7:S7=S7+E7^2:C7=C7+(P7(I)-A7)*(PM(I)-AM)
    :R7=R7+(P7(I)-A7)^2:O7=O7+(PM(I)-AM)^2:B7=B7+ABS(E7):EE7=ABS(E7)
280 E8=100*(P8(I)-PM(I))/PM(I):T8=T8+E8:S8=S8+E8^2:C8=C8+(P8(I)-A8)*(PM(I)-AM)
    :R8=R8+(P8(I)-A8)^2:O8=O8+(PM(I)-AM)^2:B8=B8+ABS(E8):EE8=ABS(E8)
290 PRINT I;:PRINT USING "#####,##";EE1:EE2:EE3:EE4:EE5:EE6:EE7:EE8
300 NEXT I
310 N=82:N1=72
320 T1=T1/N:B1=B1/N:SD1=(1/N)*(N*S1-T1^2)^.5:CF1=C1/(R1*O1)^.5
330 T2=T2/N:B2=B2/N:SD2=(1/N)*(N*S2-T2^2)^.5:CF2=C2/(R2*O2)^.5
340 T3=T3/N:B3=B3/N:SD3=(1/N)*(N*S3-T3^2)^.5:CF3=C3/(R3*O3)^.5
350 T4=T4/N:B4=B4/N:SD4=(1/N)*(N*S4-T4^2)^.5:CF4=C4/(R4*O4)^.5
360 T5=T5/N1:B5=B5/N1:SD5=(1/N1)*(N1*S5-T5^2)^.5:CF5=C5/(R5*O5)^.5
370 T6=T6/N:B6=B6/N:SD6=(1/N)*(N*S6-T4^2)^.5:CF6=C6/(R6*O6)^.5
380 T7=T7/N:B7=B7/N:SD7=(1/N)*(N*S7-T7^2)^.5:CF7=C7/(R7*O7)^.5
390 T8=T8/N:B8=B8/N:SD8=(1/N)*(N*S8-T8^2)^.5:CF8=C8/(R8*O8)^.5
400 LPRINT "CORRELATIONS      APE      AAPE        SD          CF"
410 LPRINT "=================================================="
420 LPRINT "WYLLIE      ";T1;"   ";B1;"    ";SD1;"    ";CF1
430 LPRINT "MATRIX      ";T2;"   ";B2;"    ";SD2;"    ";CF2
440 LPRINT "FLUID       ";T3;"   ";B3;"    ";SD3;"    ";CF3
450 LPRINT "AVERAGE     ";T4;"   ";B4;"    ";SD4;"    ";CF4
460 LPRINT "EFFECTIVE   ";T5;"   ";B5;"    ";SD5;"    ";CF5
470 LPRINT "NEUTRON     ";T6;"   ";B6;"    ";SD6;"    ";CF6
480 LPRINT "DENSITY     ";T7;"   ";B7;"    ";SD7;"    ";CF7
490 LPRINT "BOOK CHART  ";T8;"   ";B8;"    ";SD8;"    ";CF8
```

Table (A-1)

Measured-calculated porosity values and shale volume of the chosen intervals of Zubair formation

Well No.	Depth m	Measured porosity %	Porosity calculated from logs %				Shale volume %
			Sonic log	Neutron log	Density log	ρ_b-ϕ_s crossplot (triangle method)	
EB-77	3001.5	20	17.1	19.5	19.5	19.8	1.8
	3015	24.5	21.9	22.3	22.1	22.4	zero
	3030	22	19.7	23	23	23.3	zero
	3041	21	17.7	20.8	20.9	21	1.8
	3057	22	19.5	23.8	24	24	0.8
	3074	22	19.1	23	23	23.2	zero
	3078.5	19.2	17.3	18.5	18.3	18.7	zero
	3082	16.1	13.7	15.7	15.7	16	2.7
	3093	22	18.2	21.5	21.3	21.7	2
	3104	22	19.8	21	20.9	21	5
	3114.5	22.5	19.1	21.9	21.6	22	zero
	3161	22.2	19.1	21	20.7	21.0	zero
	3175	22.5	20.8	24	24.2	24.3	zero
EB-55	3243	17.5	14.5	16.05	16.03	16.2	5
	3255	22.2	19.0	21.2	21.09	22	0.8
	3278	23	19.1	22.3	22.4	22.5	zero
	3295	20	16.8	19.8	19.8	19.7	0.5
	3298	22	18.6	21.4	21.2	21.4	zero
	3305	24	20.8	23.3	22.8	23	zero
	3309.5	21.5	17.6	21.1	20.9	21.1	2
	3316.5	19.5	16.2	18.8	18.5	18.8	2.5
	3330.5	21.5	18.0	21.2	20.7	21.1	zero
	3338.5	19	15.4	18.3	17.8	18.3	2.5
	3365	20	16.09	18.9	18.6	19.0	zero
	3405	21.5	17.9	20.9	20.6	20.8	3.5
	3417.5	20	16.9	19.3	18.9	19.3	zero
	3445	20.8	18.0	19.8	19.3	19.6	zero

18-18	3766	16	14.1	15.3	15.1	15.3	zero
	3785	19.6	15.2	18.4	18.1	18.4	zero
	3795.5	18	14.4	17.3	17.1	17.5	4
	3816.5	19.5	15.2	18.4	18.1	18.4	zero
	3827	19	16.2	18.2	18	18.3	1
	3835	20	16.4	19.5	19.3	19.7	3
	3841.5	15	13.9	13.5	12.8	14	5
	3843.5	18.5	14.8	18.1	17.5	18	3
	3921.5	17	13.1	16.3	16.1	16.5	7.5
18-18	3697	16	14.1	15	13.6	15.1	zero
	3744	17	13.6	15.4	15.2	15.7	7.5
	3750	17.1	13.9	16.9	16.6	17	1.0
	3767.5	17.5	15.2	16.8	17.0	17	zero
	3774	19	16.9	19	18.9	19	zero
	3787	17.5	15.2	16.5	16.3	16.6	zero
	3803	18.3	14.8	17.3	17.2	17.3	zero
	3841	20.8	13.0	18	18.2	18.2	zero
18-79	3096.5	22.7	19.3	21.1	20.9	21.2	2
	3105.5	21.5	20.6	21.2	21	21.4	1
	3112.8	19.5	17.6	19.2	19.09	19.5	2
	3117.5	16	13.0	14.5	14.3	14.7	13
	3136	17.5	15.4	15.9	15.7	16.3	13
	3141.5	22.5	19.7	21.4	21.2	21.2	zero
	3150	20	16.5	19.5	19.3	19.6	2.0
	3160	21	16.9	21.4	21.2	21.5	zero
	3169.5	22.5	20.4	22.2	22.1	22.4	2.0
	3183.5	21	17.4	20.3	20.3	20.3	zero
	3248	23.5	20.8	22.1	21.9	22.2	zero
	3261	20	15.8	18.4	18.1	18.4	zero
18-56	3022	17.5	13.8	15.9	15.5	16	10.0
	3127.5	22.2	18.4	21.04	20.6	21	4.0
	3137.5	21.6	20.1	21.4	21.1	21.5	3.4
	3153.5	24	21.9	24	23.5	24	zero
	3180	20	17.8	21.8	21.5	21.8	1.2
	3185	18	15.3	19.8	19.6	19.8	3
	3192.5	20	18	21	20.7	21	zero
	3196	21	18.6	22.6	22.1	22.6	zero
	3200	20	17.0	19.5	19.3	19.7	6.0
	3205	21	16.3	22.3	21.9	22.3	zero
	3217.5	22.5	18.0	21.9	21.6	22	zero
	3228	19.8	17.7	19.3	19.1	19.4	zero
	3268	19.1	15.8	18	17.7	18.1	zero
	3287.5	20	17.7	17.1	16.9	17.3	8

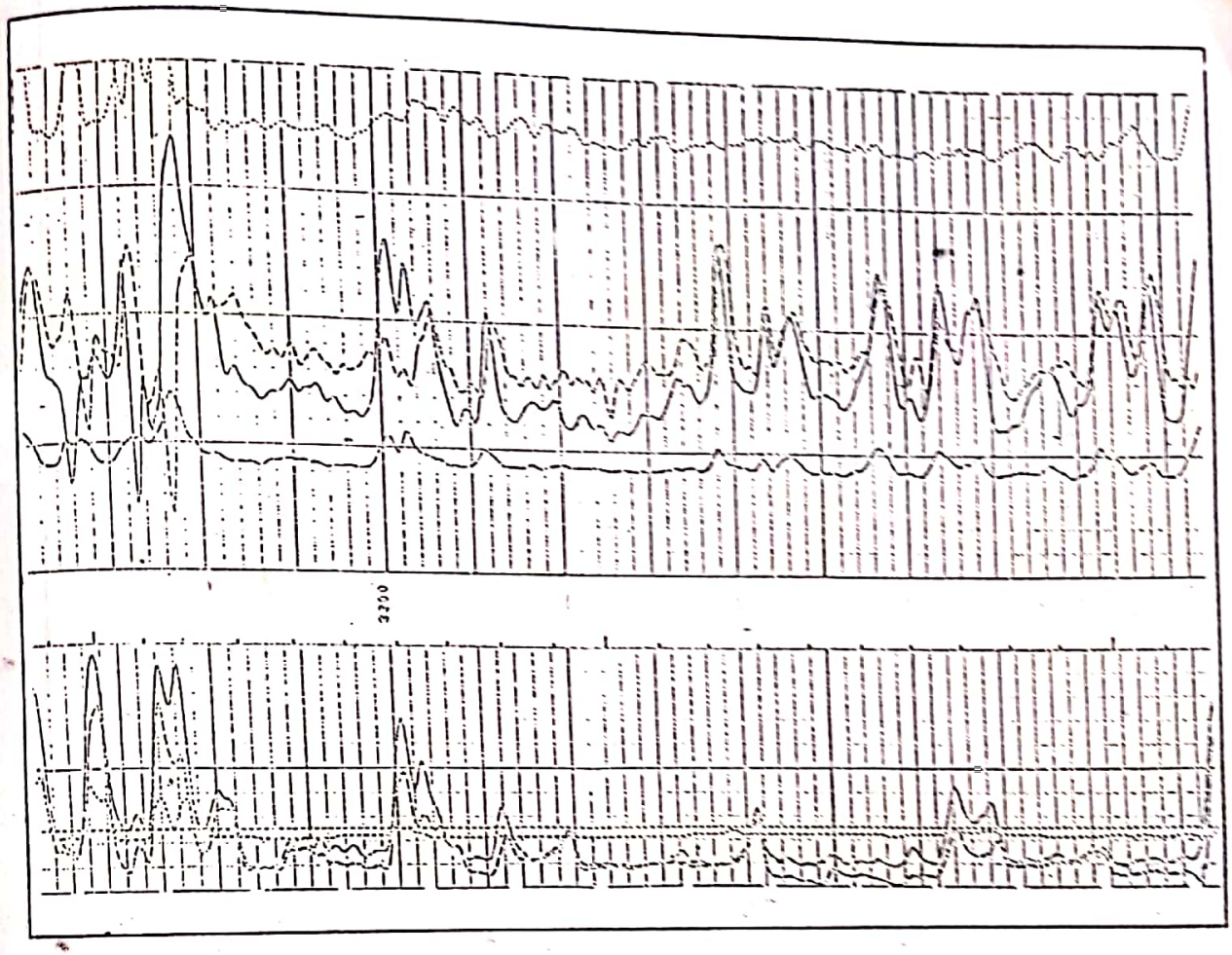

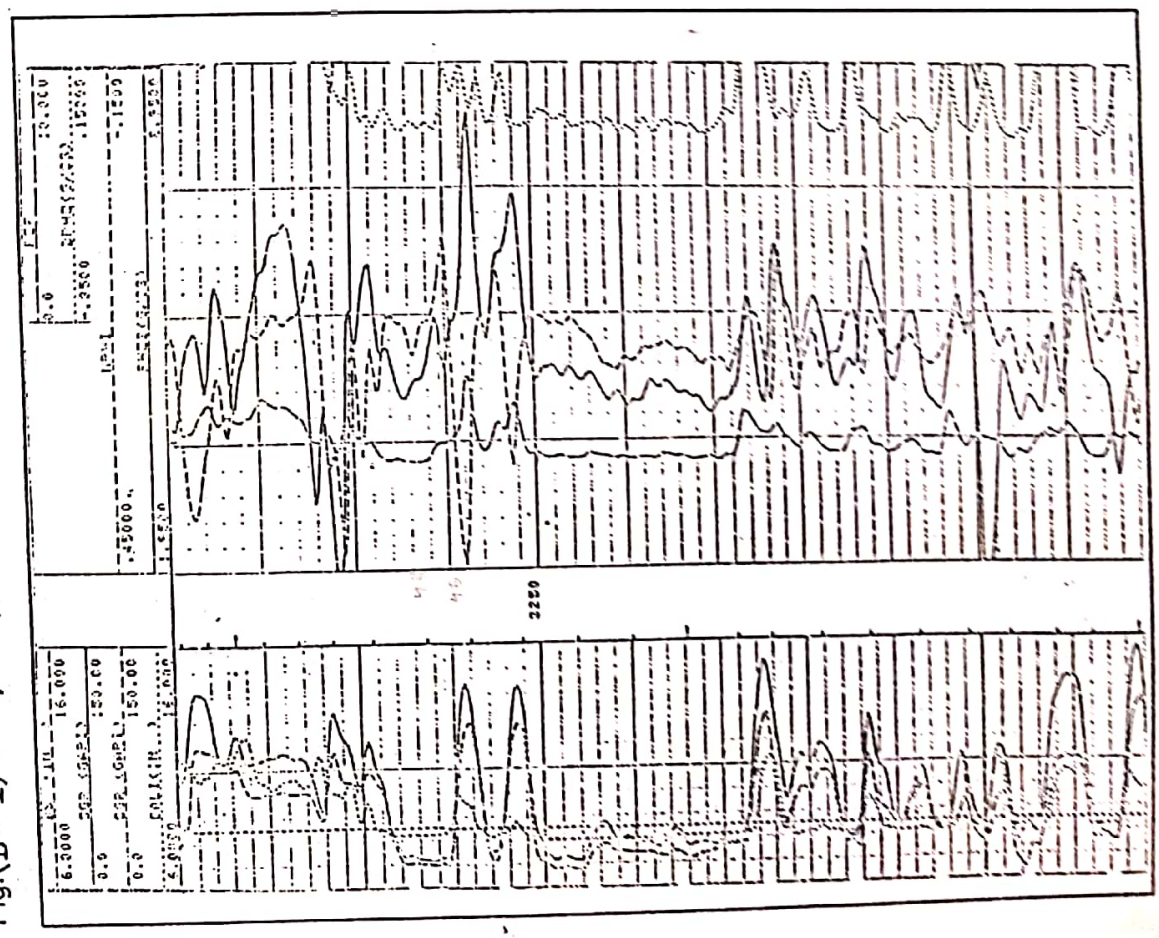

Fig.(B - 1) FDC/CNL/CAL/GR Logs for Well No.(EB-55)

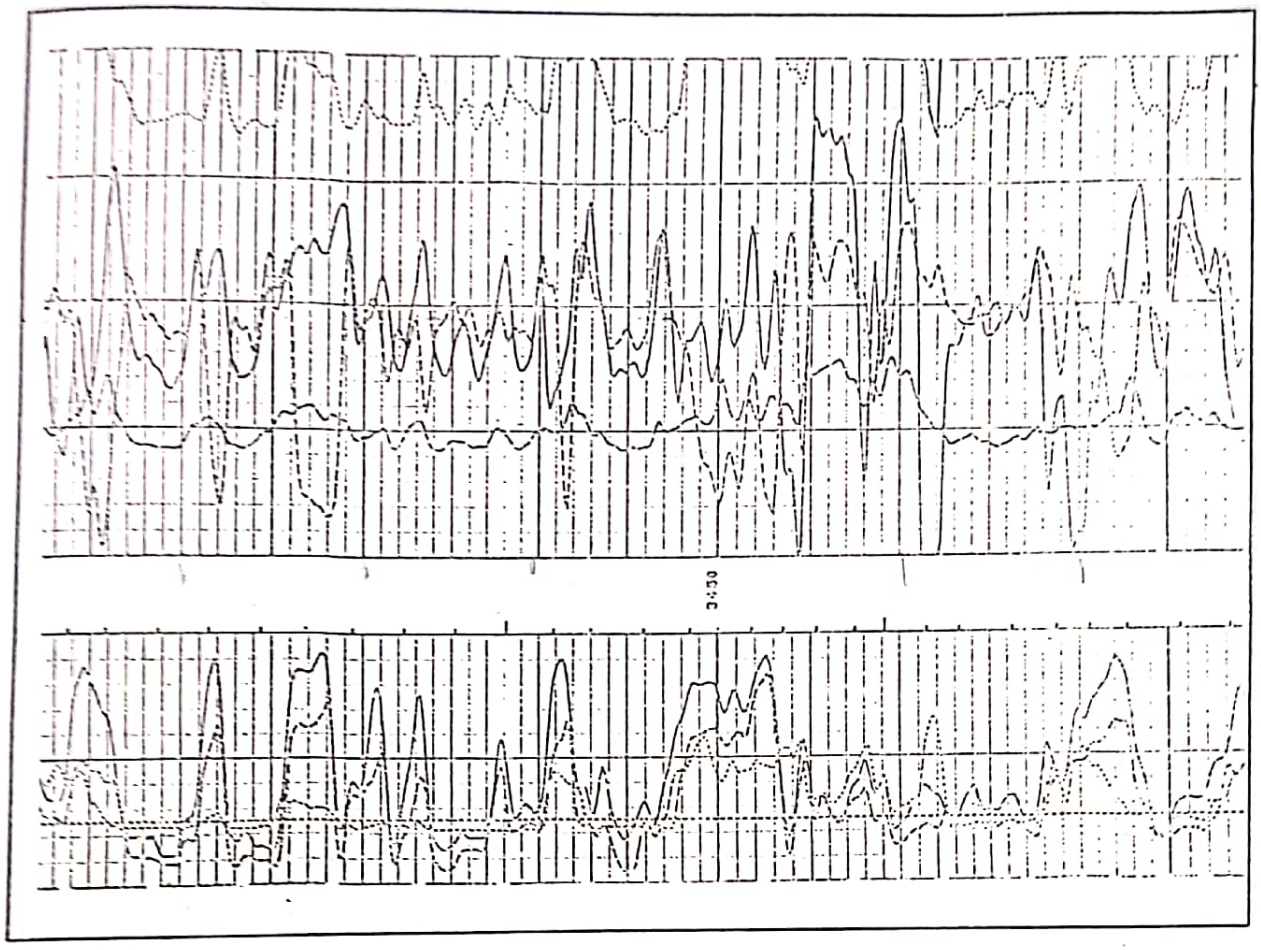

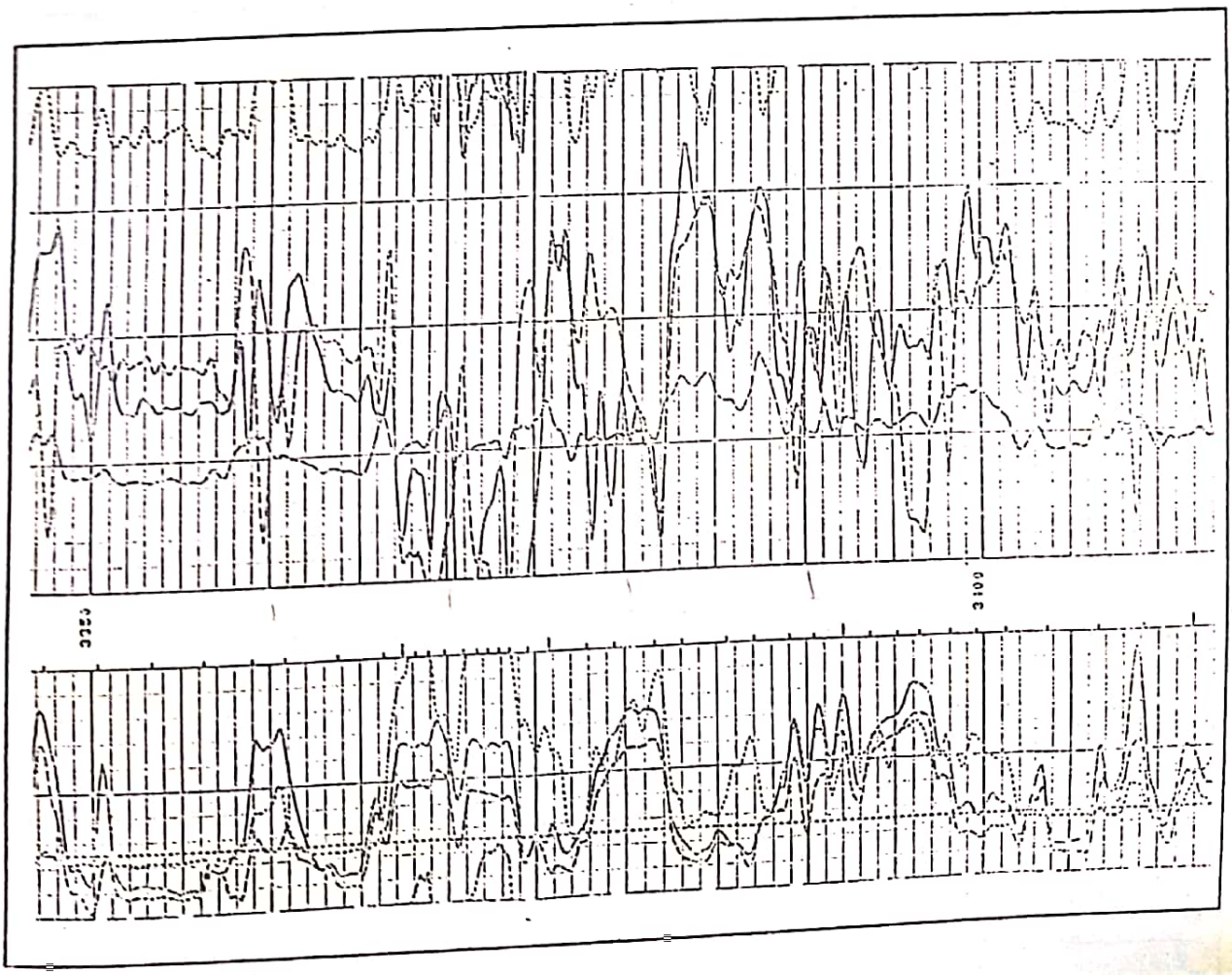

Fig.(B-2) MSFL/SFL/ILD/DT/SP/Rwa for Well No.(EB-55)

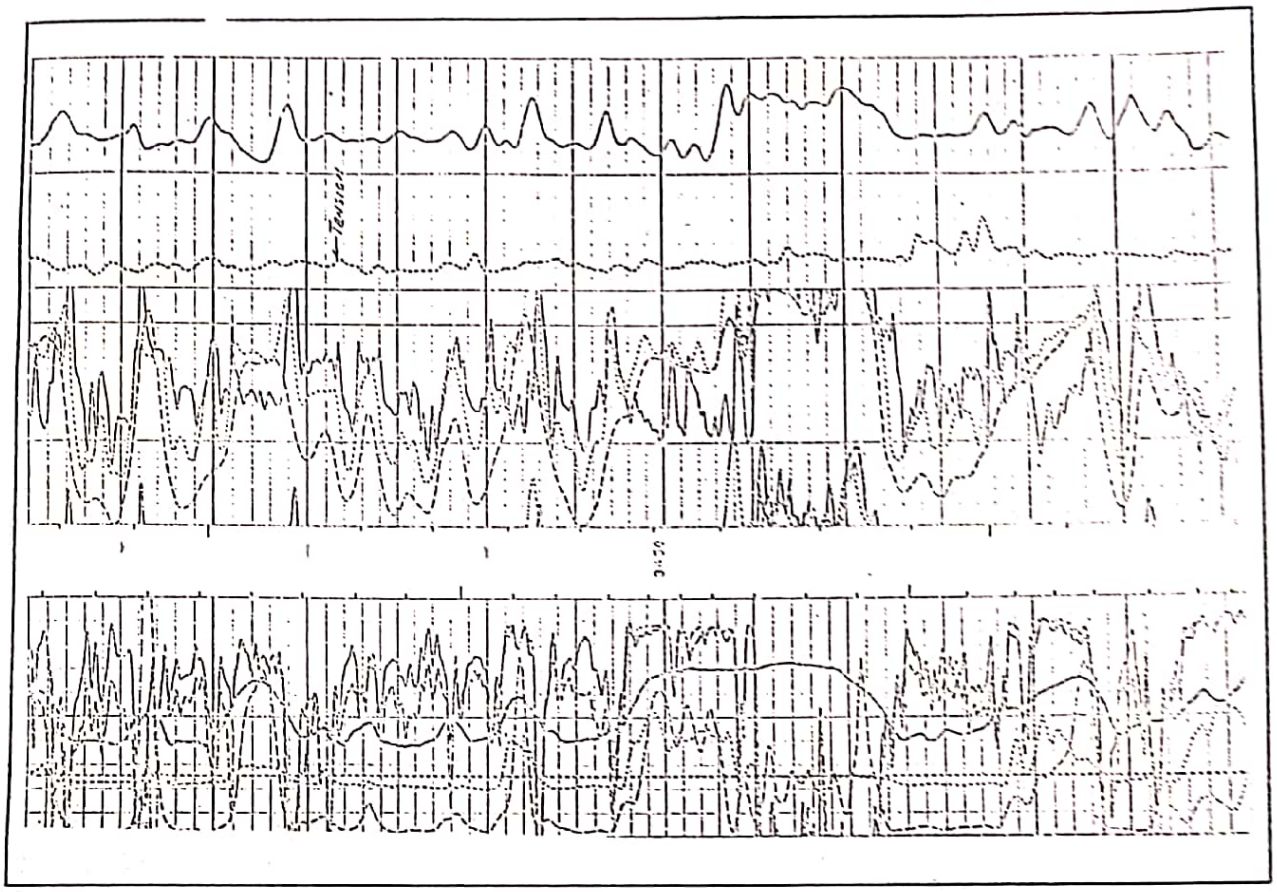

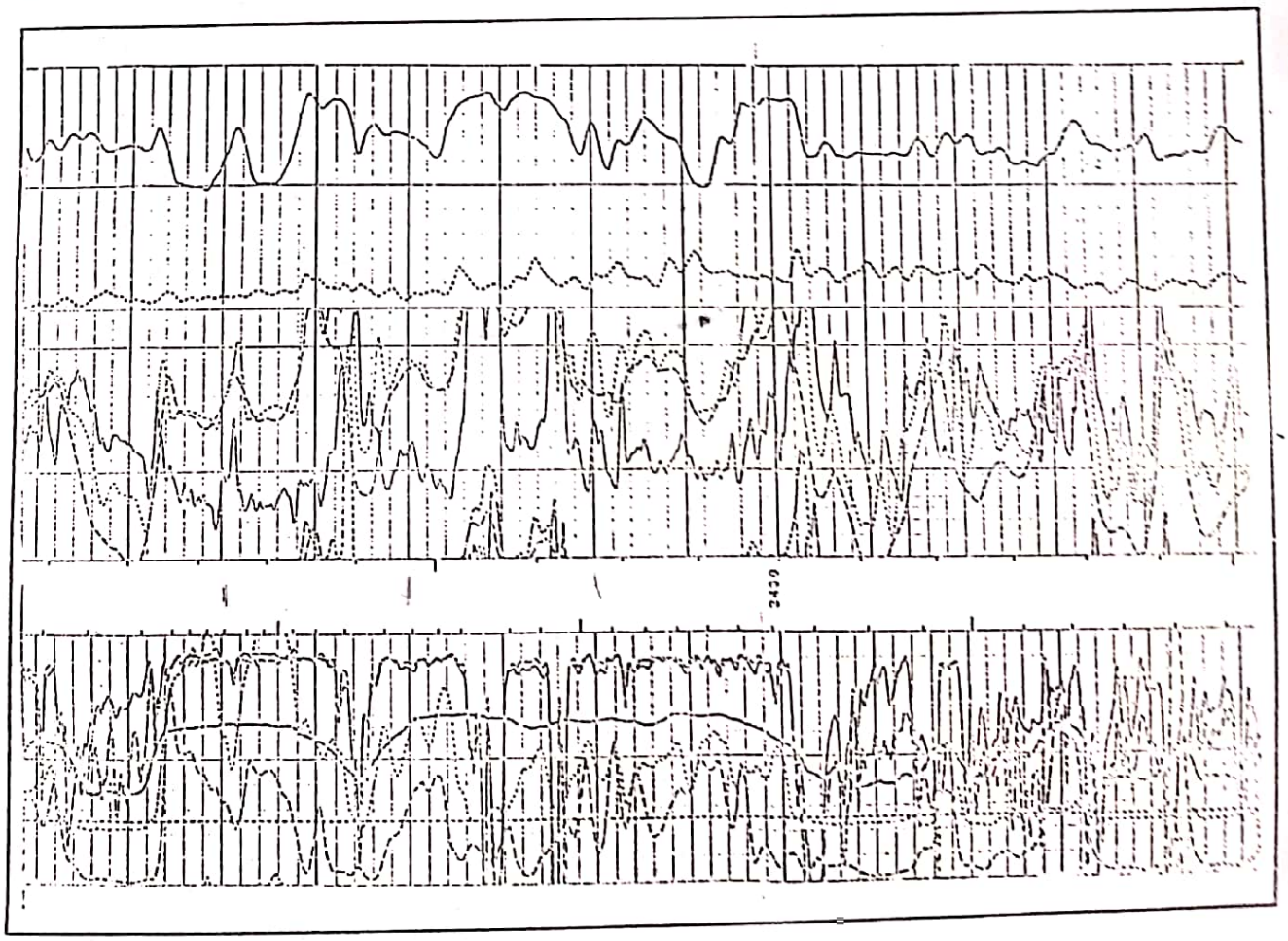

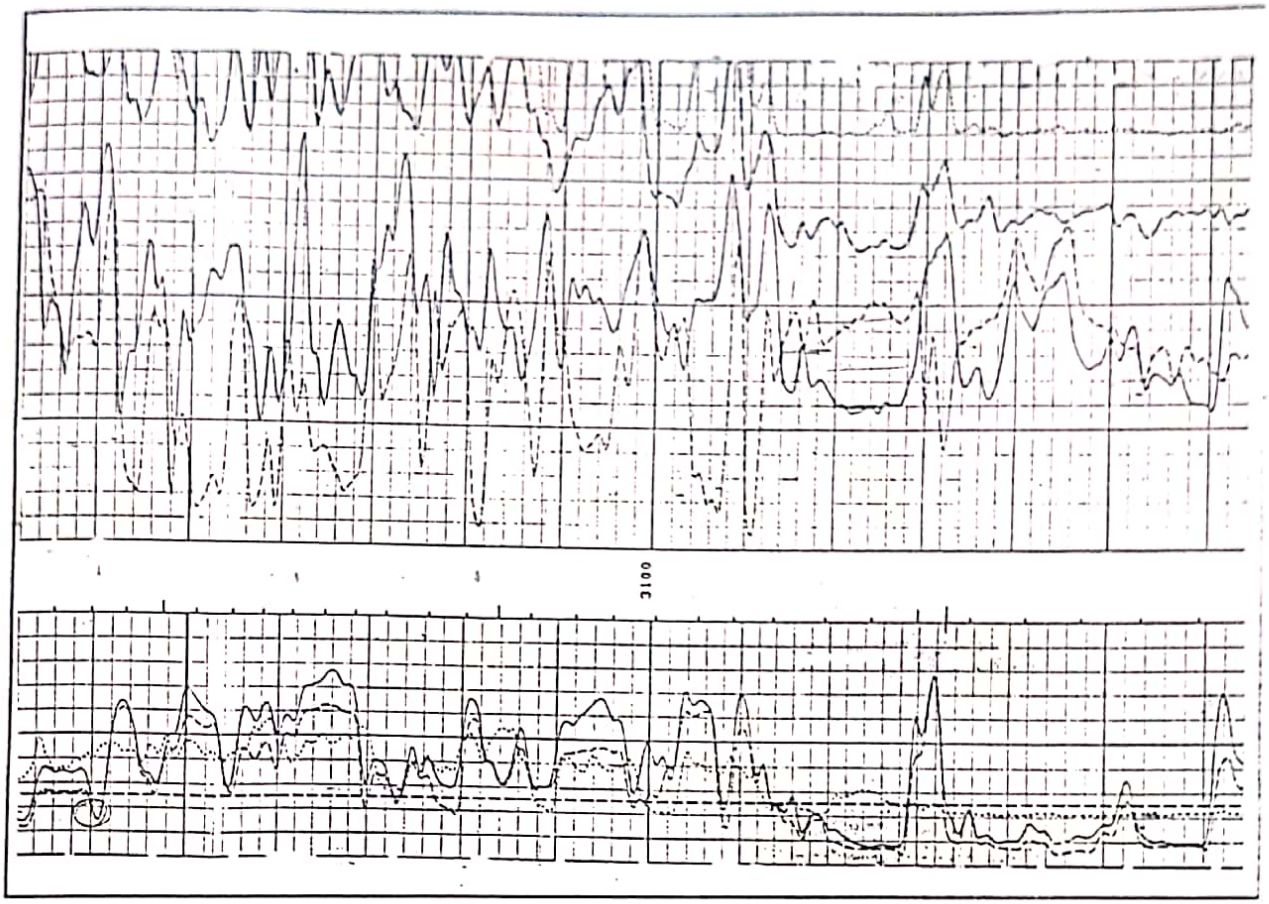

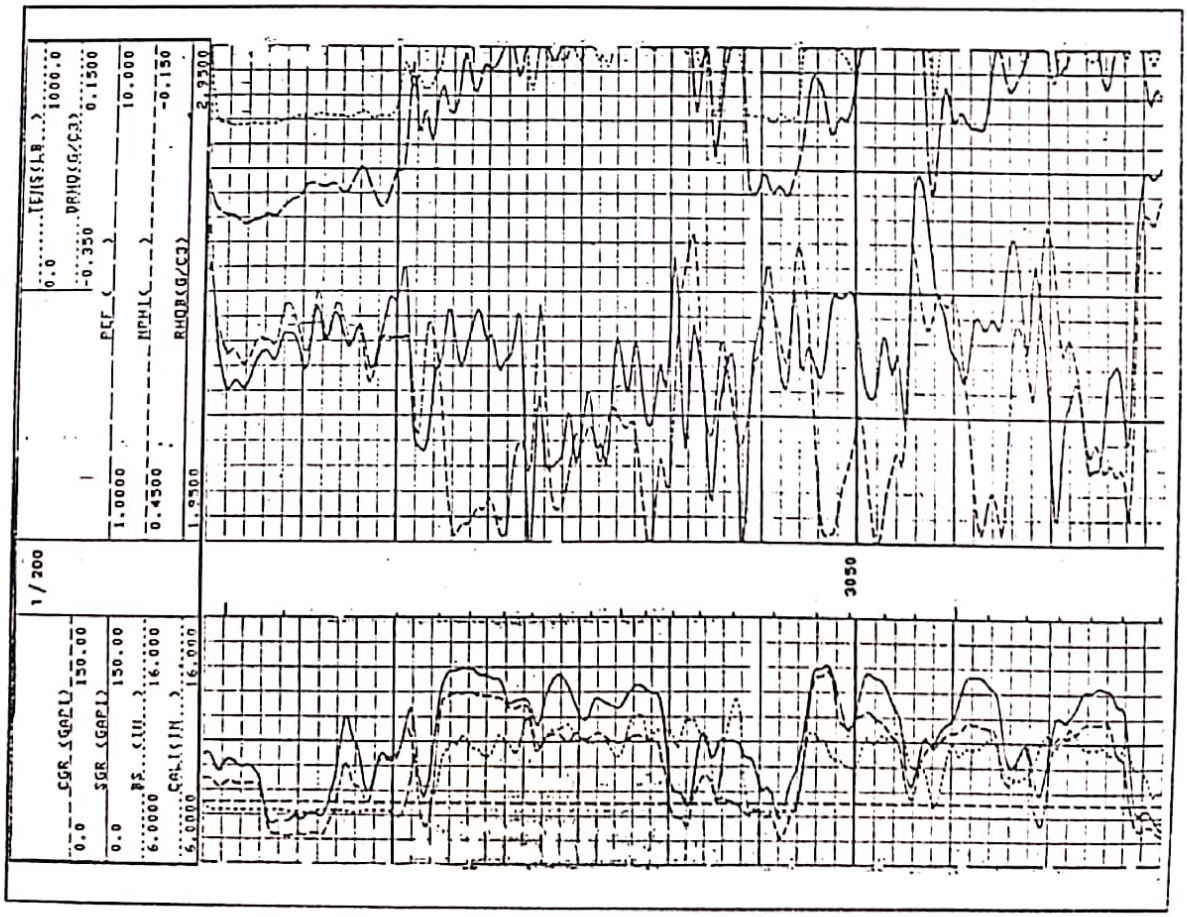

Fig.(B-3) FDC/CNL/CAL/GR Logs for Well No.(EB-56)

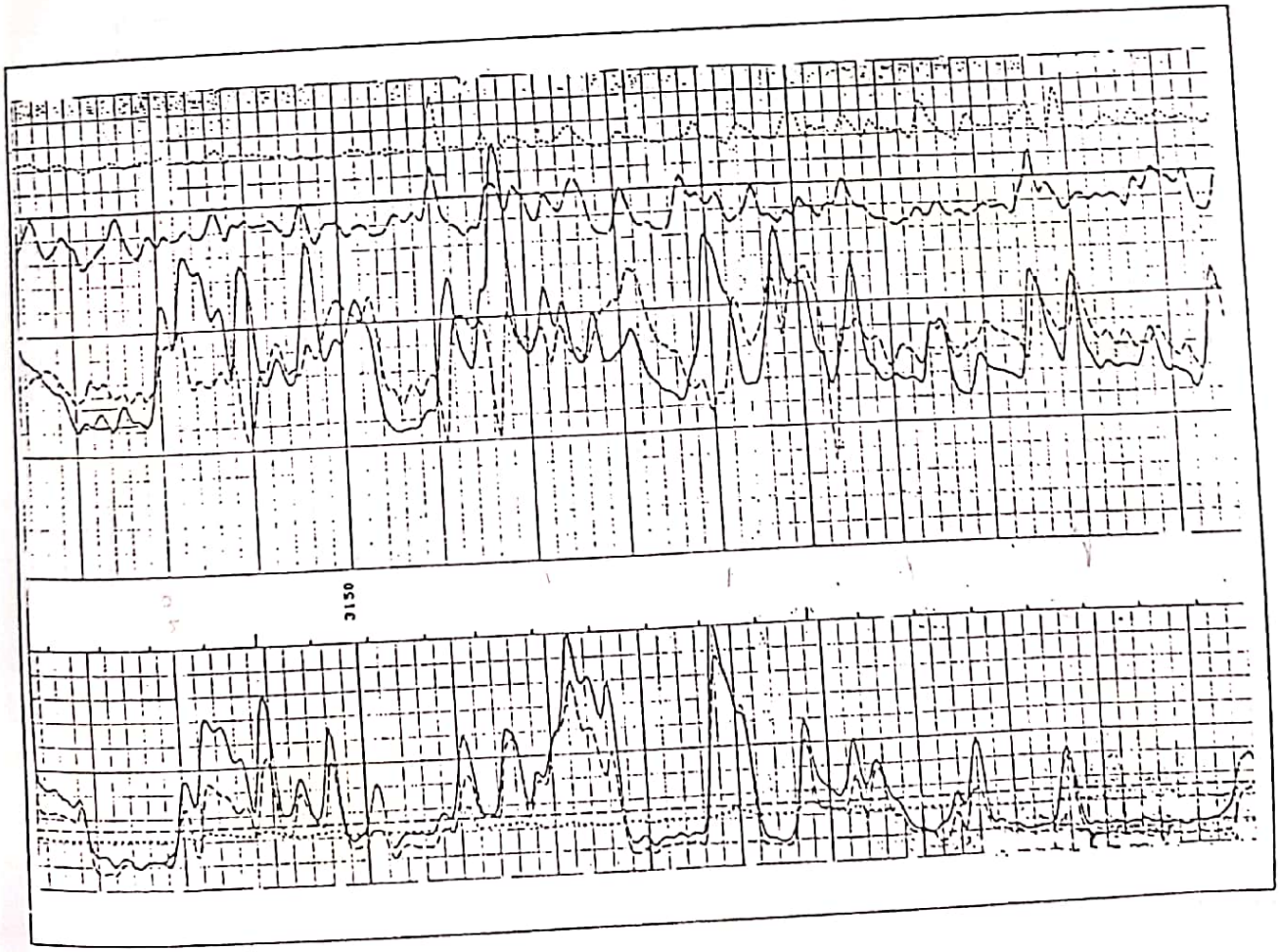

Fig.(B-4) MSFL/SFL/ILD/DT/SP/Rwa for Well No.(EB-56)

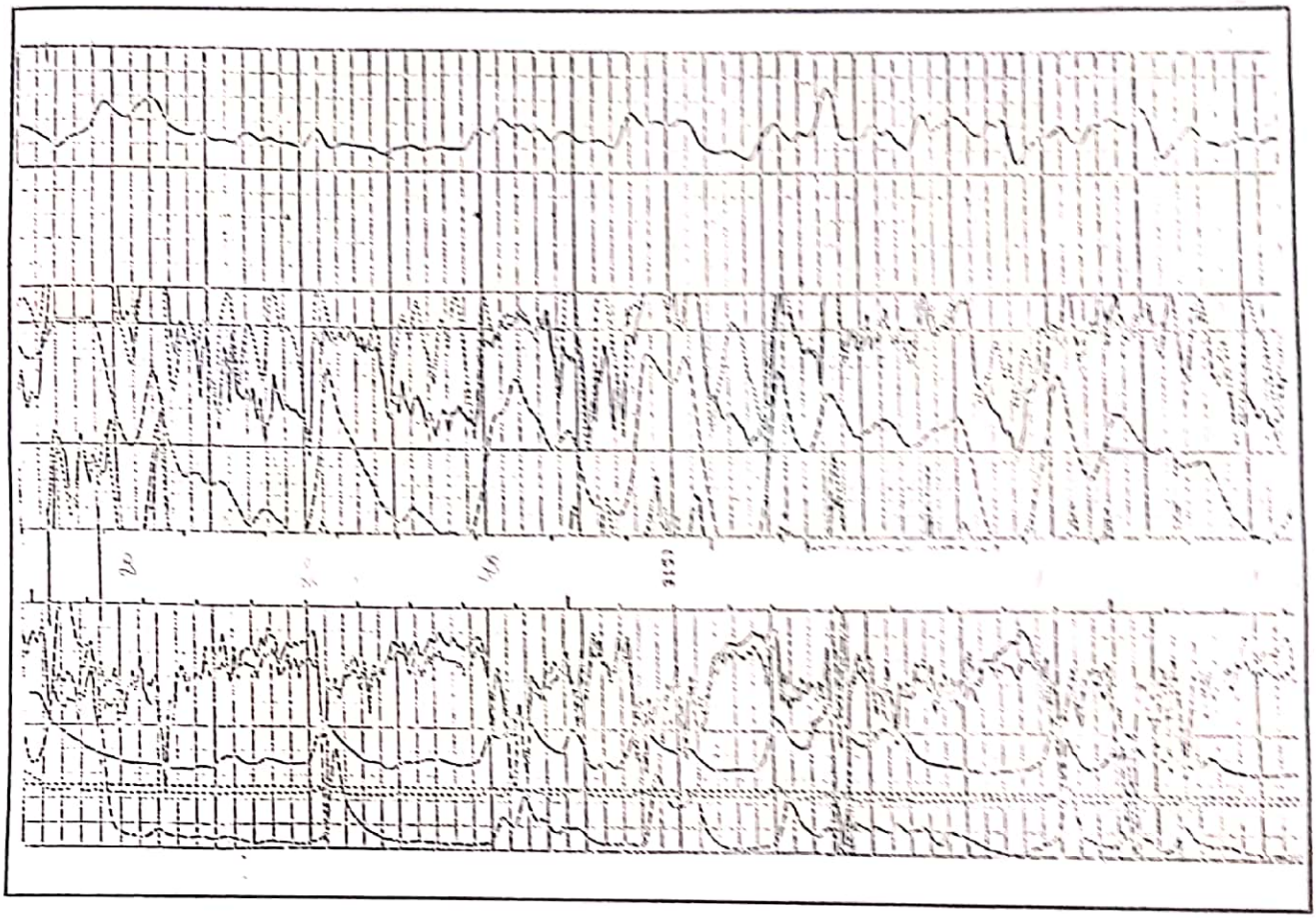

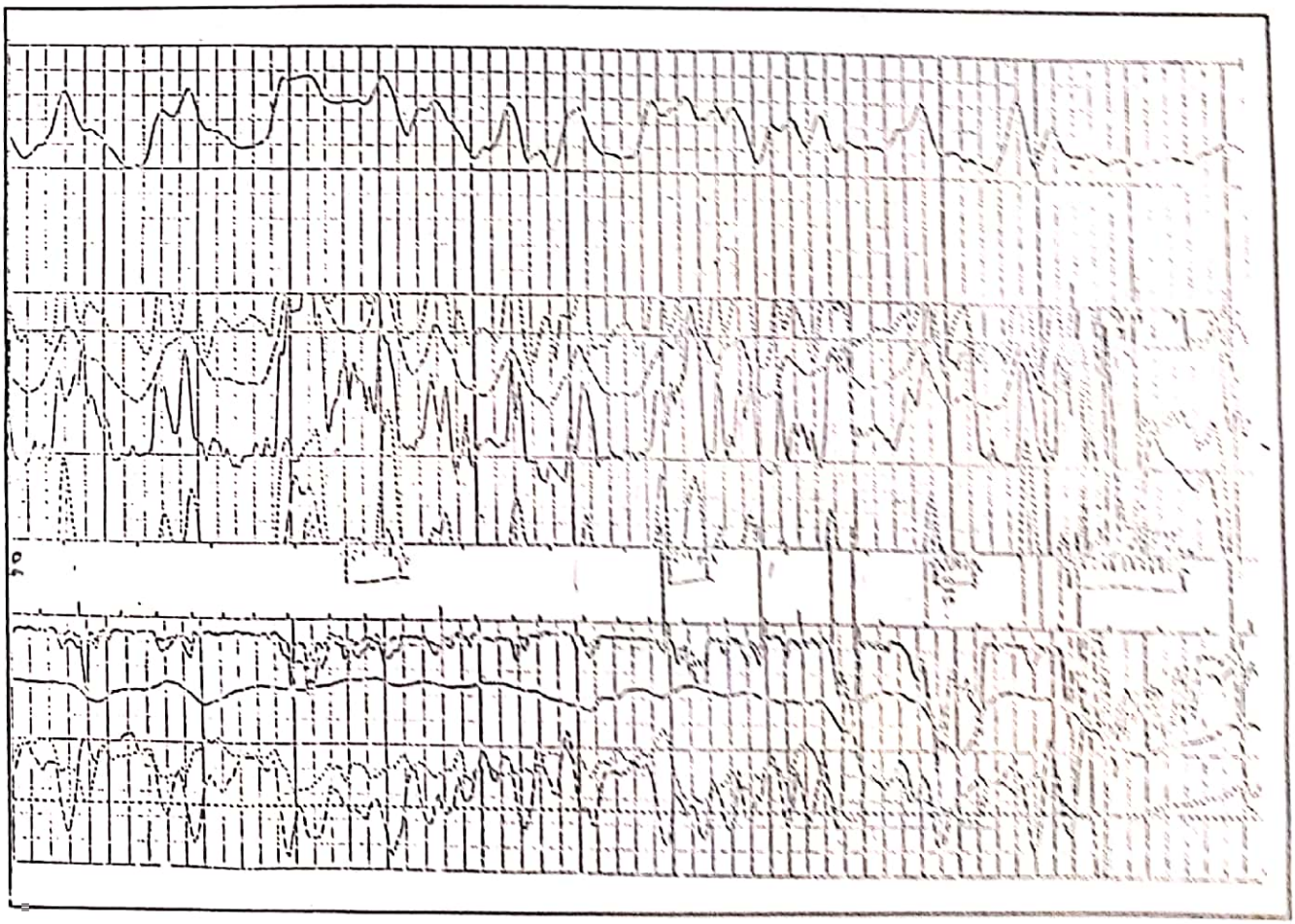

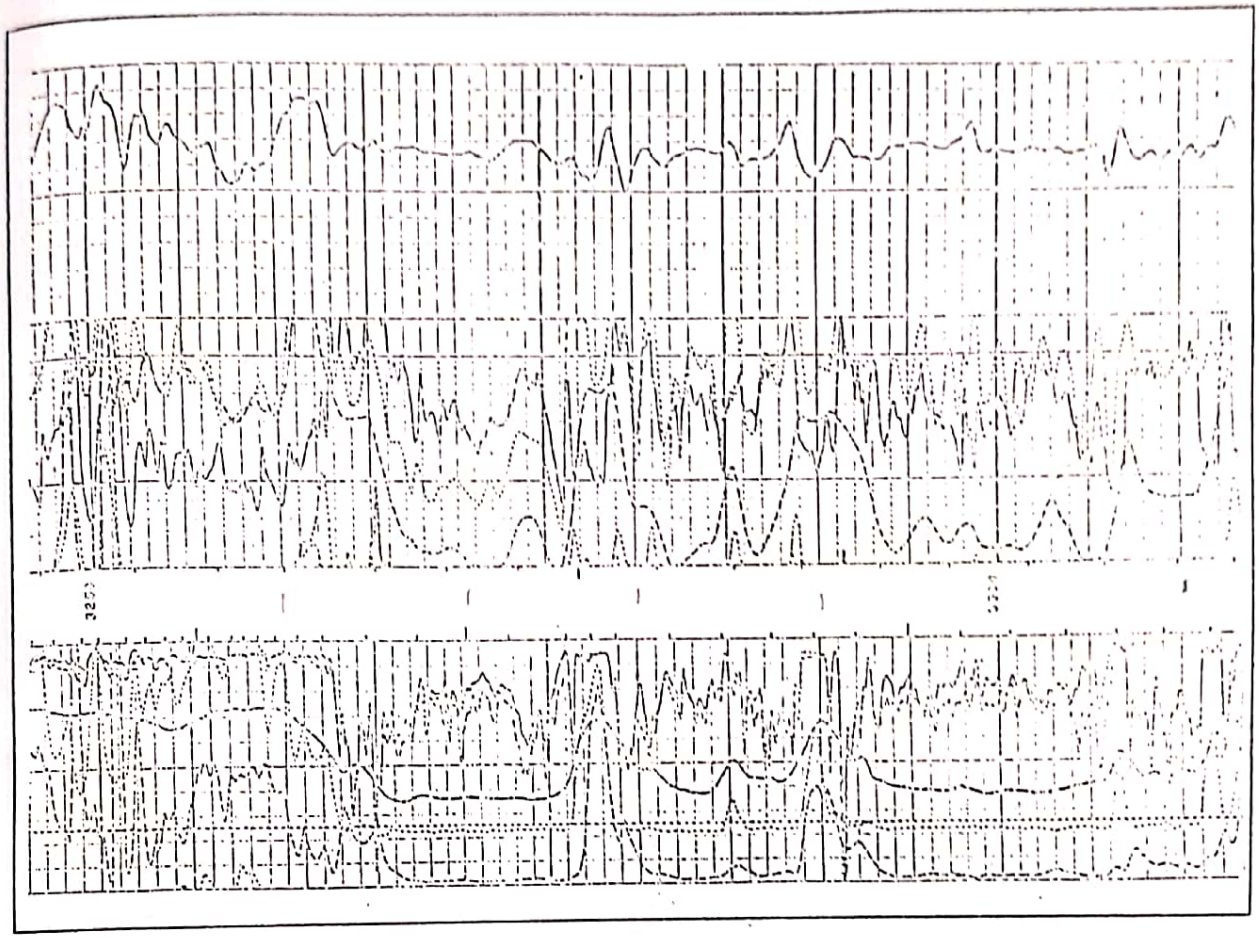

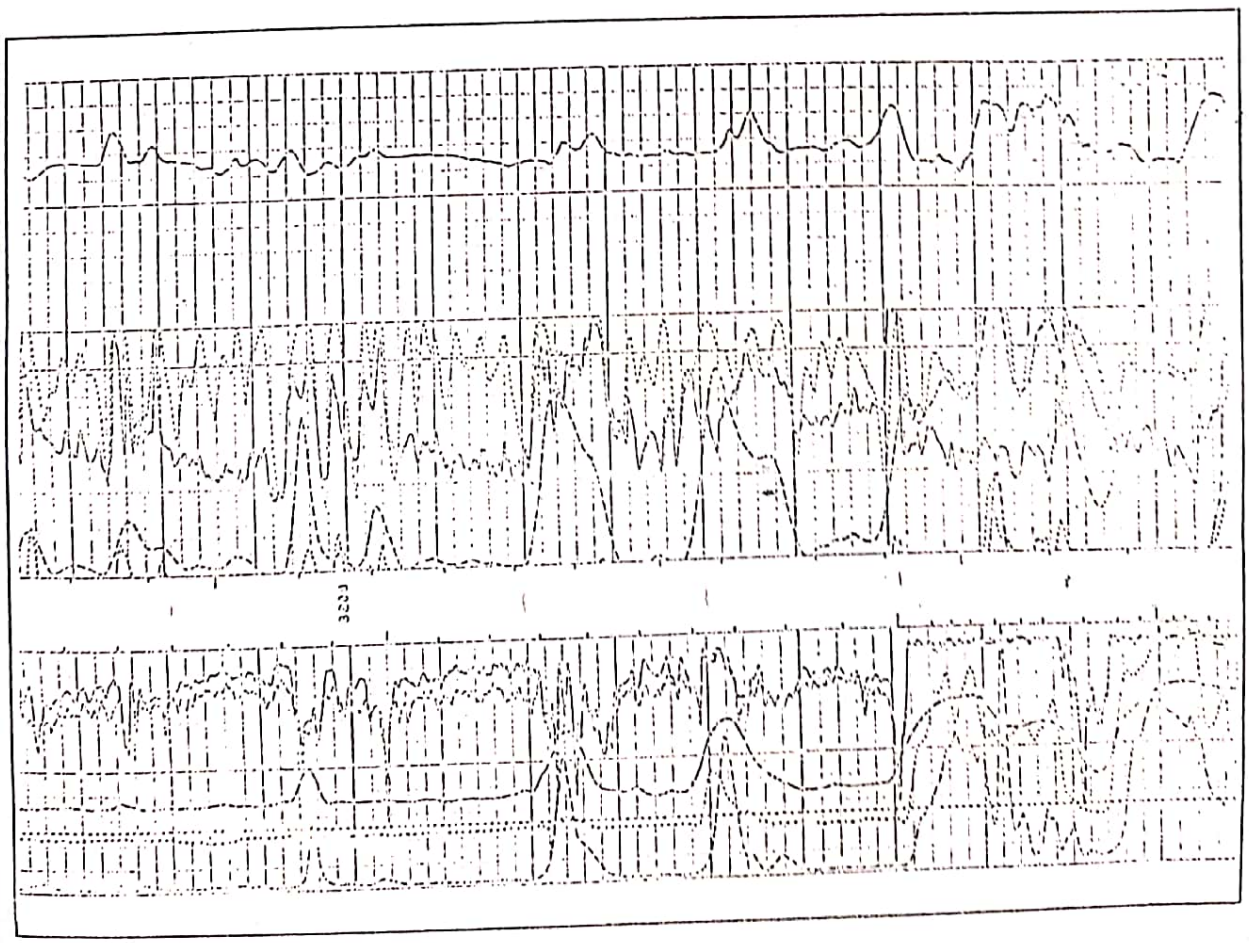

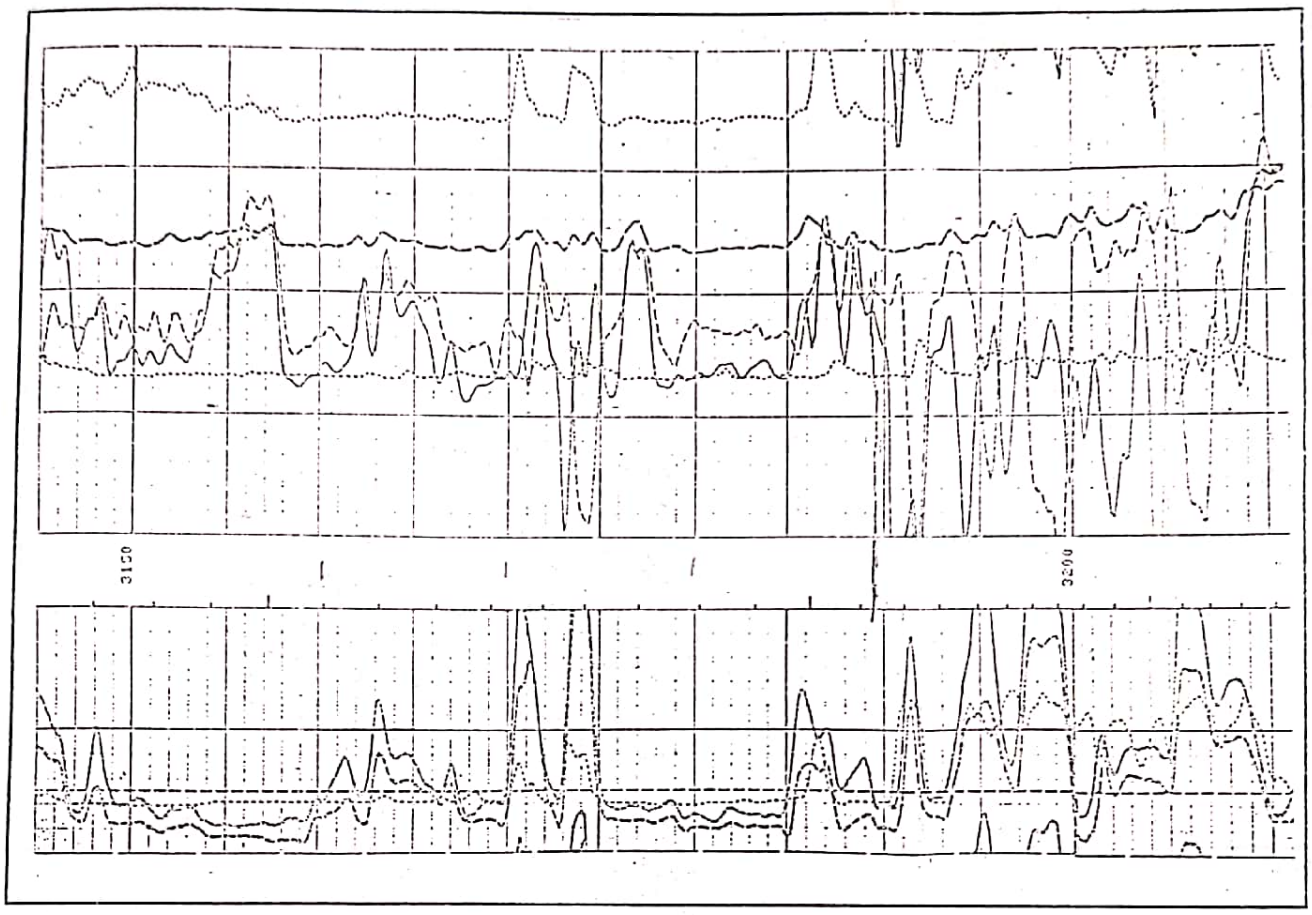

Fig.(B-5) FDC/CNL/CAL/GR Logs for Well No.(EB-79)

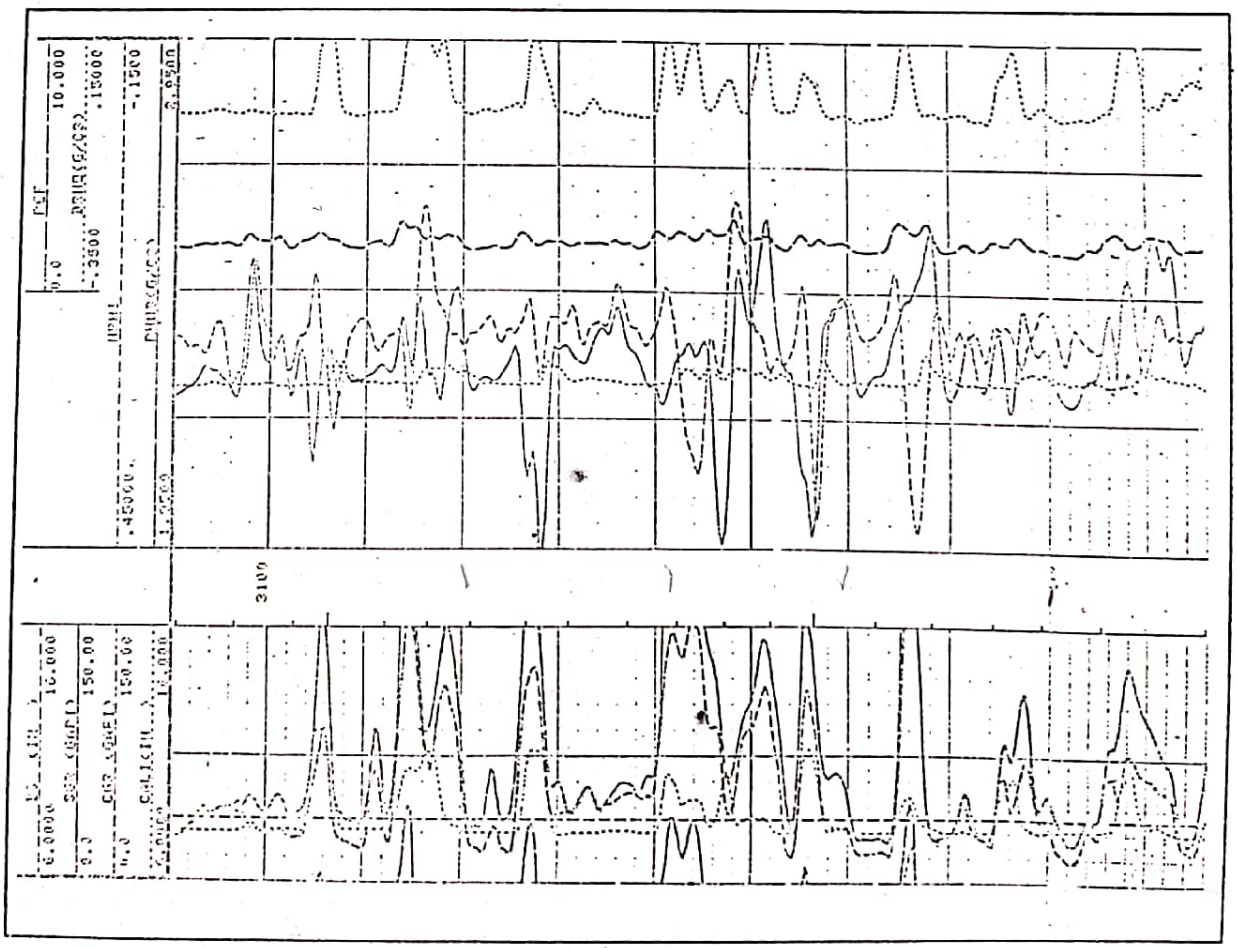

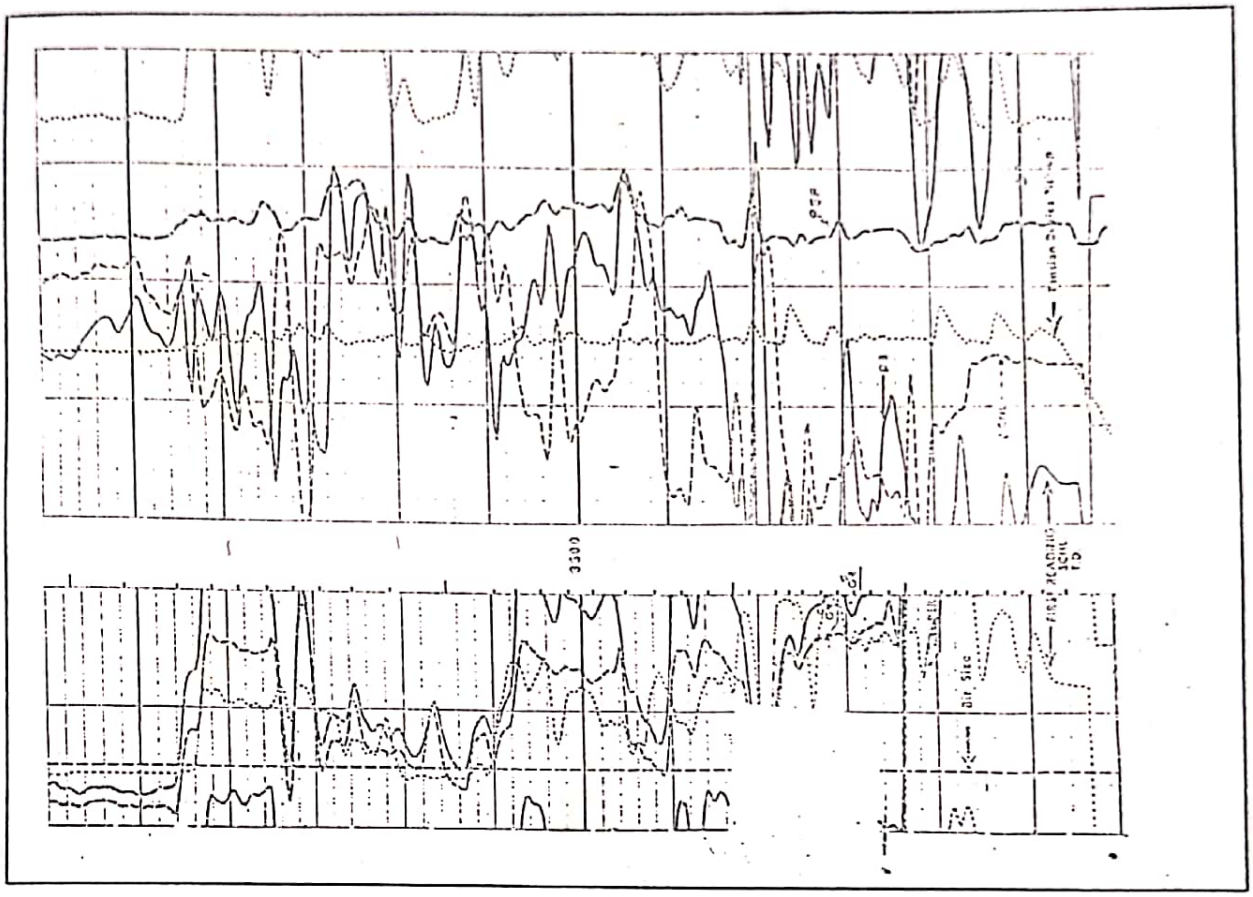

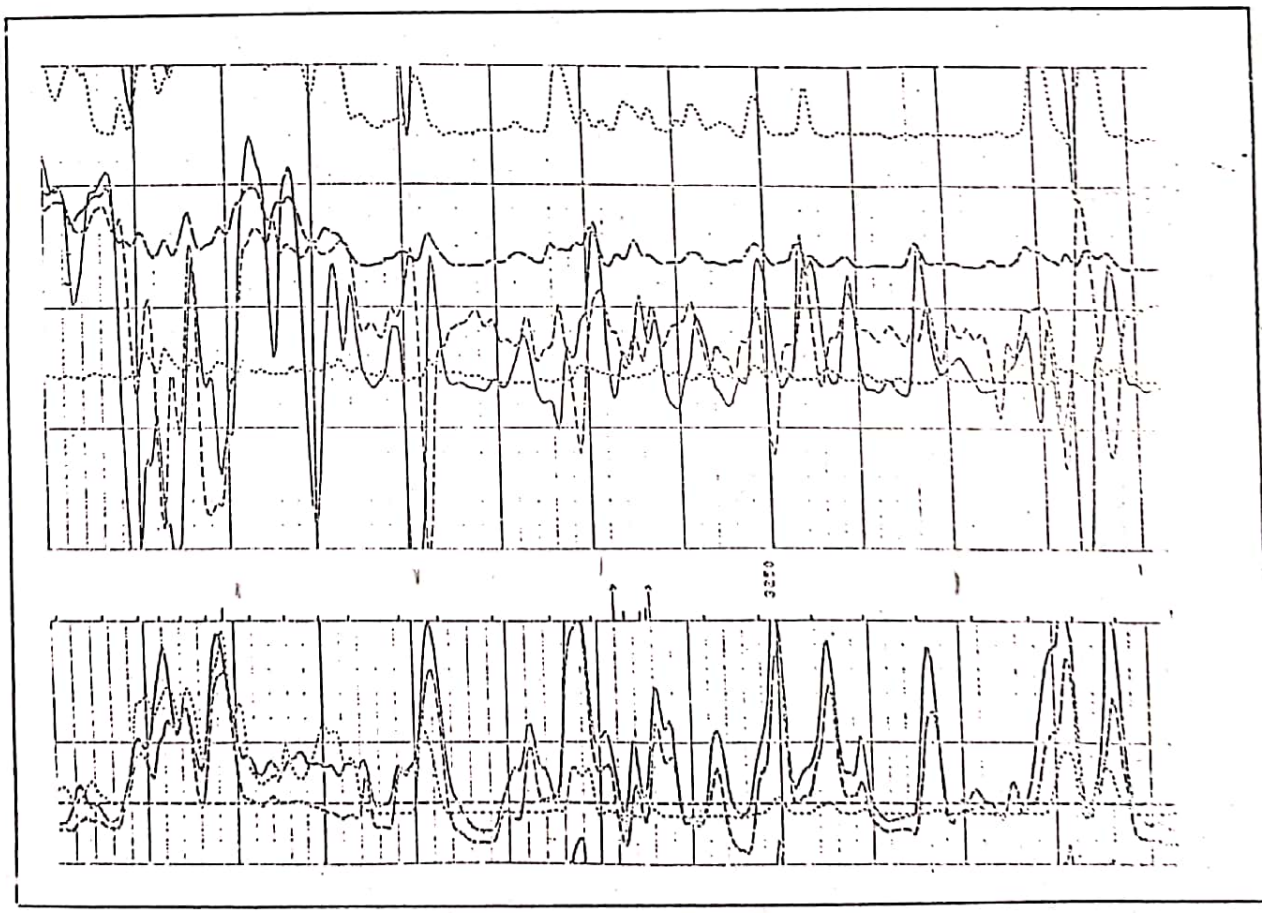

Fig.(3-6) MSFL/SFL/ILD/DT/SP/Rwa for Well No.(EB-79)

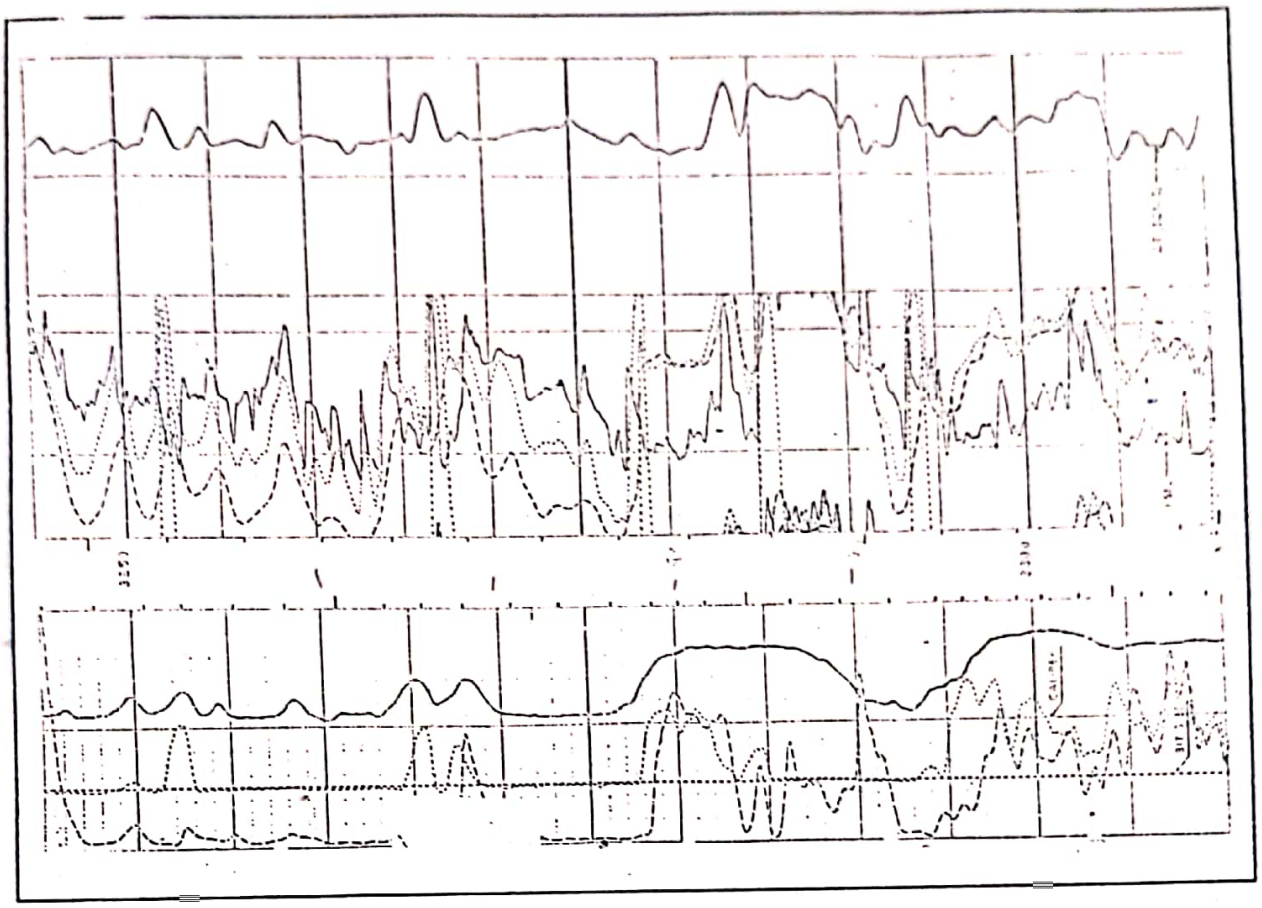

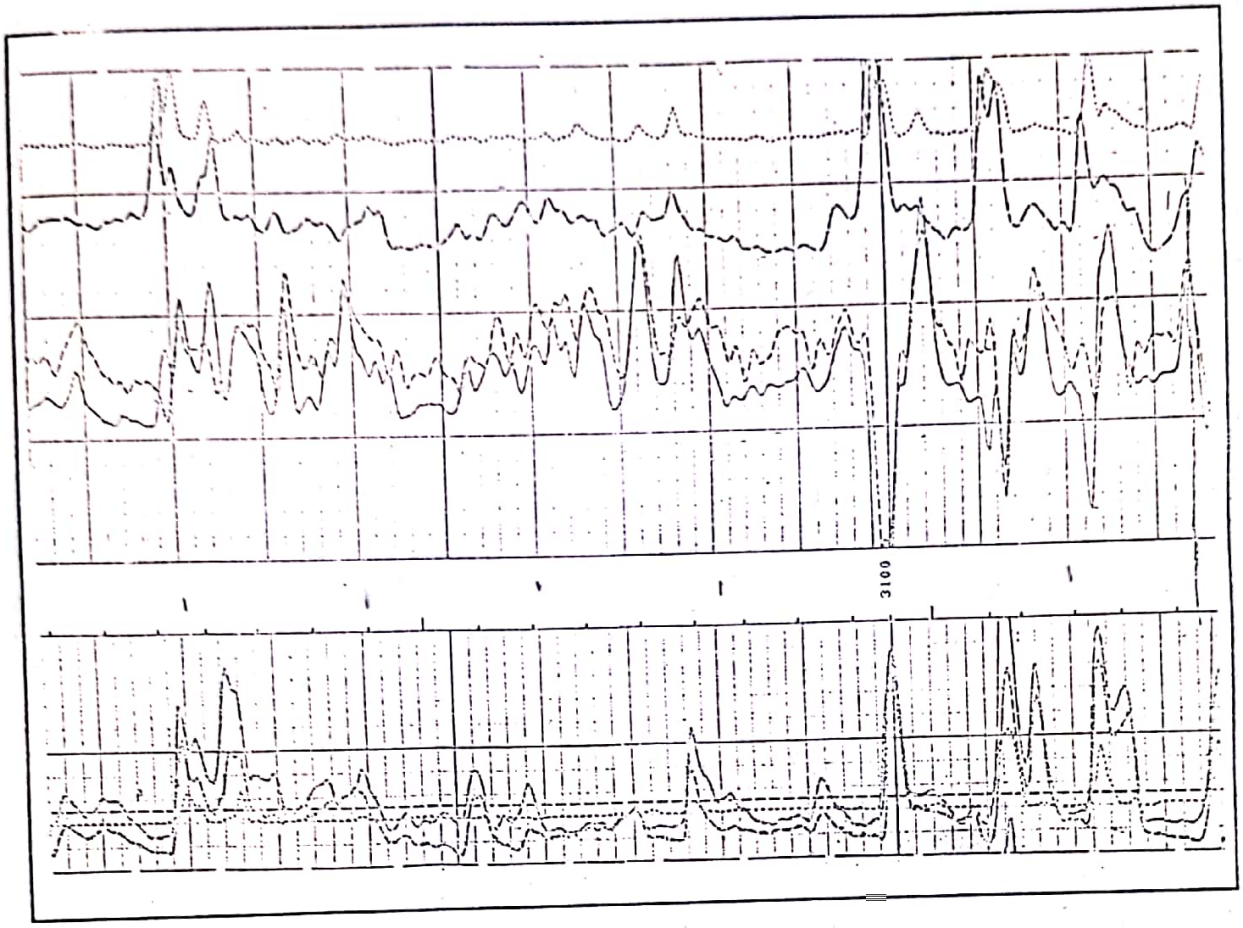

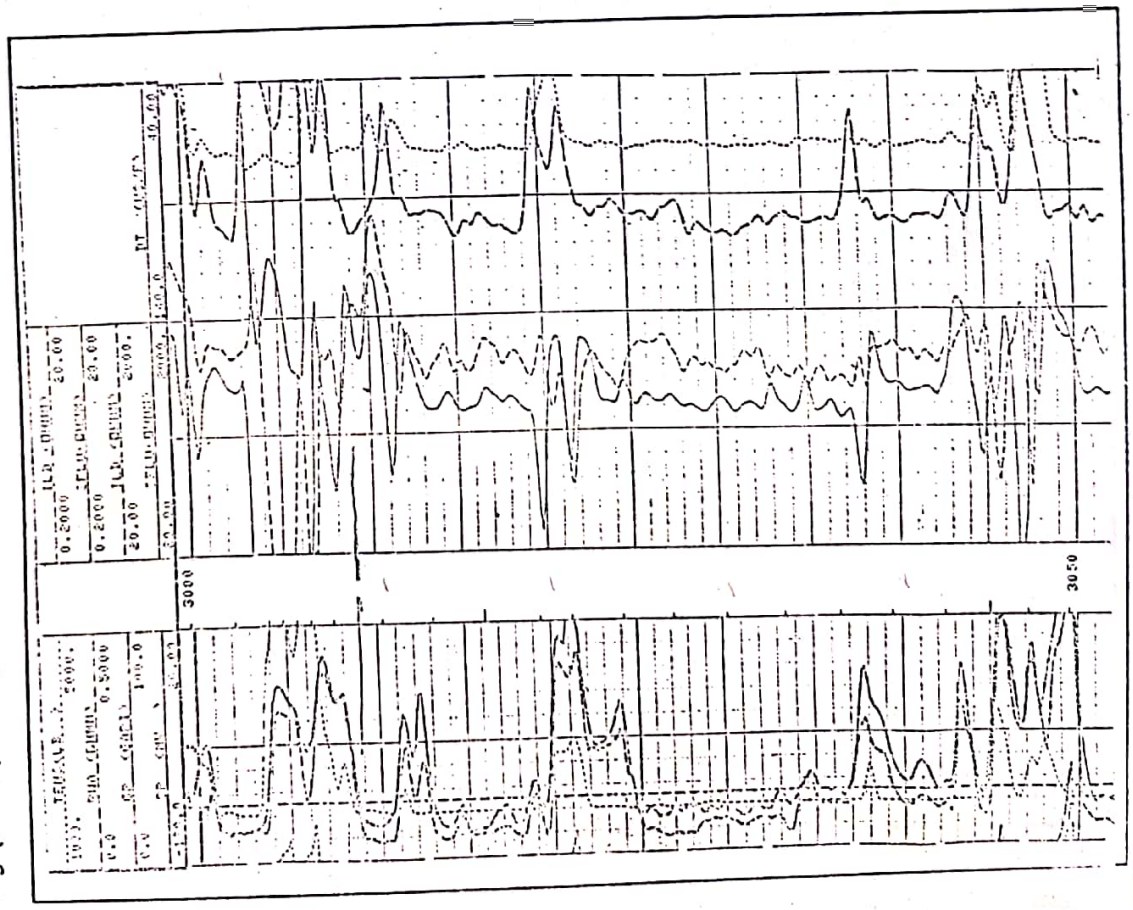

Fig.(B-7) FDC/CNL/CAL/GR Logs for Well No.(EB-77)

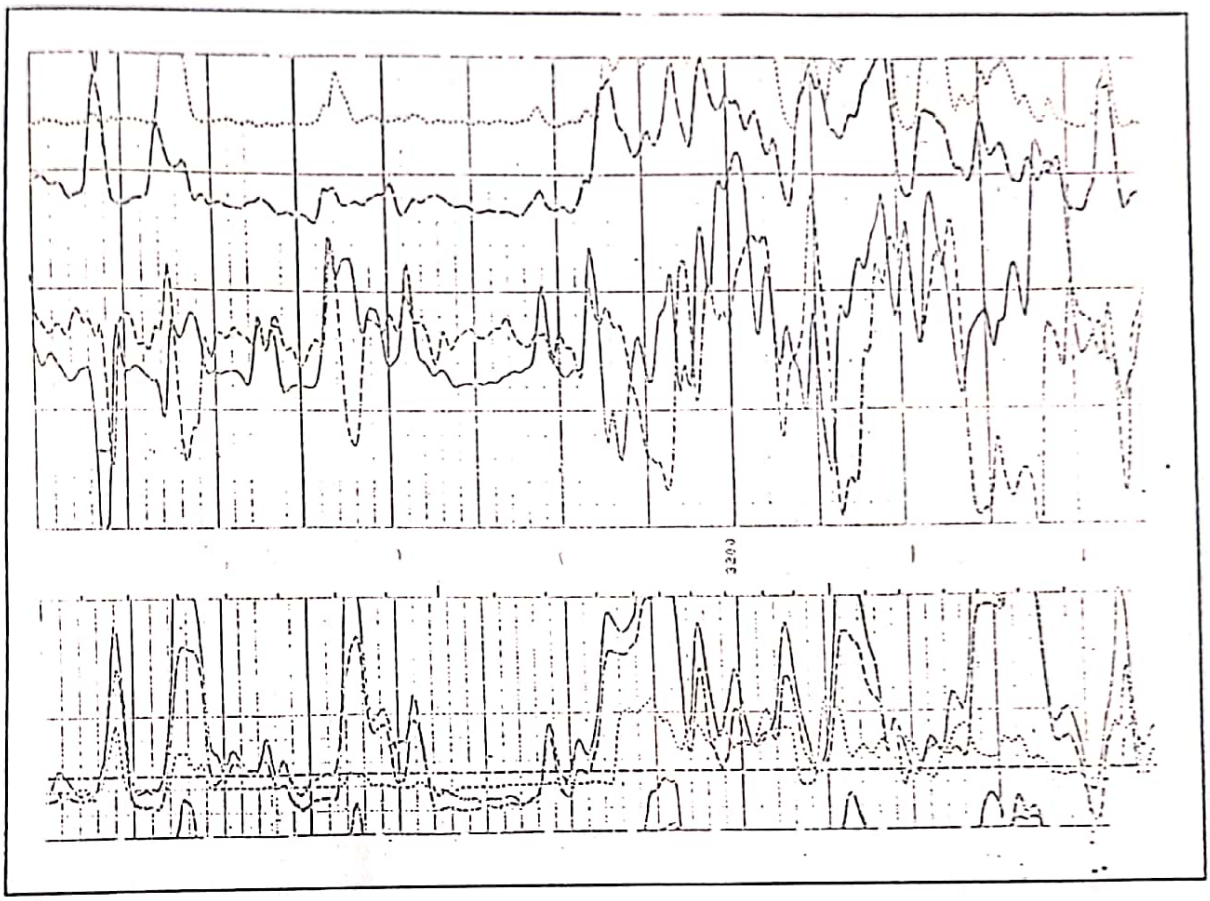

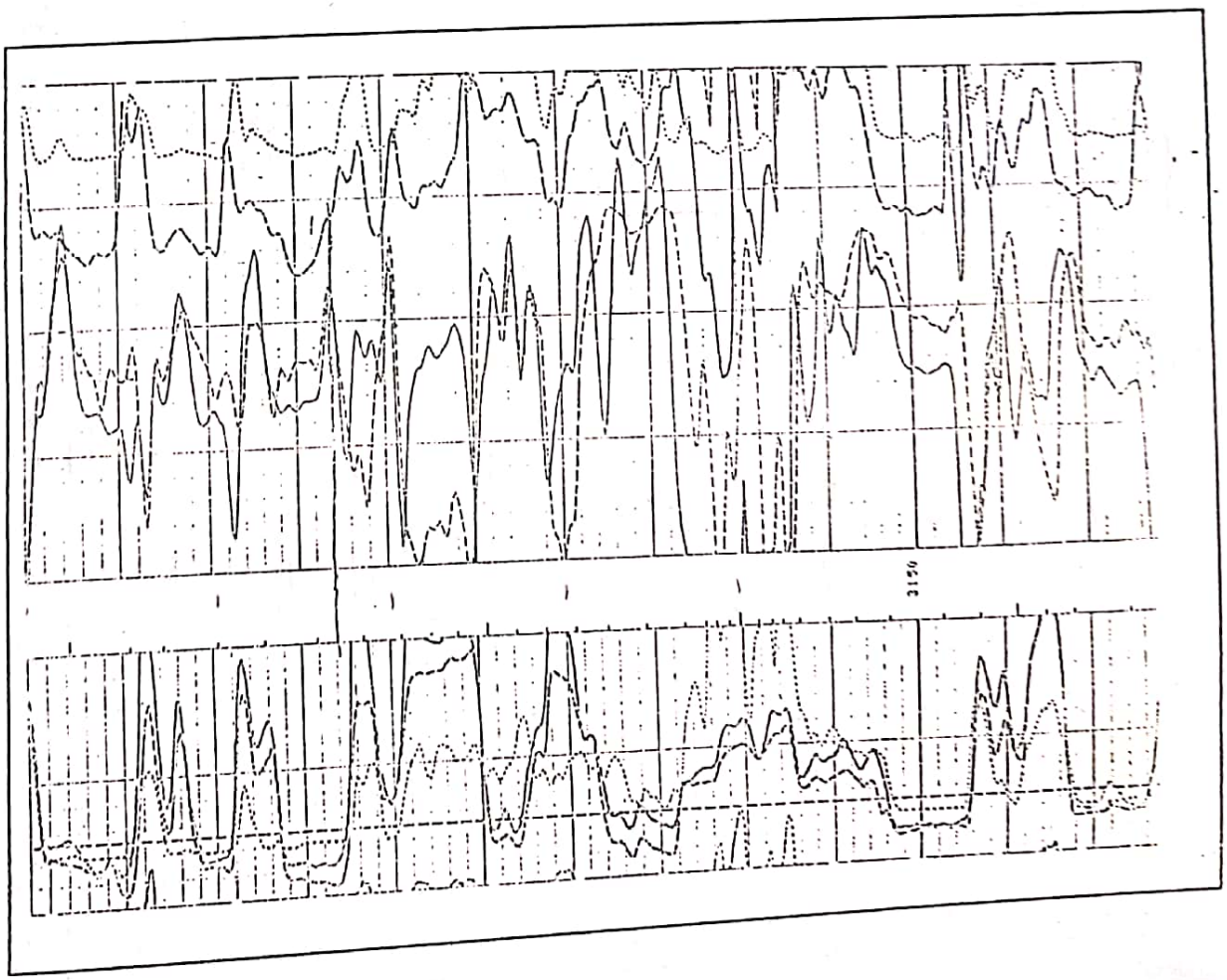

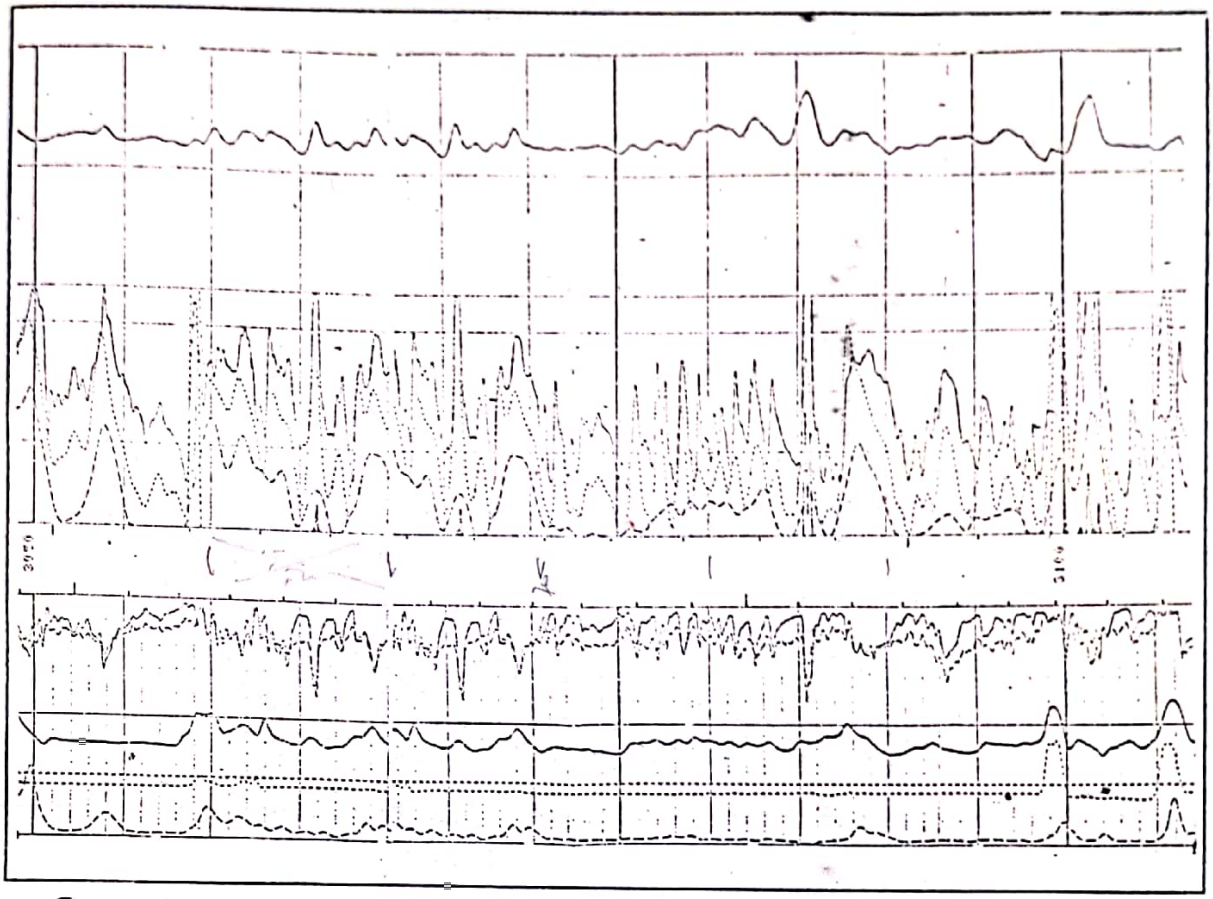

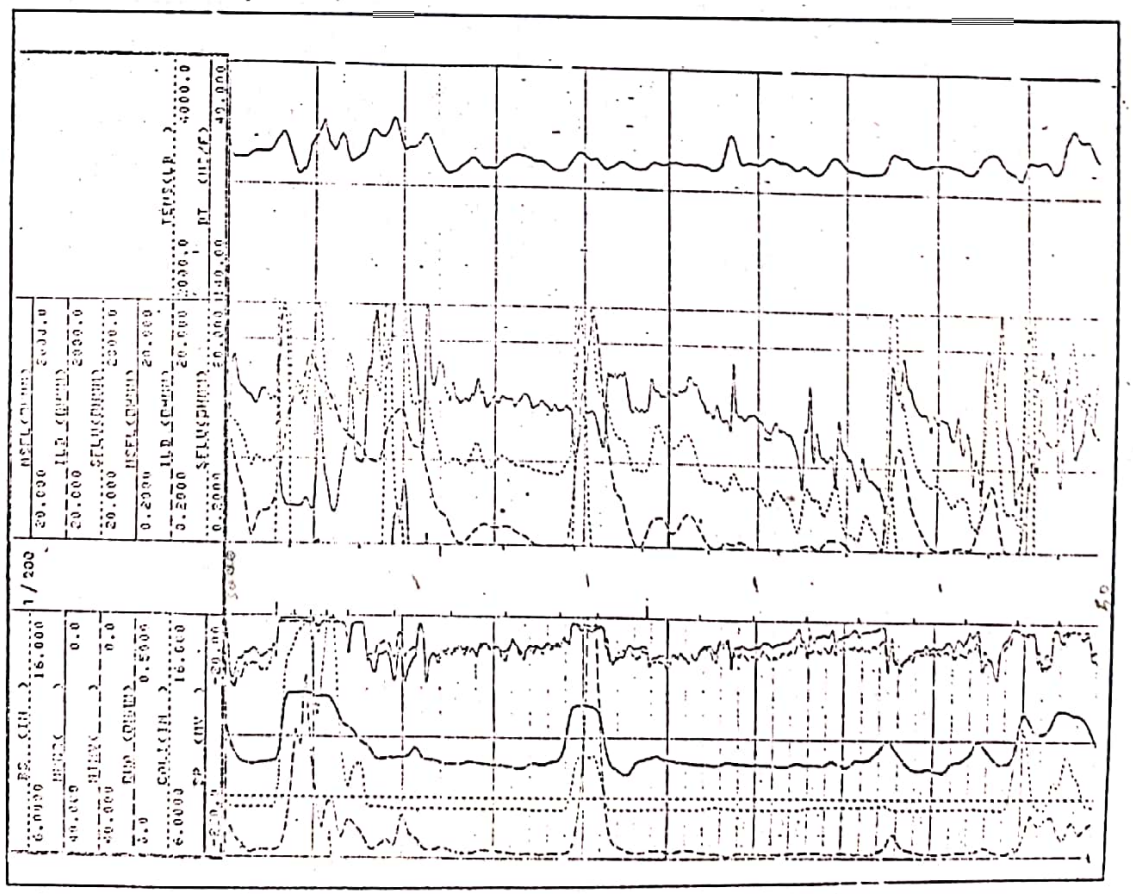

Fig.(B-8) MSFL/SFL/ILD/DT/SP/Rwa for Well No.(EB-77)

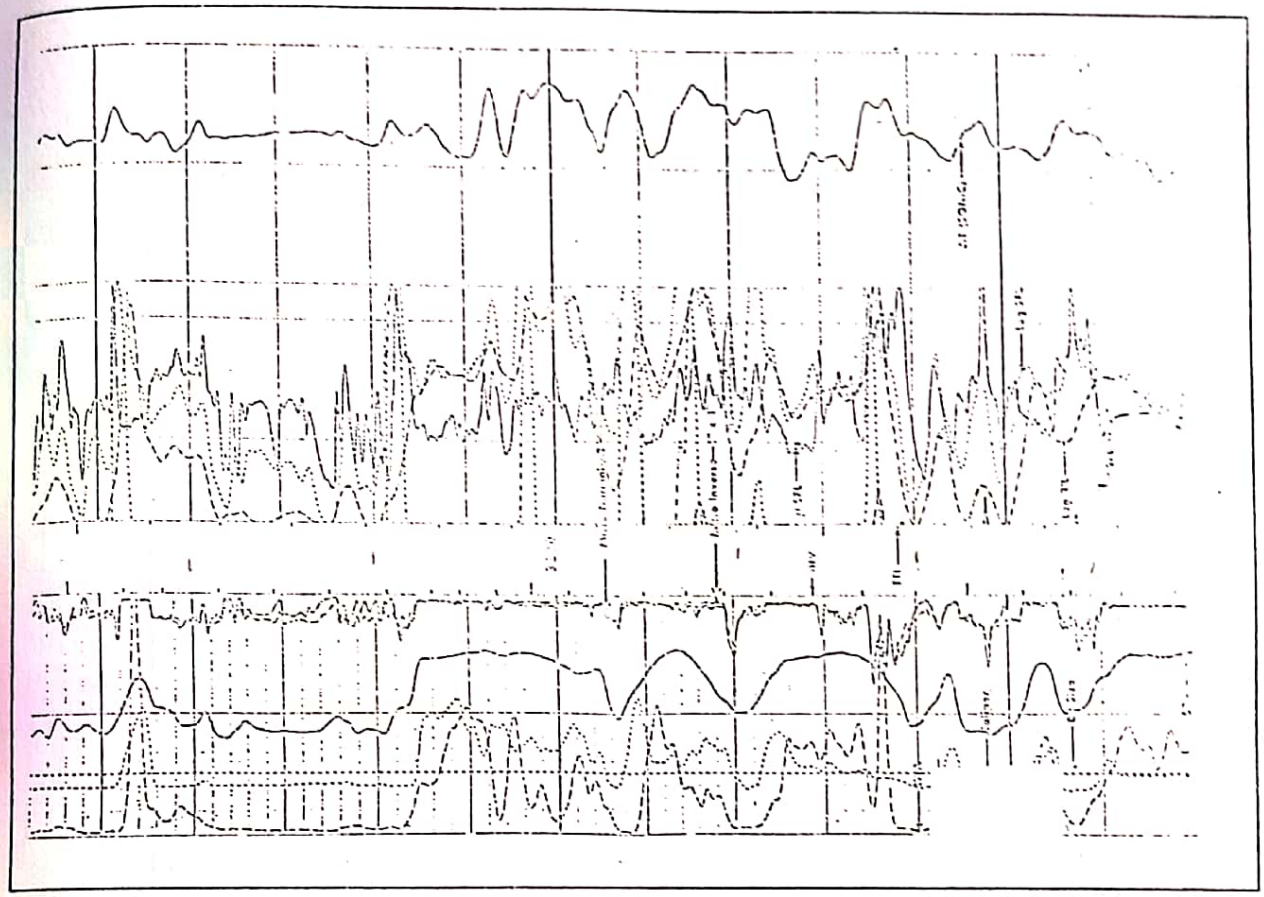

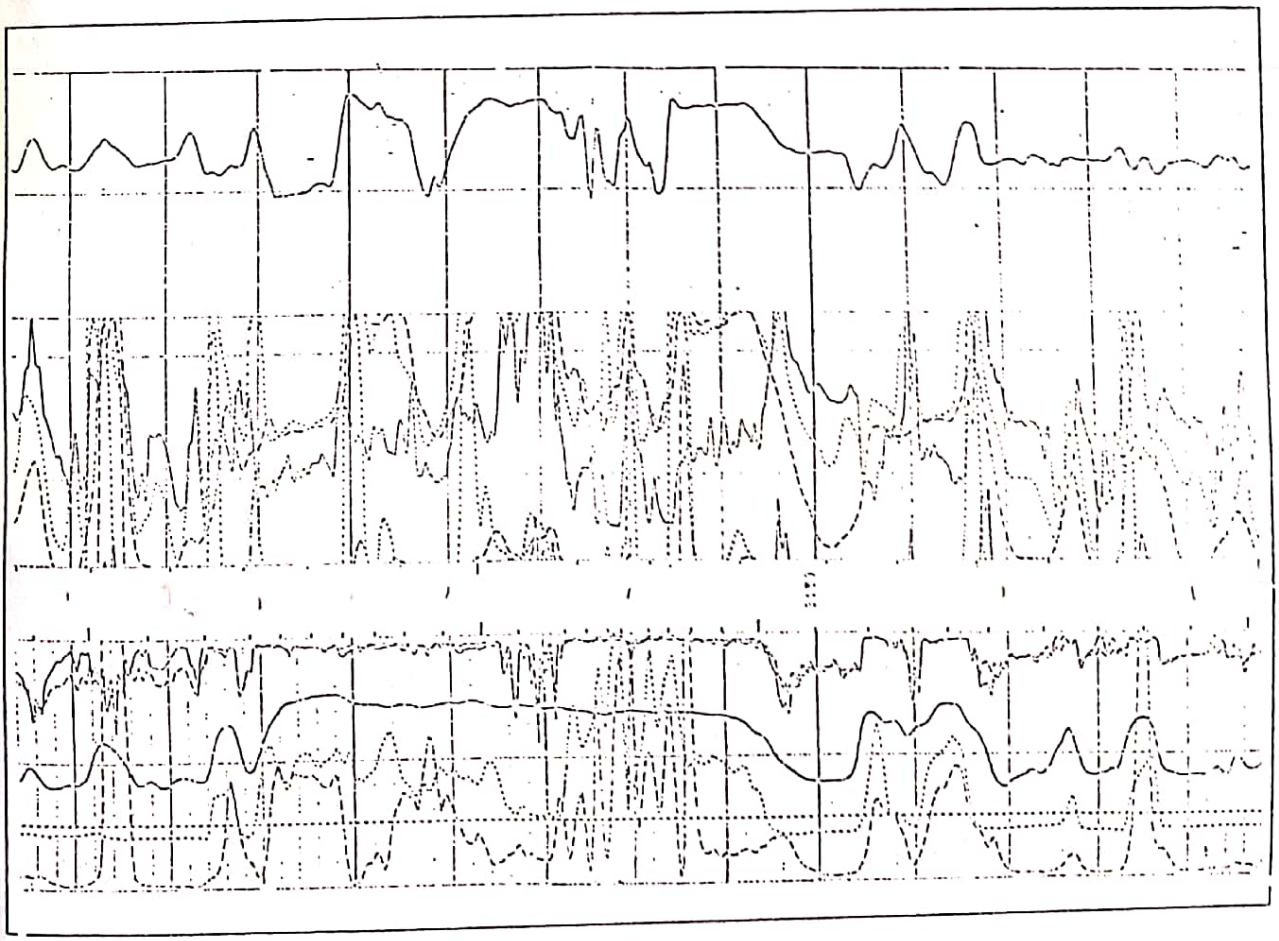

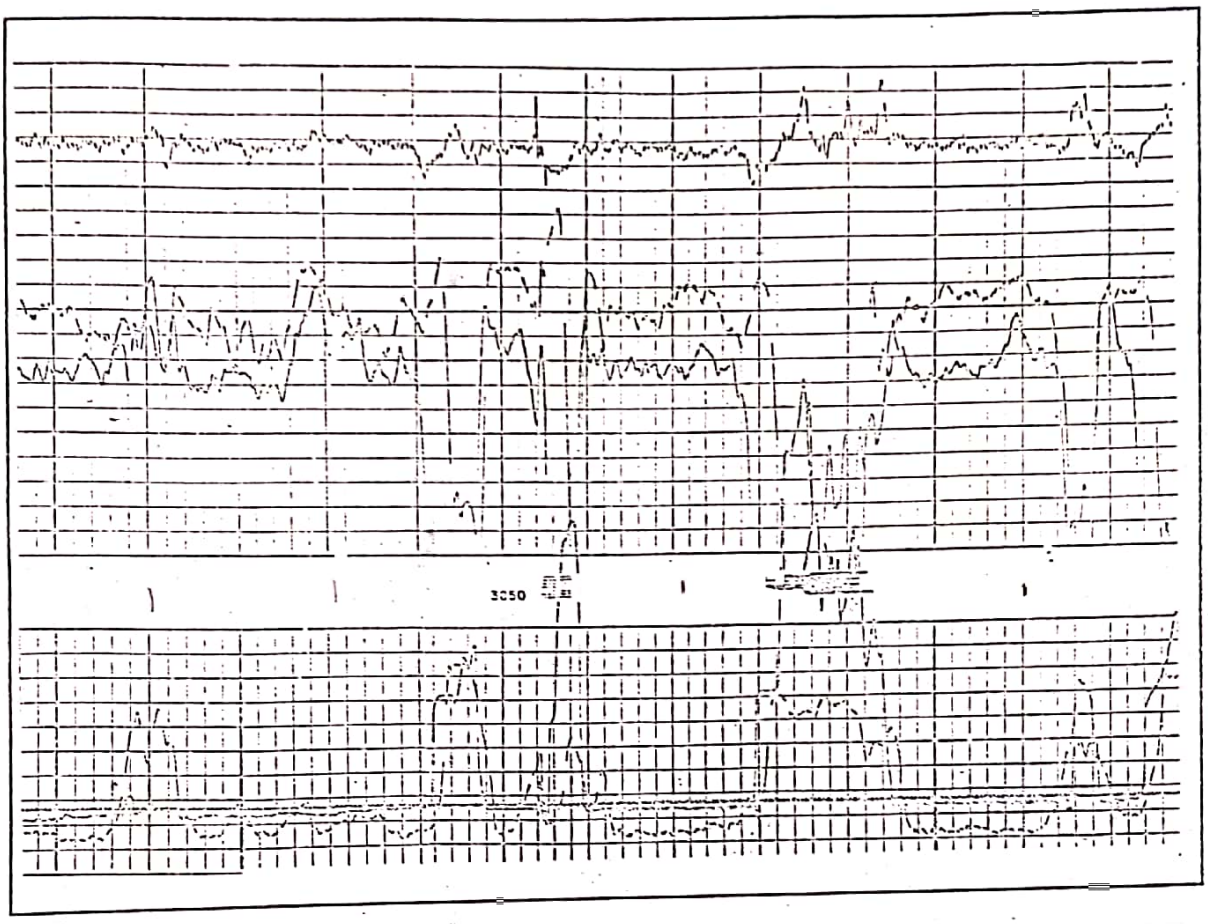

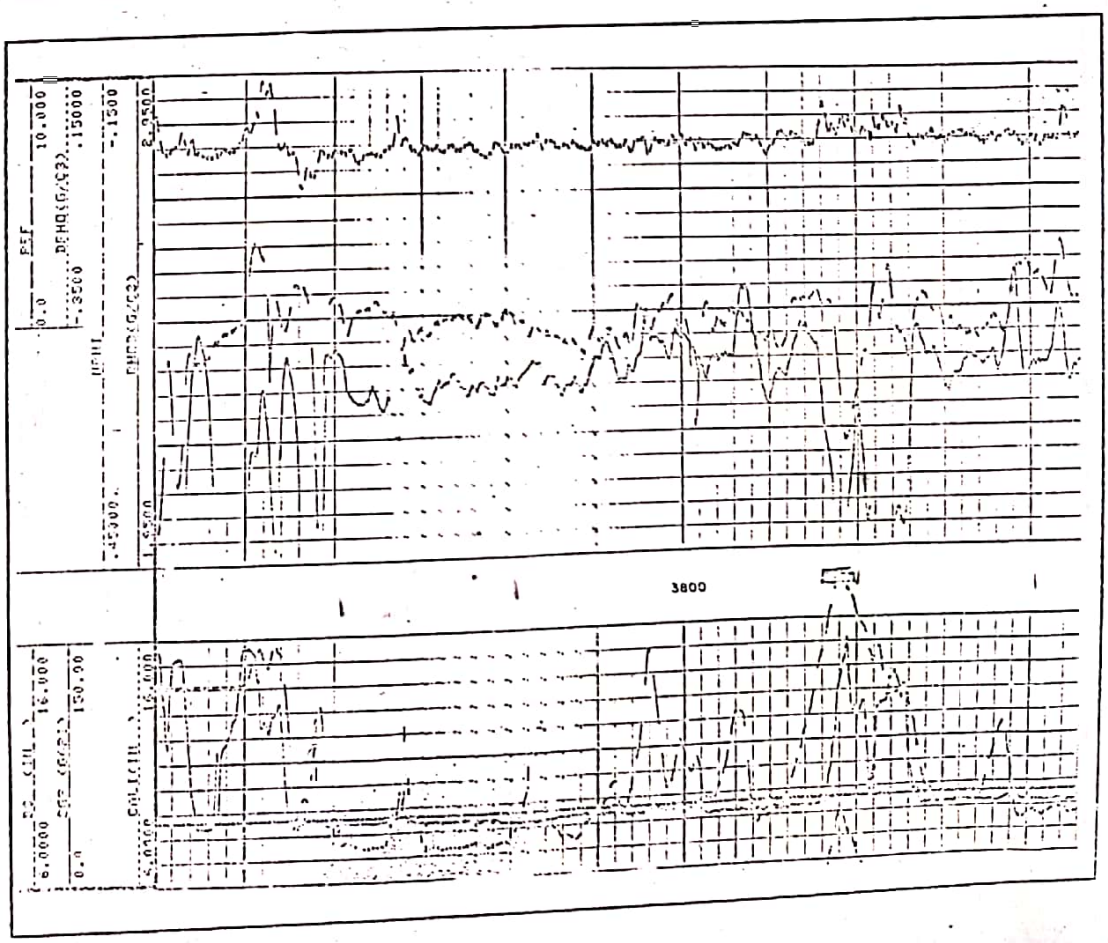

Fig.(B-9) FDC/CNL/CAL/GR Logs for Well No.(EB-15)

Fig. (B-10) MSFL/SFL/ILD/DT/SP/Rwa for Well No.(EE.15)

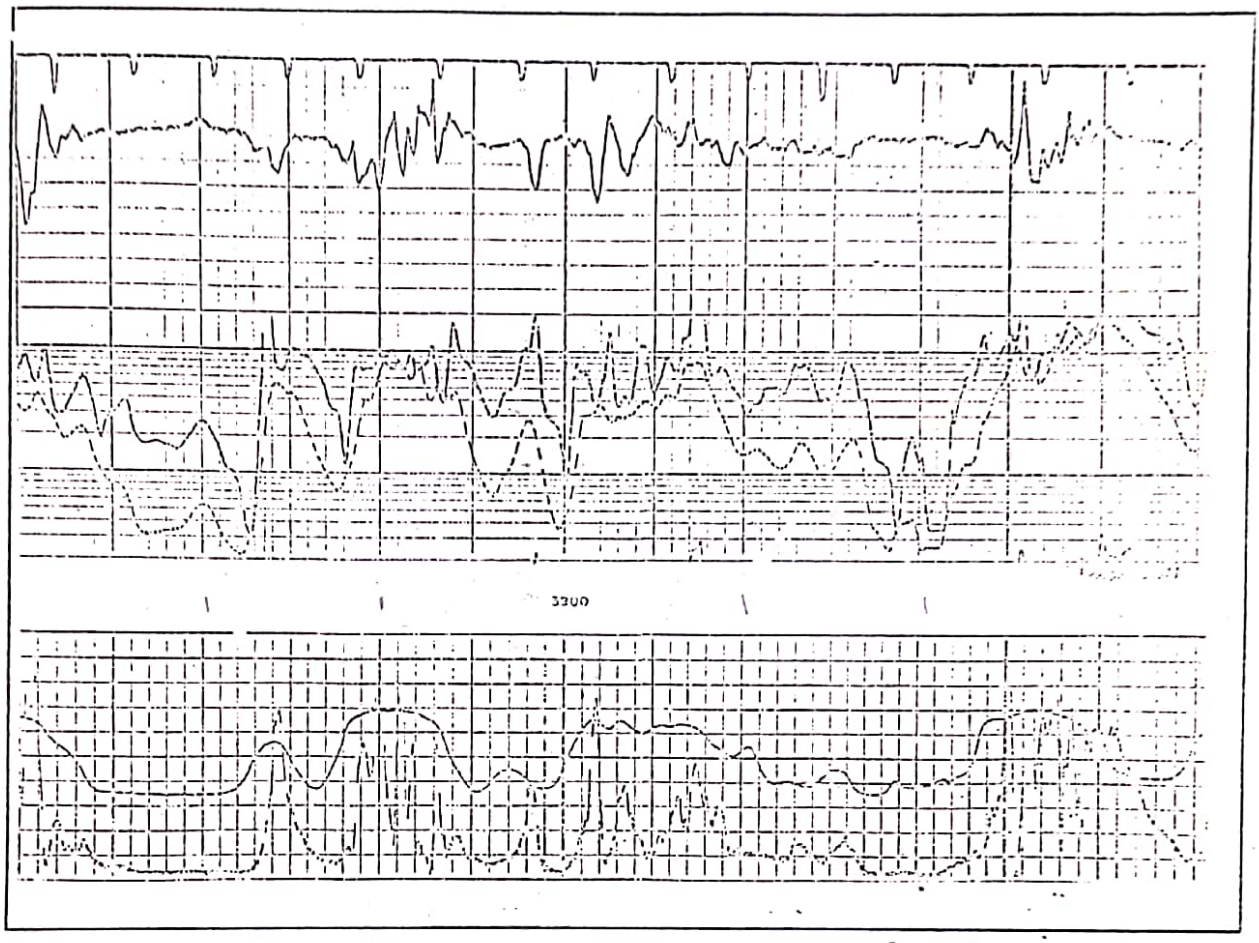

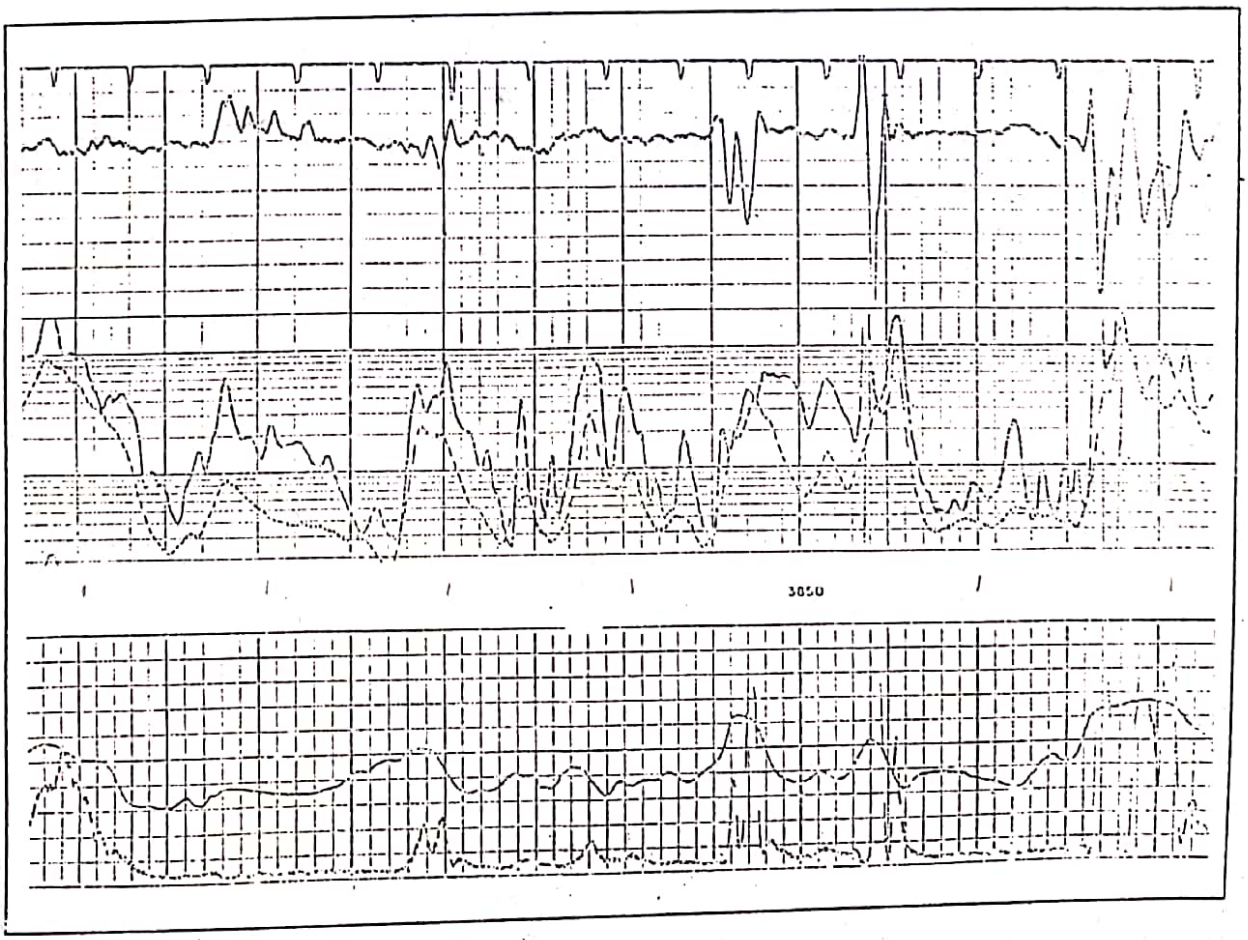

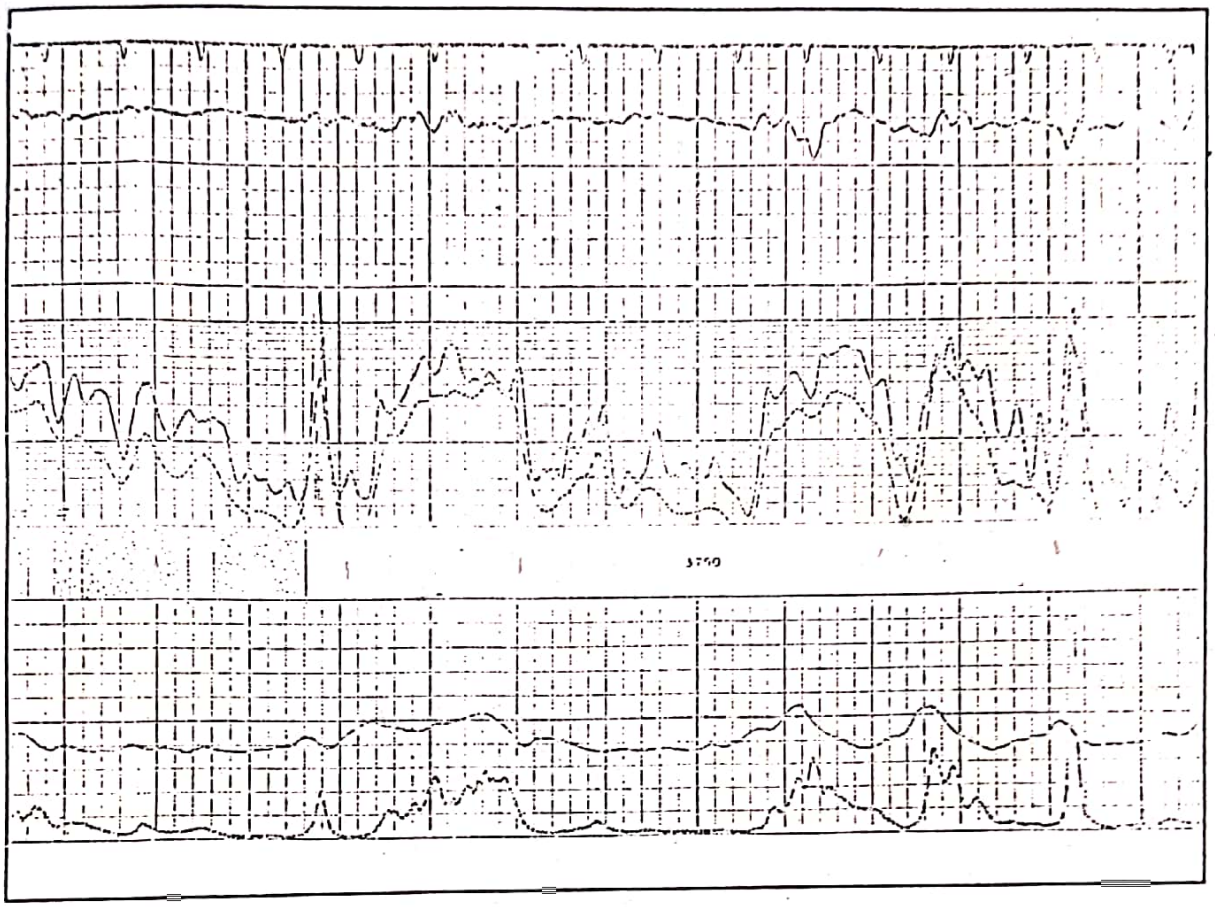

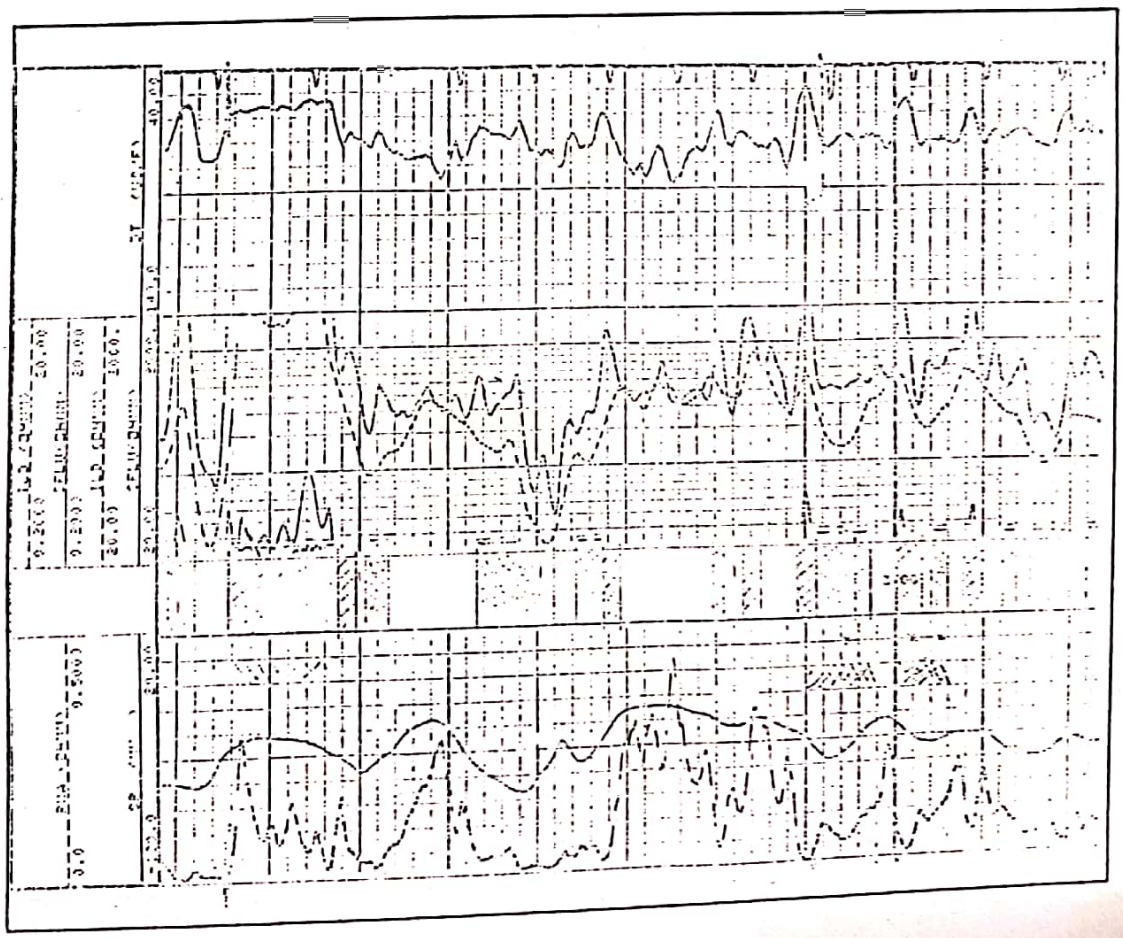

Fig (3.11) MSFL/SFL/ILD/DT/Rwa/SP Logs for KB-18

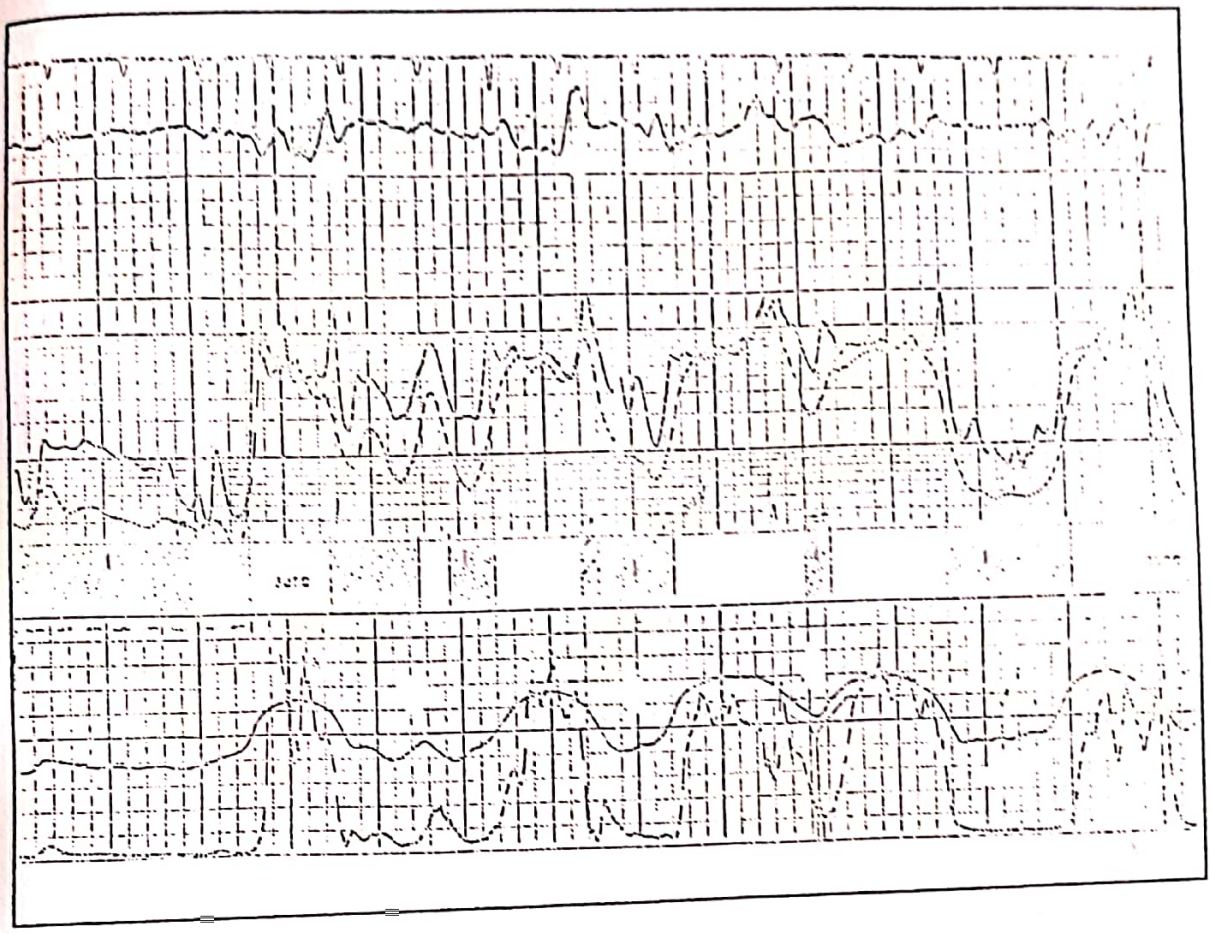

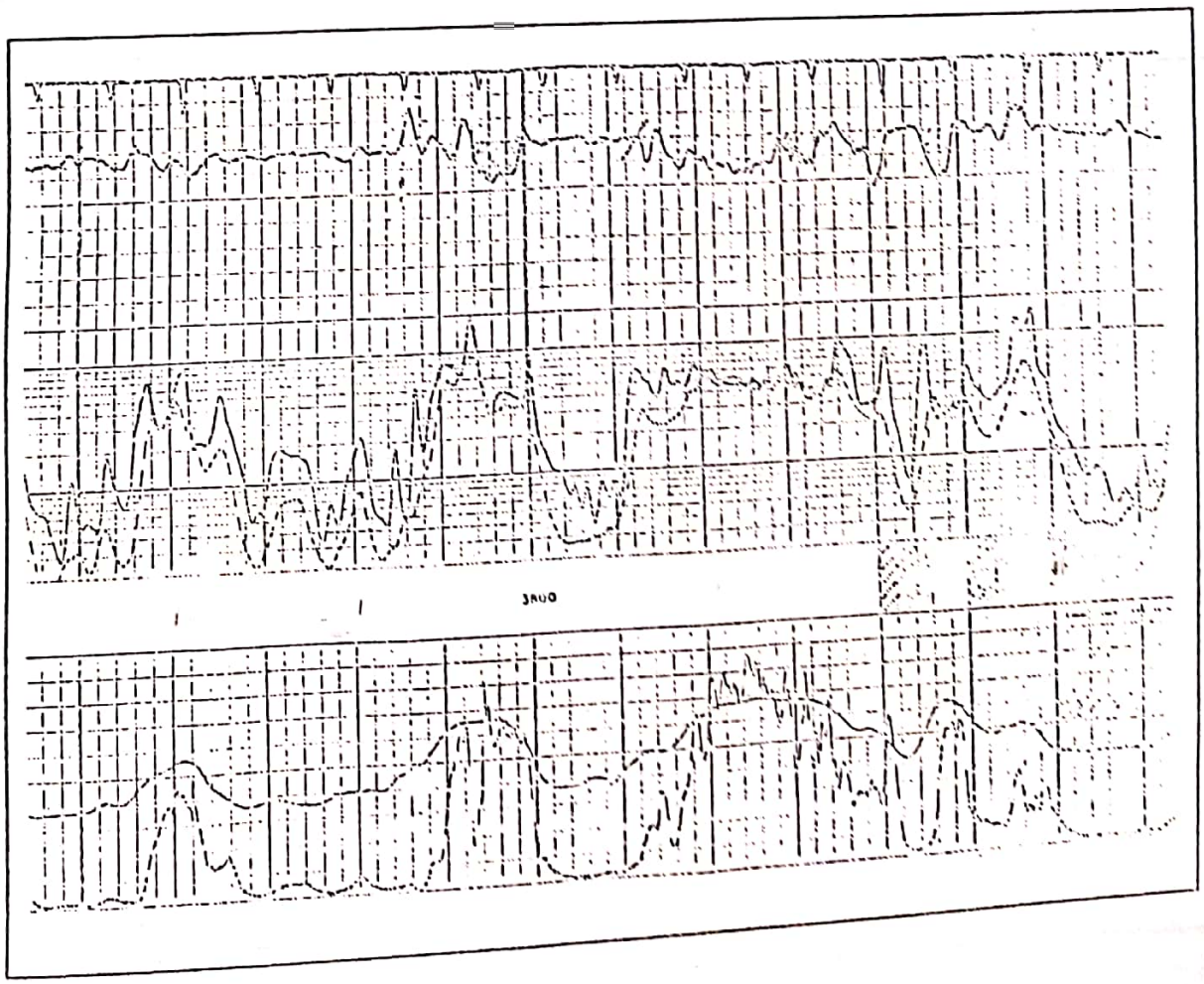

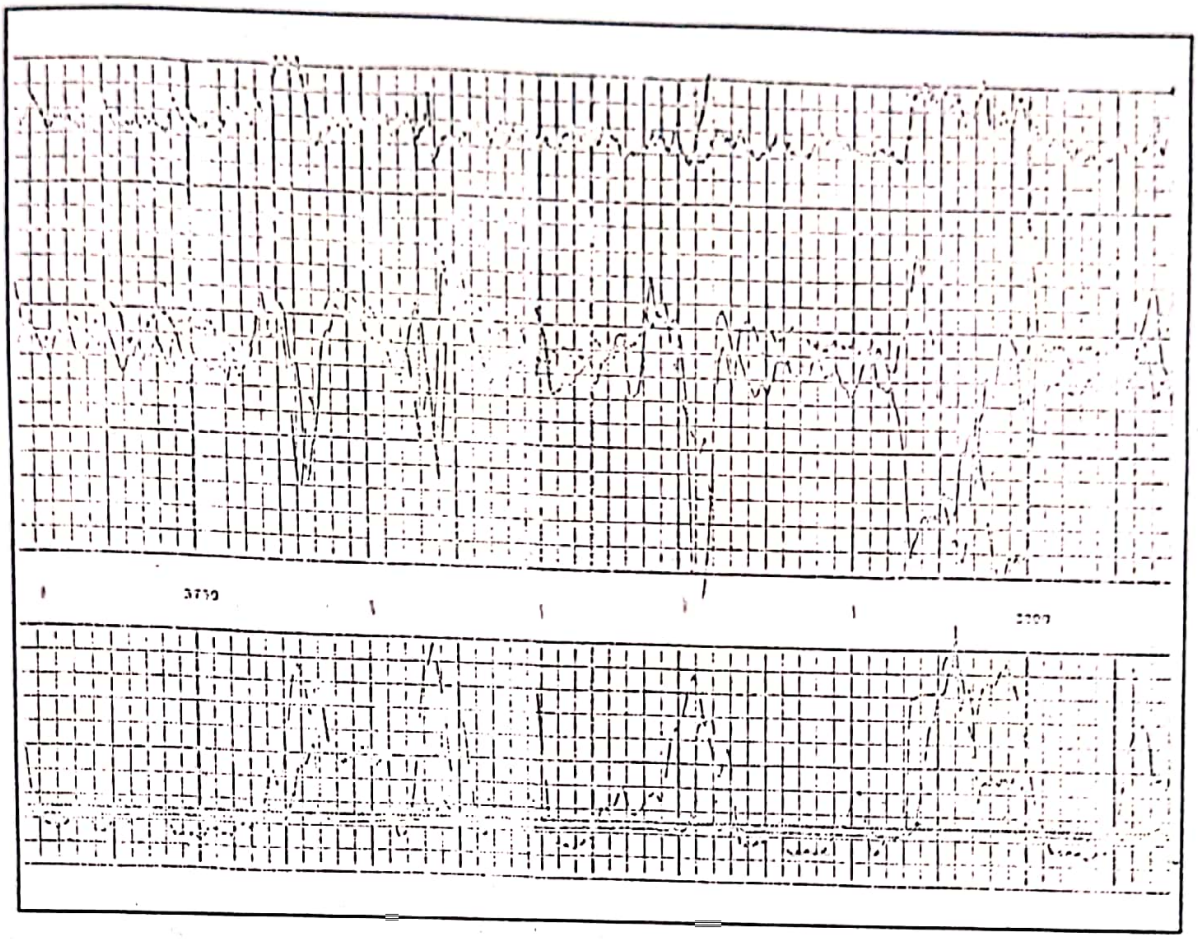

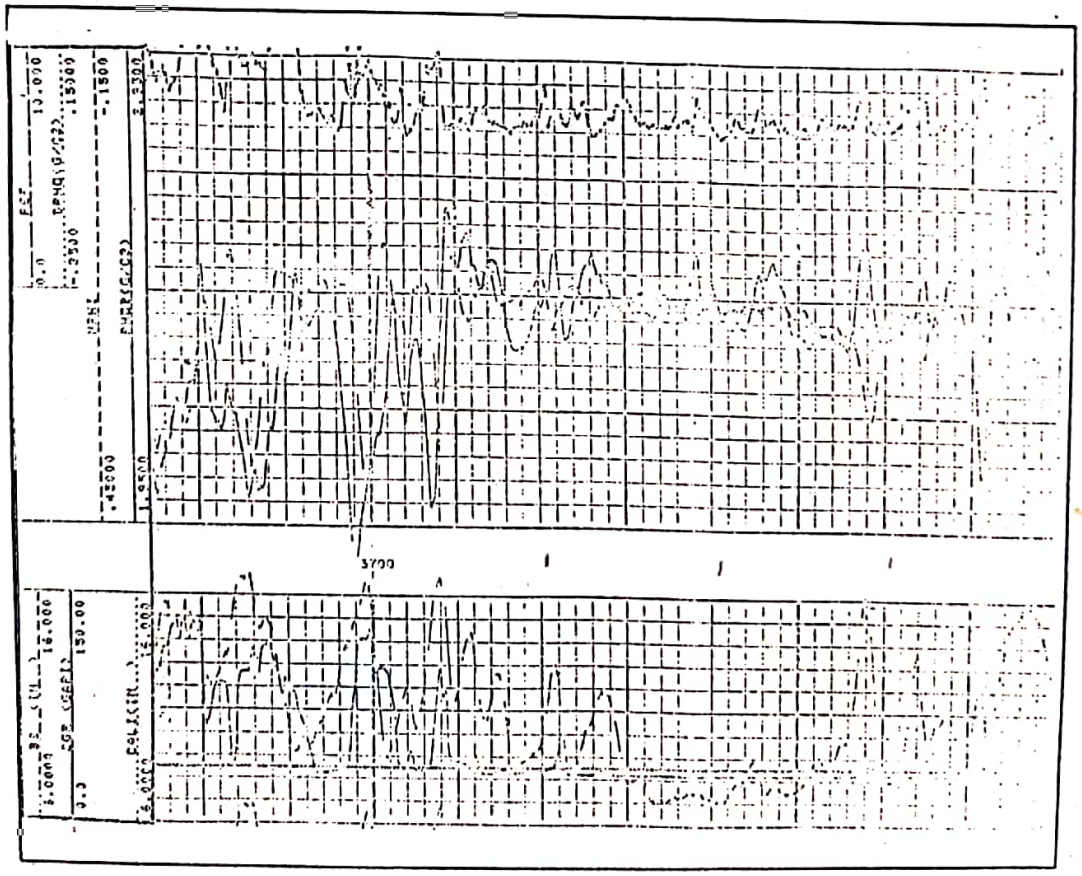

Fig.(B.12) FDC/CNL/CAL/GR Logs for Well No.(EB-18)

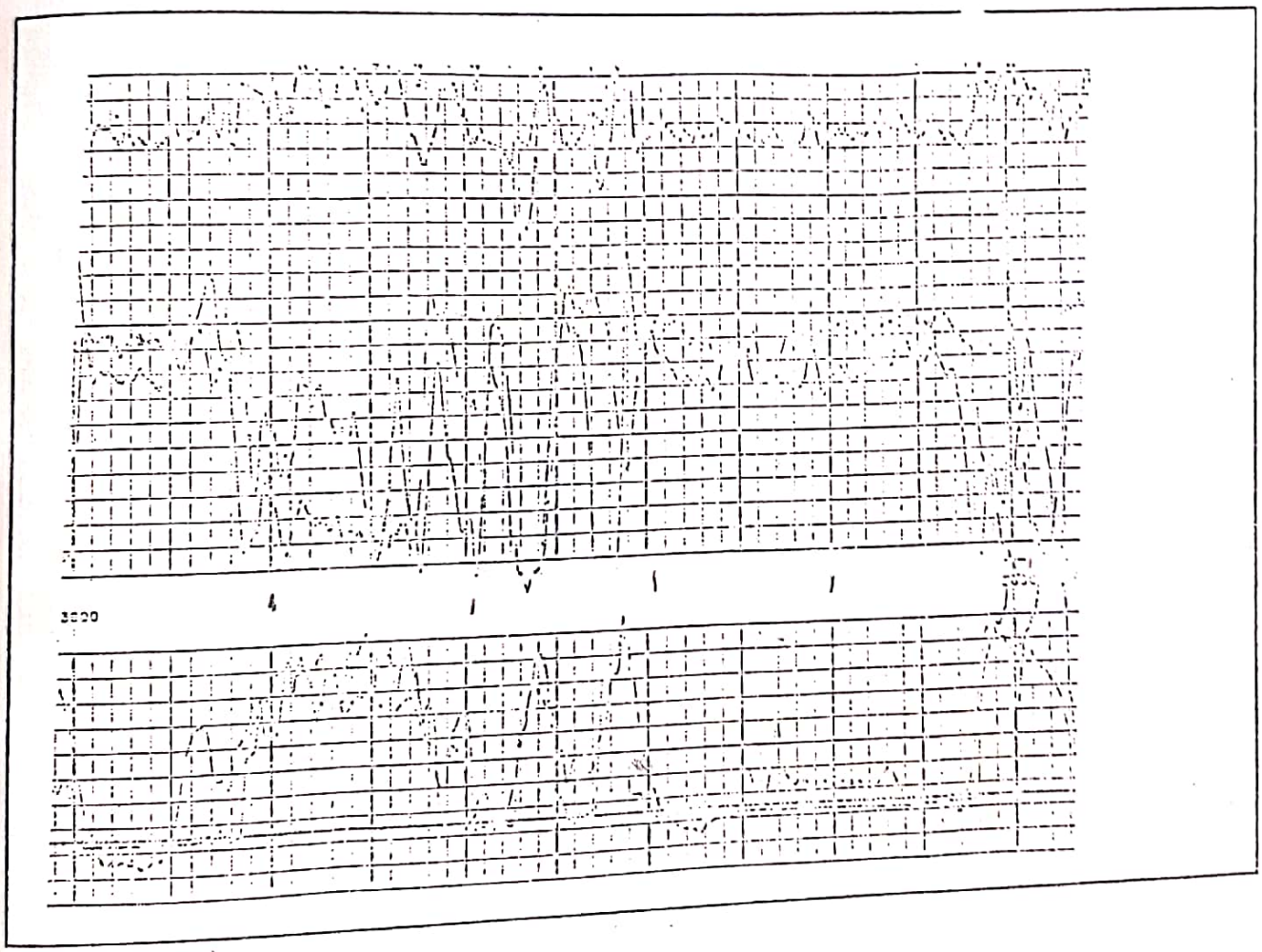

ملخـــص البحـــث

أن الغرض من هذه الدراسة هو احتساب درجات التشبع لتكوين الزبير في حقل شرقي بغداد من خلال تفسير المجسات.

و تم استخدام اربعة طرق في احتساب المسامية من خلال ثلاثة مجسات هي مجسات النيوترون و الكثافة و الصوت حيث جرى تحديد دقة هذه المسامية بمقارنتها مع المسامية المقاسة من نماذج اللباب الصخري مأخوذة من تسعة و ثمانين مقطعا لهذا التكوين. و جرى تقييم كل طريقة احصائيا عن طريق احتساب معامل الارتباط و الخطأ المعياري و معدل الخطأ المئوي اضافة الى معدل الخطأ المئوي المطلق. ووجد ان اسلوب التقاطع البياني (باستعمال طريقة المثلث) لبيانات مجسي الكثافة والنيوترون يعطي افضل المتغيرات التقييمية الاحصائية المذكورة اعلاه و لهذا تم استخدامها لاحتساب قيم المسامية الاكثر دقة فضلا عن التوصل الى تبني هذه الطريقه في تحديد المسامية سينتج عنه تحديد اكثر دقة لتشبع الماء (Sw) خاصة عند استخدام معادلة ارجي (Archie's equation) في حساب(Sw).

الجهات المستفيدة من البحث:

١- وزارة النفط

٢- مجلس البحث العلمي - مركز بحوث النفط

٣- جامعة بغداد

٤- شركة نفط الشمال

٥- شركة نفط الجنوب

٦- معهد التدريب النفطي - بغداد

٧- معهد التدريب النفطي - كركوك